PATENT ABSTRACTS OF JAPAN

(11)Publication number : 2002-334836
(43)Date of publication of application : 22.11.2002

(51)Int.Cl. H01L 21/027
G03F 7/20

(21)Application number : 2002-097334
(22)Date of filing : 22.02.2002

(71)Applicant : ASML NETHERLANDS BV
(72)Inventor : SOCHA ROBERT JOHN

(30)Priority
Priority number : 2001 271305 Priority date : 23.02.2001 Priority country : US

(54) OPTIMIZATION OF ILLUMINATION FOR SPECIFIC MASK PATTERN

(57)Abstract:
PROBLEM TO BE SOLVED: To provide a method and device for optimizing an illumination profile for a pattern of selected patterning means.
SOLUTION: The method and device for microlithography includes optimizing illumination modes, based on the features of a specific mask pattern. The illumination is optimized by determining an appropriate illumination mode, based on the diffraction order of a reticle and the autocorrelation of a projection optics. By eliminating the part of the illumination pattern which has no influence on modulation, excess DC light can be reduced, thereby improving the depth of focus. Optimization of the mask pattern includes addition of sub-resolution features, to reduce pitches and truncate the probability density function of a space width.

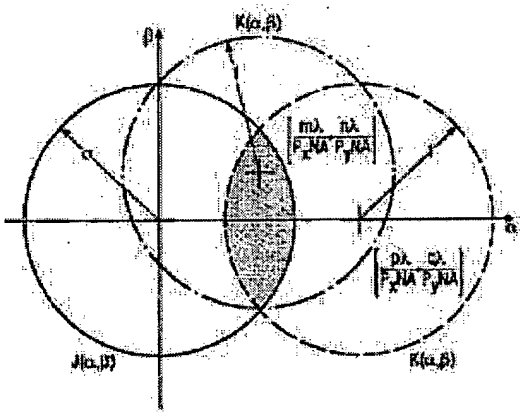

CLAIMS

[Claim(s)]
[Claim 1]A step which specifies a mutual transmission coefficient function for an optical system which is the method of optimizing the Lighting Sub-Division profile for a pattern of a selected patterning means, and contains a pattern of :lighting system and said selected patterning means; to said selected pattern. A step which is based and searches for relative relevance over image formation of a diffraction order; Illumination shape optimized from said mutual transmission coefficient is computed, A step which performs a weighting to a field of said illumination shape based on said relative relevance over image formation of said diffraction order, and a method of optimizing the Lighting Sub-Division profile provided with;.
[Claim 2]A method indicated to Claim 1 which a step which searches for relative relevance over image formation of said diffraction order equips with a step which asks for a characteristic pitch of said selected mask pattern further.
[Claim 3]Before asking for said characteristic pitch, it has a step which identifies a critical field of said selected pattern, A method indicated to Claim 2 to which asking for said characteristic pitch of said selected pattern is performed by asking for said characteristic pitch of said critical field.
[Claim 4]A step which identifies said critical field, What asking for said characteristic pitch of said critical field compares for a pitch of each critical region of which :discernment was done including identifying two or more critical fields; When a pitch of each of said identified critical region is almost equal, A method indicated to Claim 3 containing judging that said characteristic pitch of said critical region is equal to said one characteristic pitch among said identified fields, and;.
[Claim 5]A method indicated in any 1 clause from Claim 1 which includes performing a weighting to a field of said lighting-system form based on selected optimization metrics chosen from the depth of focus, a line end, a picture log inclination (ILS), a picture inclination (IS), and a group that comprises aberration sensitivity to 4.
[Claim 6]A step which asks for each pitch of a critical region which carried out the; aforementioned discernment with a step which identifies two or more critical regions; Optimization illumination shape is computed from said mutual transmission coefficient function, A method indicated to a step which performs a weighting for an order based on relevance over image formation of a diffraction order for every critical region, Claim 1 further provided with;, or 2.
[Claim 7]A method indicated in any 1 clause from Claim 1 to 6 further provided with a step which changes said selected pattern by reducing the total number of a different pitch in said mask pattern by an optical contiguity amendment technique.
[Claim 8]A method indicated to Claim 7 including that a step which changes said selected pattern by said optical contiguity amendment technique adds a feature of subresolution to said selected mask pattern further.
[Claim 9]A method indicated to Claim 7 which repeats a step which computes a step and optimization illumination shape which change said selected pattern.
[Claim 10]It is a computer program for optimizing the Lighting Sub-Division profile, A computer program provided with a program code meaning ordering said computer systems to perform said step of a method of any 1 clause of Claims 1-9, when it performs on computer systems.
[Claim 11]A step which supplies a substrate which is a device manufacturing method and was selectively covered with a layer of quality of :(a) radiation sense object at least;
(b) A step which supplies a projection beam of radiation using a lighting system;
(c) A step which gives a pattern to a section of said projection beam using a patterning means;
(d) A step which projects said patterned radiation beam on a target part of said radiation perception material layer;
A device manufacturing method fitted to said pattern which uses section intensity distribution in said projection beam generated in a step (b) in a step (c) before a step (d) using a preparation and a method by any 1 clause of Claims 1-9.
[Claim 12]It is a lithography projection apparatus and is the supporting structure for supporting a lighting system and; patterning means for supplying a projection beam of :radiation, . Function as said patterning means patterning said projection beam according to a desired pattern. A board table for holding the supporting structure and; board; Have a projection system for projecting said patterned beam on a target part of said substrate, and;, and said equipment, : — a mutual transmission coefficient function of said lighting system and said patterning means, [specify and] Based on said pattern generated by said patterning means, relative relevance over image formation of a diffraction order is searched for, . Compute illumination shape optimized from said mutual transmission coefficient function, and perform a weighting to a field of said illumination shape based on said relative relevance over image formation of said diffraction order. A calculating means; a lithography projection apparatus provided with a selecting means for choosing section intensity distribution in said projection beam ejected from said lighting system according to said illumination shape computed by said calculating means, and;.
[Claim 13]Selected mask designing. it is the method of optimizing — : — identifying a critical feature of said selected mask designing, and; — asking for the Lighting Sub-Division profile optimized based on a diffraction order of said critical feature, and; — a pitch number which exists in said selected mask feature. How to optimize changing said selected mask designing by using an optical contiguity amendment technique chosen so that it might reduce, and selected mask designing provided with;.
[Claim 14]A method by which said optical contiguity amendment added a feature of subresolution further chosen so that a continuation frequency function of spatial width of said selected mask designing might be changed, and said changed frequency

function was indicated to Claim 11 including making it have many closes.
[Claim 15]A method indicated to Claim 13 which a step which asks for said optimized Lighting Sub-Division profile equips with said step of a method of any 1 clause of Claims 1-9, or 14.
[Claim 16]It is a computer program for optimizing selected mask designing. A computer program provided with a program code meaning ordering said computer to perform a method of any 1 clause of Claims 13-15, when it performs on a computer.

[Translation done.]

* NOTICES *

1.This document has been translated by computer. So the translation may not reflect the original precisely.
2.**** shows the word which can not be translated.
3.In the drawings, any words are not translated.

DETAILED DESCRIPTION

[Detailed Description of the Invention]
[0001]
[Field of the Invention]Generally this invention relates to the method and equipment for a micro lithography method of image. If specified, this invention relates to the equipment and the method for optimizing the form of Lighting Sub-Division according to the specific pattern which is carrying out image formation.
[0002]
[Description of the Prior Art]Optical lithography is used now in manufacture of the product of other detailed features, such as an integrated circuit and a programmable gate array. In the most general explanation, a lithography device contains the lighting system which supplies the projection beam of radiation, the supporting structure holding a patterning means, the board table which supports a substrate, and the projection system (lens) for carrying out image formation of the patterned beam on the target part of a substrate.
[0003]The term of a patterning means shall be widely interpreted as what points out usable equipment and structure, in order to give the patterned section to the radiation beam which carries out ingress corresponding to the pattern generated by the target part of a substrate. The term of a "light valve" is also used in this context. Generally, a pattern corresponds to the specific stratum functionale in elements currently generated to the target part, such as an integrated circuit or other elements.
[0004]An example of this mechanism is a mask and this is usually held with a mask table (movable). The concept of a mask is well-known in lithography, and this includes mask types, such as a binary, a police box phase shift, an attenuation phase shift, and various hybrid mask types. If this mask is arranged in a projection beam, the radiation which enters into a mask will be selectively penetrated or (in the case of a transmission type mask) reflected according to the pattern on a mask (in the case of a reflection type mask). The mask table can hold a mask certainly in the position of the request in the entering projection beam, and further, in being a request, it also becomes certainly possible to move a mask to a beam.
[0005]Another example of this mechanism is a matrix address possible side including a viscoelasticity control layer and a reflector. As for the fundamental principle which is behind this equipment, the field where the address of the reflector (for example) was carried out reflects incident light as the diffracted light.
It is that the field by which an address is not carried out reflects incident light as the non-diffracted light on the other hand.
Using a suitable filter, said non-diffracted light can be removed from a reflective beam, and it can leave only the diffracted light. Thus, a beam is patterned according to the addressing pattern of a matrix address possible side. According to the alternative embodiment of a programmable mirror array, the small mirror arranged to the matrix is used. Each mirror can be leaned focusing on an axis, respectively by impressing a suitable local electric field or using a piezo-electric operating means. Also in this case, a matrix address is possible for a mirror and an ingress radiation beam is reflected in the direction in which the mirror by which the address was carried out differs from the mirror by which an address is not carried out. Thus, a reflective beam is patterned according to the addressing pattern of a matrix address possible mirror. Required matrix addressing can be performed using a suitable electronic means. In the both sides of an above-mentioned situation, a patterning means shall comprise one or more programmable mirror arrays. Furthermore it is related with the mirror array referred to here, detailed information can be acquired from US,5,296,891,B, No. 5,523,193, the PCT patent application WO 98/No. 38597, and WO 98/No. 33096, for example. These shall be contained also in an application concerned by citation. in the case of a programmable mirror array, embodying said supporting structure as a frame or a table, for example, accepting necessity -- immobilization -- or suppose that it is movable.
[0006]Another example is a programmable LCD array. In this case, the supporting structure can be too used as a frame or a table. An example of this structure is given to US,5,229,872,B. This shall also be contained also in an application concerned by citation.
[0007]For simplification, the example accompanied by a mask may be specified and treated in the portion after this document in some parts. However, he shall understand the general principle discussed in this example in the still larger context of an above-mentioned patterning means.
[0008]The term of a projection system includes a projection system various type. In an amateur's understanding, although a "lens" usually means a dioptric system, this term is used in a broad sense here so that a catoptric system and a catadioptric system may be included, for example. A lighting system may contain the element which operates according to either of these principles, in order to orient a projection beam, and to operate orthopedically or to control, below it may also summarize this element, or may be independently called a "lens."
[0009]In addition, the term of a "wafer table" can be used without showing tacitly that the substrate which receives a picture is a silicon wafer, and can show a suitable stage to support all the substrates processed by the lithography device.
[0010]A lithography projection apparatus can be used in manufacture of an integrated circuit (IC), for example. In this case, the patterning means can generate the circuit pattern corresponding to each layer of IC, and can carry out image formation of this pattern on the portion (one or more dies are comprised) of the object on the substrate (silicon wafer) covered with the layer of the quality of a radiation sense object (resist). Generally, a single wafer contains the network which comprises the adjoining target part which was continuously irradiated with one at a time at once by the projection system. In the present equipment using patterning with the mask on a mask table, the machine of two different types is distinguishable. In the lithography projection apparatus of one type,

when irradiating with each set elephant portion, the whole mask pattern is exposed on a target part by once. Generally this equipment is called a wafer stepper. In the equipment of another side generally called step and scan equipment, when irradiating with each set elephant portion, the mask pattern under a projection beam is gradually scanned to a given reference direction (the "scanning" direction), and a board table is scanned to parallel or non parallel to this direction synchronizing with this. Generally, since a projection system has a certain magnification M (generally <1), the speed V which scans a board table applies the speed which scans a mask table for the magnification M. Furthermore it is related with the lithography device described here, detailed information can be acquired from US,6,046,792,B, for example. This patent shall be included also in an application concerned by citation.

[0011]In the manufacturing process using a lithography projection apparatus, image formation of the pattern (for example, inside of a mask) is carried out on the substrate selectively covered with the layer of the quality of a radiation sense object (resist) at least. In advance of this image formation step, various procedures, such as priming, resist covering, and soft bake, may be given to a substrate. Other procedures, such as after-exposure bake (PEB), development, postbake, and measurement/inspection of a feature that carried out image formation, may be given to a substrate after exposure. The arrangement of this procedure is used as the foundation for patterning each layer of an element like IC, for example. This patterned layer may rank second and may pass through various processes, such as etching, an ion implantation (doping), metallization, oxidation, and chemical machinery polish. It is for these all completing each layer. When some layers are required, it is necessary to repeat the whole procedure or its modification for a new each layer. Eventually, the array of an element will exist on a substrate (wafer). These elements rank second, are mutually separated by techniques, such as dicing or sawing, and can carry each element on the carrier connected to the pin etc. from there. Furthermore it is related with this process, detailed information, for example Peter van Zant, McGraw Hill PublishingCo. 1997, The books of ISBN 0-07-067250-4 "Microchip Fabrication: A Practical Guideto Semiconductor Processing (manufacture of a microchip:.) It can obtain from the 3rd edition of the practical guidance for a semiconductor process." This document shall be contained also in an application concerned by citation.

[0012]For simplification, a projection system may be henceforth called a "lens." However, this term shall be widely interpreted as what includes dioptrics parts, a reflected-light faculty article, and a projection system various type [including a catadioptric system], for example. The radiation system can include the component which operates according to these design types of either, in order to orient the projection beam of radiation, and to operate orthopedically or to control, below it may summarize this component, or may call it a "lens" independently. A lithography device may be a thing of a type which has two or more board tables (and/or, two or more mask tables). It is also possible to use other one or more tables for exposure, performing a preparation step on one or more tables in this equipment of "being a stage in large numbers" using the table of a parallel addition. The lithography device of two stages is indicated to US,5,969,441,B and WO 98/No. 40791, for example. These shall be contained also in an application concerned by citation.

[0013]The number of control parameters has increased further now as the lighting system develops so that annular, a quadrupole, and the form of still more complicated Lighting Sub-Division may be generated from the conventional thing. The only adjustment which illuminates a circular area including an optic axis in the conventional illumination pattern, and is added to this pattern is changing a circumradius ($sigma_r$). Annular Lighting Sub-Division needs to specify an inradius ($sigma_c$), in order to specify the ring illuminated. A controllable number of parameters continues increasing in a multipolar pattern. For example, the illumination shape of a quadrupole prescribes the angle defined by each pole between the inradius and circumradius which the angle alpha of the pole other than two radii chose.

[0014]Simultaneously, mask technology is also progressing. The binary intensity mask has replaced with the advanced mask of a phase shift mask and others. Although a binary mask sends out, reflects or prevents image formation radiation only in a given point, the phase shift mask can attenuate a part of radiation, or after it performs a phase shift, it can send out reflect light, or can perform the both sides. The phase shift mask is used in order to carry out image formation of the wavelength of image formation radiation, or the feature of an order smaller than this. The diffraction effect in such resolution is because there is a possibility of causing the error of insufficient contrast and a line end especially also in various problems.

[0015]The feature of resolution, the depth of focus, contrast, and other printing pictures is improvable using illumination shape various type. However, each Lighting Sub-Division type is accompanied by a certain trade-off. For example, an improvement of contrast can be obtained at the sacrifice of the depth of focus. The mask of each type has the performance also depending on the pattern by which image formation is carried out.

[0016]In order to choose conventionally the optimal illumination mode that carries out image formation of the given pattern on a wafer, it was casual, and a series of test wafers were exposed, and were compared. As mentioned above, in the latest lighting system, the number of operational variables is increasing increasingly. The cost of optimization of the illumination shape by trial and error becomes very large, and the quantitive method of choosing illumination shape is needed as various rearrangement of variable setting increases.

[0017]The necessity checked previously and in order to cope with it in addition to this, this invention provides the method of optimizing the Lighting Sub-Division profile for the pattern of the selected patterning means. This method :lighting system. And the step which specifies the mutual transmission coefficient function for the optical system containing the pattern of the selected patterning means; The step which searches for the relative relevance over the image formation of a diffraction order based on the selected pattern, and the illumination shape optimized from; mutual transmission coefficient function are computed, It has the step and; which perform a weighting to the field of illumination shape based on the relative relevance over the image formation of a diffraction order.

[0018]According to another mode of this invention, a device manufacturing method is provided. Step which supplies the substrate by which this method was selectively covered at least in the layer of the quality of :(a) radiation sense object;

(b) Step which supplies the projection beam of radiation using a lighting system;

(c) Step which gives a pattern to the section of a projection beam using a patterning means;

(d) Step which projects the radiation beam patterned on the target part of a radiation perception material layer;

The section intensity distribution in the projection beam generated in the step (b) before the step (d) is fitted to the pattern used in a step (c) using a preparation and the above-mentioned method.

[0019]According to another mode of this invention, a lithography projection apparatus is provided. This method is the supporting

structure for supporting the lighting system and; patterning means for supplying the projection beam of :radiation, . Function as this patterning means patterning a projection beam according to a desired pattern. Have a projection system for projecting the beam patterned on the board table for holding the supporting structure and; board, and the target part of; board, and;, and this equipment, : -- the mutual transmission coefficient function of a lighting system and a desired pattern, [specify and] Based on the pattern generated by the patterning means, the relative relevance over the image formation of a diffraction order is searched for, . Compute the illumination shape optimized from the mutual transmission coefficient function, and perform a weighting to the field of illumination shape based on the relative relevance over the image formation of a diffraction order. It has a selecting means for choosing the section intensity distribution in the projection beam ejected from a lighting system according to the illumination shape computed by the calculating means and; calculating means, and;.

[0020]According to another mode of this invention, the method of optimizing the selected mask designing is provided. This method : the critical feature of the selected mask designing. It identifies.; so that the pitch number which exists in asking [for the Lighting Sub-Division profile optimized based on the diffraction order of a critical feature]; and the selected mask feature may be reduced. It has changing-mask designing selected by using optical selected contiguity amendment technique;.

[0021]This invention provides the computer program for performing a further above-mentioned method.

[0022]In this Description, although especially the thing for which the equipment by this invention is used for manufacture of IC can be mentioned, it will be understood clearly that this equipment has many other possible uses. For example, this can be used for manufacture of the derivation for an integrated optics system and magnetic domain memories and detecting patterns, liquid crystal display panels, thin film magnetic heads, etc. A "reticle", [in / on the situation of this alternative use, and / this document] A person skilled in the art will be permitted what is regarded as a term "mask" with any more common use of the term of a "wafer" or a "die", a "substrate", and a thing replaced by an "object position", respectively.

[0023]This invention is further explained below with reference to an illustration embodiment and attached Drawings.

[0024]

[Mode for carrying out the invention]This invention is taken into consideration about a lighting source and the details of a pattern, and includes carrying out the modeling of the image formation of a pattern (from a mask to a substrate top) mathematically first.

[0025]In order to compute an aerial image about a limited lighting source, there are mainly two methods. These methods are Abbe's formulation and formulation of Hopkins. In Abbe's formulation, the source of each point in illumination shape generates the plane wave which enters on a pattern, and image formation of each of these point sources is carried out on a wafer. Since a point source is incoherency spatially, the sum total intensity in a wafer is the sum of the intensity generated by each of these point sources. Therefore, in Abbe's formulation, integration in illumination shape is performed, after finding the integral in a pattern.

[0026]An order of integration is changed in formulation of Hopkins. That is, integration in a source is performed first. In formulation of Hopkins, a 4-dimensional mutual transmission coefficient (TCC) is specified, and inverse Fourier transform of TCC serves as intensity of a picture. Derivation of TCC is explained to Principles of Optics (principle of optics) of Born and Wolf, the 6th edition, and 528 thru/or 532 pages, for example. This shall be contained also in an application concerned by citation.

[0027]TCC is the autocorrelation of the projection pupil which carried out multiplication with the Lighting Sub-Division pupil. TCC is shown in drawing 1 as a set of three overlapping circles. When it explains to the right from the left, the 1st circle expresses Lighting Sub-Division pupil J_S (alpha, beta), and alpha and beta are coordinates of illumination shape here. For next calculation, the radius of J_S can be set as the greatest circumradius $sigma_r$ possible to the lithography device used for image formation, for example. In order to study implementability, and in order to clarify the advantage of still bigger $sigma_r$, it is also possible to set $sigma_r$ or more to 1.0.

[0028]A central circle expresses the projection pupil K consisting mainly of (-m lambda/P_xNA and -n lambda/P_yNA) (alpha, beta). Since the coordinate system is normalized by the factor of lambda/NA, the radius of K is 1.0. Although a right-hand side circle expresses a projection pupil similarly, this centers on (p lambda/P_xNA and q lambda/P_yNA). In these last two formulas, m, n, p, and q are equivalent to a separate diffraction order, and it becomes clear that TCC(s) are the above 4-dimensional (4-D) formulas. The diffraction order of a x direction is expressed by m and p, and the diffraction order of a y direction is expressed by n and q. Although x and a y-coordinate are used for this explanation, he changes a coordinate system appropriately by the following formulas, and an usable thing will be understood by the person skilled in the art in an alternative coordinate system.

[0029]TCC about a point (m, n, p, q) with separate 4-D is the integration of the field which attached the shade with which all the three circles overlap. Since it is assumed that structure is periodic, the Fourier transform of a pattern is discrete and TCC is discrete. In a continuous pattern image, a pitch can be lengthened until an adjoining feature stops affecting the Fourier transform of an object pattern. TCC of drawing 1 is mathematically expressed in writing by the formula 1.

$$\iint_{\sqrt{\alpha^2+\beta^2}\le\sigma} J_s(\alpha,\beta)K\left(\alpha+\frac{m\lambda}{P_xNA},\beta+\frac{n\lambda}{P_yNA}\right)K^*\left(\alpha-\frac{p\lambda}{P_xNA},\beta-\frac{q\lambda}{P_yNA}\right)d\alpha d\beta \qquad \text{式(1)}$$

[0030]By specifying both the diffraction order coefficient (DOCC), TCC is extensible so that the effect of a pattern may be included. DOCC is specified at a ceremony 2. This is obtained by carrying out the multiplication of the Fourier conversion factor of a pattern to TCC.

$$DOCC(m,n,p,q)=T(m,n)T^*(-p,-q)TCC(m,n,p,q) \qquad \text{式(2)}$$

[0031]The radiant intensity in a wafer is computable by inverse Fourier transform of DOCC, as shown in the formula 3.

$$I(x,y)=\sum_m\sum_n\sum_p\sum_q e^{ix\left[\frac{2\pi}{P_x}(m+p)\right]}e^{iy\left[\frac{2\pi}{P_y}(n+q)\right]}DOCC(m,n,p,q) \qquad \text{式(3)}$$

[0032]Since a projection optical system acts as a low-pass filter selectively and a diffraction order decreases by this, in the computed image strength, an important diffraction order is only a decimal. As a result, TCC is a band limiting function. The greatest

required order of x and y is computable according to the formulas 4 and 5, respectively. In each case, the order of negative and positive both sides is required. For example, m ranges from negative m_{max} to positive m_{max} ($-m_{max}<=m<=+m_{max}$). Since the order of negative and positive both sides is required, the size of TCC is $2q_{max}+1$ to hang, which is hung $2n_{max}+1$ and which is hung $2p_{max}+1$ 2 $m_{max}+1$. However, since the zone is limited, happiness and TCC need to calculate no pattern diffraction orders. The same with setting to TCC, it is pattern diffraction order $m_{max}<=m<=+m_{max}$ Accepted and only order $n_{max}<=n<=+n_{max}$ is required in a y direction in a x direction.

$$f_{x\,max} = m_{max} = p_{max} = floor\left[\frac{P_x NA(1+\sigma_o)}{\lambda}\right] \qquad 式(4)$$

$$f_{y\,max} = n_{max} = q_{max} = floor\left[\frac{P_y NA(1+\sigma_o)}{\lambda}\right] \qquad 式(5)$$

[0033]If the formulas 1 and 2 are substituted for the formula 3, the formula 6 about the radiant intensity in a wafer will be obtained. As shown in the formula 7, it can ask for the portion of the Lighting Sub-Division pupil which affects image formation most by changing an order of integration, i.e., use not formulation of Hopkins but Abbe's formulation. It comments on each of the formulas 6 and 7 amounting to two lines.

$$I(x,y)=\sum_m\sum_n\sum_p\sum_q e^{ix\left[\frac{2\pi}{P_x}(m+p)\right]}e^{iy\left[\frac{2\pi}{P_y}(n+q)\right]}T(m,n)T^*(-p,-q) \qquad 式(6)$$

$$\bullet \iint_{\sqrt{\alpha^2+\beta^2}<\sigma} J_s(\alpha,\beta)K\left(\alpha+\frac{m\lambda}{P_x NA},\beta+\frac{n\lambda}{P_y NA}\right)K^*\left(\alpha-\frac{p\lambda}{P_x NA},\beta-\frac{q\lambda}{P_y NA}\right)d\alpha d\beta$$

$$I(x,y)=\iint_{\sqrt{\alpha^2+\beta^2}<\sigma} d\alpha d\beta\sum_m\sum_n\sum_p\sum_q e^{ix\left[\frac{2\pi}{P_x}(m+p)\right]}e^{iy\left[\frac{2\pi}{P_y}(n+q)\right]} \qquad 式(7)$$

$$\bullet J_s(\alpha,\beta)T(m,n)T^*(-p,-q)K\left(\alpha+\frac{m\lambda}{P_x NA},\beta+\frac{n\lambda}{P_y NA}\right)K^*\left(\alpha-\frac{p\lambda}{P_x NA},\beta-\frac{q\lambda}{P_y NA}\right)$$

[0034]Since alpha and beta express the coordinates of the Lighting Sub-Division pupil, new function J_{opt} can be specified. New function J_{opt} shows which portion (alpha, beta) of illumination shape is used to the given diffraction order (m, n, p, q), and is expressed in writing by the formula 8. Image strength is computable in totaling all the six variables (m, n, p, q, alpha, beta), as the multiplication of the reverse Fourier coefficient (e^{ikx}) is carried out to this and it is shown in the formula 9 from the formula 8.

$$J_{opt}(\alpha,\beta,m,n,p,q)=J_s(\alpha,\beta)T(m,n)T^*(-p,-q)K\left(\alpha+\frac{m\lambda}{P_x NA},\beta+\frac{n\lambda}{P_y NA}\right)K^*\left(\alpha-\frac{p\lambda}{P_x NA},\beta-\frac{q\lambda}{P_y NA}\right)$$

式(8)

$$I(x,y)=\iint_{\sqrt{\alpha^2+\beta^2}<\sigma} d\alpha d\beta\sum_m\sum_n\sum_p\sum_q e^{ix\left[\frac{2\pi}{P_x}(m+p)\right]}e^{iy\left[\frac{2\pi}{P_y}(n+q)\right]}J_{opt}(\alpha,\beta,m,n,p,q)$$

式(9)

[0035]Although it will become clear, J_{opt} is a 6-dimensional function, therefore it is difficult to apply this to illumination shape. In order to ask best for which portion of illumination shape is important for image formation, it is desirable to remove some among six variables.

[0036]It asks for the aerial image intensity I (x, y) by taking inverse transformation about m+p and n+q. When it is m+p=n+q=0, aerial image intensity is not modulated. Since one of the targets of the Lighting Sub-Division optimization is removing the portion of the illumination shape which does not almost have the influence which it has on abnormal conditions, or is not, it can remove the portion of the illumination shape used as m+p=n+q=0. In order to remove these portions and to visualize the portion of important illumination shape further for image formation, by conversion of a variable, two of the variables of a 6-dimensional J_{opt} function (4 diffraction orders) are removed, and it is changed into four dimension functions (2 diffraction orders). These four dimension functions are called J_{opt-2D}. The formula 12 can be obtained by substituting for the formula 9 about the formulas 10 and 11 I (x, y).

$$\eta = m + p \Rightarrow p = \eta - m \qquad \text{式(10)}$$

$$\xi = n + q \Rightarrow q = \xi - n \qquad \text{式(11)}$$

$$I(x,y) = \iint_{\sqrt{\alpha^2+\beta^2}<\sigma} d\alpha d\beta \sum_{\eta=-2f_{x\max}}^{+2f_{x\max}} \sum_{\xi=-2f_{y\max}}^{+2f_{y\max}} e^{ix\left[\frac{2\pi}{P_x}\eta\right]} e^{iy\left[\frac{2\pi}{P_y}\xi\right]} \underbrace{\sum_{m=-f_{x\max}}^{+f_{x\max}} \sum_{n=-f_{y\max}}^{+f_{y\max}} J_{opt}(\alpha,\beta,m,n,\eta-m,\xi-n)}_{J_{opt-2D}(\alpha,\beta,\eta,\xi)} \qquad \text{式(12)}$$

[0037]In the formula 12, after J_{opt-2D} changes a variable according to the formulas 10 and 11, it can be regarded as the sum of J_{opt} about m and n. It can express with substituting the formula 8 for the formula 12 so that in the formula 13 for J_{opt-2D}, and it can write as a function of J_{opt-2D} so that in the formula 14 for the intensity I (x, y).

$$J_{opt-2D}(\alpha,\beta,\eta,\xi) = J_s(\alpha,\beta) \sum_{m=-f_{x\max}}^{+f_{x\max}} \sum_{n=-f_{y\max}}^{+f_{y\max}} T(m,n)T^*[-(\eta-m),-(\xi-n)] \qquad \text{式(13)}$$

$$\cdot K\left(\alpha+\frac{m\lambda}{P_x NA}, \beta+\frac{n\lambda}{P_y NA}\right) K^*\left(\alpha-(\eta-m)\frac{\lambda}{P_x NA}, \beta-(\xi-n)\frac{\lambda}{P_y NA}\right)$$

$$I(x,y) = \iint_{\sqrt{\alpha^2+\beta^2}<\sigma} d\alpha d\beta \sum_{\eta=-2f_{x\max}}^{+2f_{x\max}} \sum_{\xi=-2f_{y\max}}^{+2f_{y\max}} e^{ix\left[\frac{2\pi}{P_x}\eta\right]} e^{iy\left[\frac{2\pi}{P_y}\xi\right]} J_{opt-2D}(\alpha,\beta,\eta,\xi) \qquad \text{式(14)}$$

[0038]Function J_{opt-2D} shows the portion of important illumination shape for every diffraction order, when a value is calculated. Since the weighting of the J_{opt-2D} is carried out by each diffraction order T (m, n), the influence which exerts a large diffraction order on an aerial image becomes large.

[0039]The starting point for the optimal illumination shape can be indicated to be J_{tot} about a specific pattern, and as shown in the formula 15, this totals J_{opt-2D} about eta and xi, and is called for by subtracting J_{opt-2D} (alpha, beta, eta= 0, xi= 0). In the case of eta= 0 and xi= 0, an aerial image is not modulated but a J_{opt-2D} (alpha, beta, eta= 0, xi= 0) ingredient expresses the order or DC light of zero with the formula 15. The whole quantity of DC light increases with the point in Lighting Sub-Division which is not contributed to image formation. Since DC light which increased does not cause abnormal conditions, this is not very useful and there is a possibility that the depth of focus may become shallow as a result, further.

[0040]For this reason, the illumination shape by J_{tot} stops the quantity of DC light to the minimum, and a process window improves it as a result. It can be shown using formula J_{tot} whether which portion of a lighting system of importance is high for image formation (or is importance low?).

$$J_{tot}(\alpha,\beta) = \left[\sum_{\eta=-2f_{x\max}}^{+2f_{x\max}} \sum_{\xi=-2f_{y\max}}^{+2f_{y\max}} \left|J_{opt-2D}(\alpha,\beta,\eta,\xi)\right|\right] - \left|J_{opt-2D}(\alpha,\beta,0,0)\right| \qquad \text{式(15)}$$

[0041]Since illumination shape and a pattern are combined, if optical contiguity amendment (OPC) is changed, a diffraction order will be affected, therefore J_{tot} will be affected. Although it will be understood by the person skilled in the art as a result, a change to initial illumination shape J_{tot} and a pattern must be made several times using a repetition of processing with an OPC engine and the Lighting Sub-Division engine. It is necessary to adjust a pattern and illumination shape also so that specific image formation standards (sensitivity to the depth of focus (DOF), a line end (EOL), and aberration, etc.) may be optimized, and optimization software can perform this. However, since not an OPC feature but the pattern as the whole has influence of the greatest on the optimal illumination shape, J_{tot} is the optimal initial illumination shape.

It will converge most quickly for optimization of the repetition about illumination shape and a pattern.

[0042]The gray-scale illumination shape which has a continuous intensity value of the range of 0 thru/or 1 can express initial illumination shape J_{tot}. This gray-scale illumination shape is generable by using the quartz plate which performed the chrome plating which performed a diffraction optical element (DOE) or dithering. Gray-scale illumination shape is not possible, or, in the case which is not preferred, only 0 and 1 can be forced into a lighting-system profile by applying a threshold value to a gray scale. In this case, the value exceeding a threshold value is revalued to 1, and the value of less than a threshold value is omitted to 0. It is being able to apply arbitrary threshold values or simulating a process window, or the optimal threshold value can be found out by repeating a pilot run.
[0043]Example 1: the technique for computing J_{tot} outlined previously was applied to the brick-wall separation pattern. A 150-nm pattern was reduced to 130 nm and a 110-nm design basis, and the numerical aperture (NA) carried out image formation with the step and scan lithography system of 0.8. The separation pattern of a 130-nm design basis is shown in drawing 2.
[0044]The size of the diffraction order of this mask feature is shown in drawing 3. In drawing 3, the greatest order is an order (0, 0) or DC background light. The order which contributed to image formation most is an order (**2, 0).
The brick of the lengthwise direction in a brick-wall pattern is expressed.
Other important orders are (**1, **1), express a clear field and specify the end of a separation pattern. An order higher than this is useful to specify two-dimensional structures, such as an end of each line. Since the diffraction pattern is not constant, the weighting factor in DOCC changed with orders, and this has suggested that a mask pattern affects the method of Lighting Sub-Division.
[0045]J_{opt-2D} can be computed by the ability to substitute the diffraction order coefficient T in drawing 3 (m, n) for the formula 13. This is shown in drawing 4. As drawing 4 shows, the greatest contribution to J_{opt-2D} is an order (eta= 0, xi= 0). (0, 0) An order does not contribute to image formation but makes DOF shallow. As shown in the formula 15, this (0, 0) order can be subtracted from sum total Lighting Sub-Division J_{tot}. (0, 0) If an order is not taken into consideration, the greatest contribution is a diffraction (eta= **2, xi= 0) order, and this expresses formation of the separating line along a x direction. It is large and another ingredient which specifies the end of a separating line is a diffraction (eta= **1, xi= **1) order. (0, **2) Although a diffraction order is slightly small, a larger order than this is combined in eta= 0 of a lens, and the field of xi= 2 [**]. These fields are useful to specify a line end. The technique of DOCC is an effective method in order to show how the Lighting Sub-Division pupil is sampled in order to improve image formation, and to understand the image formation of a brick-wall separation pattern.
[0046]130-nm design-basis goodwill can compute the Lighting Sub-Division pupil of a wall pattern using the formula 15. This is shown in drawing 5. It is shown that the field where drawing 5 is the most important for image formation is a lateral part of illumination shape along a x axis. These lateral parts form an ellipse dipole. In addition to these ellipse dipole elements, the center of the Lighting Sub-Division pupil contributes to image formation greatly. As mentioned above, the Lighting Sub-Division pupil can be carried out in a gray scale or a binary Lighting Sub-Division profile.
[0047]According to the equipment to be used, gray-scale Lighting Sub-Division may be possible. Gray-scale Lighting Sub-Division means controllable illumination intensity, and the normalization levels from zero to one can be chosen at least about the given portion of illumination shape. For example, control of this illumination intensity can be performed using the diffraction optical element (DOE) in a lighting system. In this case, for example, illumination shape can be carried out, as shown in drawing 5. However, as mentioned above, a part of partial spike which is computed theoretically and looked at by drawing 5 is removed, after filtering illumination information with a low-pass filter as a result of a projection optical system. Therefore, the spike filtered shall be disregarded when designing illumination shape.
[0048]When using binary illumination shape, only a binary must choose a threshold value as the intensity of a lighting system as the foundation for (0 or 1) to assign each point of illumination shape the value of 0 or 1 when possible. For example, when the threshold value of 0.8 is chosen, the intensity value of the lighting system exceeding 0.8 is revalued by 1, and less than 0.8 value is omitted by 0. In a request, it is also possible to apply other threshold values.
[0049]A gray scale is used for the technique of example 2:2 value, binary illumination shape is designed about the same brick-wall separation pattern supposing the maximum circumradius sigma of 0.88, and it is shown in drawing 6.
[0050]Subsequently, it compared with the performance for which the performance of illumination shape in which drawing 6 was optimized was simulated about the binary mask on NA=0.8 and a lambda= 248-nm step and scan lithography device, and annular Lighting Sub-Division simulated it. In this simulation, since the numerical aperture exceeded 0.7, the vector (thin film) image formation resist model was used. In this model, a resist is 400 nm in thickness of the type which has refractive-index n=1.76-j0.0116, and is on 66 nm another type which has n=1.45-j0.3 on the polysilicon substance of n=1.577-j3.588. The result of the lighting system ($sigma_{out}$=0.88) which was annular-illuminated ($sigma_{in}$=0.58 and $sigma_{out}$=0.88) and was optimized to drawing 7 and 8 is shown, respectively. In drawing 7 and the both sides of 8, the result of the section in the center of an isolation region and a top-down simulation result are shown. In these figures, by equalizing the intensity through a resist, the Bossung plot B is computed from an aerial image threshold value, and the line width lw obtained as a result is graph-ized to the focus f about the intensity of a threshold value. This technique tends to carry out superfluous prediction of DOF as a loss of thickness, and the resist profile's inclination is not taken into consideration. Probably, the resist model which computes the loss of thickness at least will be required. In each of a figure, the top-down result is drawn as a curve of the solid line in optimal threshold value (optimal dose) that was computed in the Bossung plot. The picture of these simulated threshold values is compared with the actual mask data shown in the straight line of a dotted line.

[0051]130-nm design-basis goodwill shows drawing 7 the simulation result of a wall separation pattern about the binary mask feature in NA of 0.8 which used annular Lighting Sub-Division ($sigma_{in}$=0.58 and $sigma_{out}$=0.88). This annular setting out has about 0.4-micrometer DOF to a -0.4micrometer to 0.0-micrometer focus. Through an omnifocal lens, the contrast of a resist is low and image formation can be carried out by the resist of low contrast. However, in the contrast of this low strength, a mask error increase factor (MEEF) is large, and an exposure latitude (EL) is small. Although the top-down picture in drawing 7 shows that shortening of a line end (EOL) is about 20 nm, about a 130-nm design basis, this can extend a line slightly and can fix it. However, since there is a

possibility that the extended line may collide with other features when a design basis continues contracting, extension of a line cannot be performed any longer. Therefore, it is desirable to fix EOL with Lighting Sub-Division.

[0052]At drawing 8, 130-nm design-basis goodwill is illustrating the simulation result about a wall separation pattern about the binary mask feature by NA of 0.8 using the optimization binary illumination shape of drawing 6. The optimal illumination shape has about 0.6-micrometer DOF to a -0.45micrometer to +0.15-micrometer focus. The illumination shape which optimized the cross section image of drawing 8 as compared with the thing of drawing 7 has large contrast through an omnifocal lens compared with annular Lighting Sub-Division. This big contrast suggests that MEEF about optimization illumination shape is small compared with annular Lighting Sub-Division, and the exposure latitude for optimization illumination shape is large. Another advantage of this optimization illumination shape is that the performance of a line end is improved compared with annular Lighting Sub-Division. The top-down picture of drawing 8 shows that EOL can be maintained without this optimization illumination shape extending the line on a pattern, and this is convenient because of reduction of a bolder design basis.

[0053]Example 3: the result about drawing 7 and the binary mask (BIM) in 8 was compared with the simulation result about a chromium loess mask (CLM). By the known method, the chromium loess brick-wall separation pattern was designed from the experimental result of software simulation to the person skilled in the art. Chromium loess technology needs the light of an order (0, 0) so that sufficient benefit may be received from the improvement of DOF which an axis shifts and is obtained by Lighting Sub-Division. The necessity for the light of an order (0, 0) is supported by the experimental result from a simulation. For this reason, dithering must be performed to a detached core or it must be considered as half-tone. What is necessary is just to choose the pitch of half-tone so that the 1st order of a direction that performed dithering may not go into a projection pupil. In this example, the pitch of lambda/[NA (1+$sigma_{out}$)] following performed dithering on the line perpendicularly. However, the duty cycle of dithering must be adjusted so that the quantity of the light of an order (0, 0) may be optimized for optimal DOF and pattern fidelity. At the simulation result for CLM, the half-tone pitch was 155 nm in 50% of duty cycle (77.5-nm chromium island). In this pitch, it is barred mostly that an order (0, **1) goes into a projection pupil. However, this duty cycle must be adjusted so that DOF may be made into the maximum with a computer-aided-design tool.

[0054]Example 4: the simulation result about a 130nm design-basis layer was illustrated about CLM of a 155-nm half-tone pitch and a 50% duty cycle. With NA and annular Lighting Sub-Division ($sigma_{in}$=0.58 and $sigma_{out}$=0.88) of 0.8, CLM was exposed with lambda= 248-nm equipment. DOF of CLM of this annular setting out was 0.5 micrometer (from a -0.4-micrometer focus to a +0.1-micrometer focus). CLM of annular Lighting Sub-Division had large DOF compared with BIM of annular Lighting Sub-Division, and contrast was excellent through the omnifocal lens. This shows that the performance of CLM was superior to the BIM mask. It was also shown that the result of a top-down simulation excels the EOL performance by BIM in the EOL performance by CLM theoretically and that CLM was more fully able to specify the landing field of the contact hole compared with BIM.

[0055]Example 5: the simulation result about a 130nm brick-wall separation pattern detached core was illustrated about the lambda= 248-nm equipment of the optimization ellipse dipole shown in NA and drawing 6 of 0.8. These results were simulated using the same reticle as the CLM reticle used in the example before having a 155-nm half-tone pitch and 50% of duty cycle. CLM exposed with this optimization illumination shape had 0.7-micrometer DOF (from -0.5micrometer to +0.2 micrometers), and was 40% of improvement. The Bossung plot showed that parfocal intensity was about 0.21. In addition, in order to adjust a reticle so that it may become a size of exact line width, and also to improve performance, the OPC technique based on a model was able to be applied. What is necessary is to perform applying bias and just to make a change of a half-tone duty cycle, for example, in order to amend line width. The top-down simulation result showed that CLM could specify the landing field of contact and could maintain the homogeneity of CD. With this ellipse illumination shape, the disagreement of the vena contracta and other line width decreased. The CLM reticle can apply bias so that DOF may be improved, and as a result, EOL performance should improve it. OPC based on a model should be able to amend EOL further.

[0056]Example 6: about the detached core of the 110nm design basis, optimization illumination shape was generated by the formulas 13 and 15 using the mask pattern of drawing 2. In order to visualize the sampling of the Lighting Sub-Division pupil, J_{opt-2D} is illustrated to drawing 9 and y order (xi=n+q) is horizontally shown perpendicularly for x order (eta=m+p). The greatest contribution to the 110-nm design basis of drawing 11 is an order (eta= 0, xi= 0) like drawing 4 about a 130-nm design basis. The light of this (0, 0) order is harmful to DOF, and as shown in the formula 15, it is removed in J_{tot}. Drawing 9 shows that not an order (**2, 0) (**1, **1) but an order serves as the greatest contribution to optimization of illumination shape. This is for the fact that a 110-nm design basis is too positive, with the 248-nm equipment of NA=0.8.

In order to attain this resolution, slightly high NA is preferred.

The order which contributes most in order to specify separation line width is an order (**2, 0). However, the distant place edge of illumination shape has an order (**2, 0) (0.8< sigma<1.0), and this shows that enforcement of a 110-nm design basis [in / that sigma is 1 / this wavelength] can be improved.

[0057]The optimization illumination shape about a 110-nm brick-wall detached core is shown in drawing 10 using the result of the formula 15 and drawing 9. Drawing 10 shows that the illumination shape field which contributes to image formation most is the central small part and distant place edge of illumination shape. To drawing 11 a, one possible embodiment of this illumination shape is illustrated. In order to print a still more positive design basis using 248-nm equipment and to impose restriction of a projection numerical aperture, as shown in drawing 11 b, sigma is set to 1.0 and the illumination shape which has a small sector (the ring width of sigma is 0.2) is used.

[0058]The embodiment of this invention includes selection of a critical cell or a specific gate. Subsequently, these critical features are processed and it asks for J_{tot} as mentioned above. Depending for illumination shape on a pattern was shown by the section 1. Therefore, when there is no remarkable difference in a pitch about a critical feature, the single illumination shape which optimizes a process window can be generated about all the critical features. One example of a circuit which has critical gate g_1, g_2, g_3, and the critical cell cc is shown in drawing 12. The diffraction order of a critical feature with these tags can be computed, and optimization illumination shape can be computed by using the already expressed theory. A process window can be computed and it can compare with the process window by other illumination shape, after computing optimization illumination shape.

[0059]The option which optimizes the interaction of Lighting Sub-Division/pattern is changing a design pattern with a dispersion bar.

A dispersion bar closes a pitch from ASIC or the half-continuous function about a logic design. A pitch decreases, after arranging a dispersion bar. In simulation software, arranging a dispersion bar by the separation between edge of 0.61 lambda/NA can prove this. At drawing 13, the design of drawing 12 is changed by adding two or more dispersion bars. Subsequently, illumination shape can be optimized about this changed design. Subsequently, the process window performance of the illumination shape optimized about the design which has a dispersion bar can be compared with the process window of the illumination shape optimized without having a dispersion bar. Since the design which has a dispersion bar closes a pitch, a dispersion bar and the optimized axis shift and the combination with Lighting Sub-Division (OAI) has the greatest possible DOF process window.

[0060]Another concept for optimizing illumination shape is based on the arrangement of a dispersion bar based on consideration of spatial width (SW). A dispersion bar is arranged by OPC based on a rule. Spatial width can prescribe this rule. Using simulation software, when it does not have a dispersion bar, the frequency function (pdf) of the spatial width in the case of having a dispersion bar should be able to be computed. Subsequently, in consideration of pdf, Lighting Sub-Division can be optimized by changing J_{opt-2D}, as shown in the formula 16. If it assumes that a vertical line and a level line are infinite, it is also possible to compute the diffraction order T (m, n). In the formula 17, a diffraction order is computed as a function of m and n. w is line width and tau is a pitch [in / respectively / in intensity transmissivity / of a reticle /, $P_x=SW_x+w$, and $P_y=SW_y+w$ / x and a y direction] here.

$$J_{opt-2D}(\alpha,\beta,\eta,\xi) = J_s(\alpha,\beta)\sum_{m=-fx_{max}}^{+fx_{max}}\sum_{n=-fy_{max}}^{+fy_{max}}\int\int dP_x dP_y pdf(Px)pdf(Py)T(m,n)T^*[-(\eta-m),-(\xi-n)]$$

$$\cdot K\left(\alpha+\frac{m\lambda}{P_x NA},\beta+\frac{n\lambda}{P_y NA}\right)K^*\left(\alpha-(\eta-m)\frac{\lambda}{P_x NA},\beta-(\xi-n)\frac{\lambda}{P_y NA}\right) \quad \text{式(16)}$$

[0061]The formula 17 is a procession of four formulas.
In order of presentation, it is m=n=0, m= 0, n!=0, m!=0, n= 0 and m!=0, and n!=0.

$$T(m,n) = \begin{cases} 1 - w\left(1+\sqrt{\tau}\right)\left(\frac{1}{P_x}+\frac{1}{P_y}\right)+\frac{w^2}{P_x P_y}\left(1+\sqrt{\tau}\right)^2 \\ \left[1-\frac{w}{P_x}\left(1+\sqrt{\tau}\right)\right]\left(1+\sqrt{\tau}\right)\left(\frac{P_y}{\pi n}\right)\sin\left(n\frac{\pi w}{P_y}\right) \\ \left[1-\frac{w}{P_y}\left(1+\sqrt{\tau}\right)\right]\left(1+\sqrt{\tau}\right)\left(\frac{P_x}{\pi m}\right)\sin\left(m\frac{\pi w}{P_x}\right) \\ \left(1+\sqrt{\tau}\right)^2\left(\frac{P_x}{\pi m}\right)\sin\left(m\frac{\pi w}{P_x}\right)\left(\frac{P_y}{\pi n}\right)\sin\left(n\frac{\pi w}{P_y}\right) \end{cases} \quad \text{式(17)}$$

[0062]Since it is suggested that it is not so important as other things, if the optimal illumination shape is computed by pdf, some problems will produce some pitches. When it is considered that all the gates are critical in pdf, pdf must be changed with a weighting factor. This weighting factor is a function of the pitch called wf (Px). All the critical pitches are treated identically and it must be made to be set to wf(Px) and pdf(Px) =1 with this weighting factor. In replacing pdf (Px) in the formula 16 by wf(Px) and pdf (Px), this weighting factor shall be added to the formula 16. When all the pitches are critical, it is difficult for a weighting factor to generate optimization illumination shape, without it not being useful in order to opt for optimization, and changing a design (pattern).

[0063]One solution to this problem is adding an above-mentioned dispersion bar and changing a design. A dispersion bar is useful to make a pitch small about the separated feature. If a dispersion bar is added to a design, the feature separated before once has the tendency to act as a feature which crowded. For this reason, a dispersion bar closes a pitch from pdf to continuous still more nearly discrete pdf. Drawing 14 is pdf of an example about logic patterns which has the feature which carried out orientation to the y direction (namely, the "vertical" direction) when [which applied the dispersion bar] not having case and applied. Drawing 14 shows vertical gate space width (micrometer) on x (level) axis. In the design D which does not have a dispersion bar and which is not changed, pdf has three separate upheaval in 0.2, 0.6, and the spatial width of 1.5 micrometers. After arranging a dispersion bar, in D+SB, a pitch number becomes fewer and most spatial width is in the pitch which is 0.2 micrometer and which crowded. By change of this pdf, the probability which can optimize illumination shape becomes high.

[0064]The overall illumination shape about the design which has the both sides of a horizontal (x axis) and vertical feature is the sum of horizontal and vertical illumination shape. When centralizing illumination shape on $sigma_{cx}$ about a vertical feature and making it concentrate on $sigma_{cy}$ about a level feature, $\sqrt{2}\,\sigma_{cx} \leqq 1$ かつ $\sqrt{2}\,\sigma_{cy} \leqq 1$

If it comes out, the optimal illumination shape will be the "conventional" quadrupole illumination shape. In the case of others, analysis of this type serves as 4 pole illumination shape rotated 45 degrees as a result.

[0065]It can show here, and 5 Lighting Sub-Division technique can be extended so that aberration may be taken into consideration. By including aberration, the operator can determine which portion of illumination shape combines with aberration. A coupling amount relates to the sensitivity of the image strength to aberration directly. By understanding this combination, illumination shape may be able to be changed so that the aberration sensitivity of a design may be stopped to the minimum.

[0066]The projection pupil K about the Scala image formation (alpha, beta) contains the exponential function of the wave front with which it is expressed by an obliquity factor, being out-of-focus, and the Zernike polynomials. This Scala image formation pupil is shown in the formula 18. This pupil can be further divided into two portions. That is, it is non-deviating pupil K_0 (alpha, beta) and a deviation pupil (exponential function of a wave front), and as shown [both] in the formula 19, the multiplication of these two portions is carried out.

$$K(\alpha,\beta)=\underbrace{\left[\frac{1-(\alpha^2+\beta^2)/M^2}{1-(\alpha^2+\beta^2)}\right]^{1/4}}_{obliquity-factor}\underbrace{exp\left[-i\frac{2\pi}{\lambda}z\sqrt{1-\alpha^2-\beta^2}\right]}_{defocus}\underbrace{exp\left[-i\frac{2\pi}{\lambda}W(\alpha,\beta)\right]}_{aberrations}$$

式(18)

$$K(\alpha,\beta)=\underbrace{K_0(\alpha,\beta)}_{unaberrated}\underbrace{\exp\left[-i\frac{2\pi}{\lambda}W(\alpha,\beta)\right]}_{aberrations}$$

式(19)

ここで、

$$K_0(\alpha,\beta)=\underbrace{\left[\frac{1-(\alpha^2+\beta^2)/M^2}{1-(\alpha^2+\beta^2)}\right]^{1/4}}_{obliquity-factor}\underbrace{\exp\left[-i\frac{2\pi}{\lambda}z\sqrt{1-\alpha^2-\beta^2}\right]}_{defocus}$$

式(20)

$$W(\alpha,\beta)=\sum_{\nu=5}^{37}Z_\nu R_\nu(\alpha,\beta)$$

式(21)

$$e^x=1+x+\frac{x^2}{2!}+\frac{x^3}{3!}+\ldots\cong 1+x$$

式(22)

[0067]From the formula 22, a wave front can be written as linear approximation. This is shown in the formula 23. By substituting the formula 23 for the formula 22, the linear approximation about the projection pupil K (alpha, beta) is computable by the formula 24.

$$\exp\left[-i\frac{2\pi}{\lambda}W(\alpha,\beta)\right]\cong 1-i\frac{2\pi}{\lambda}W(\alpha,\beta)=1-i\frac{2\pi}{\lambda}\sum_{\nu=5}^{37}Z_\nu R_\nu(\alpha,\beta)$$

式(23)

$$K(\alpha,\beta)\cong K_0(\alpha,\beta)\left[1-i\frac{2\pi}{\lambda}\sum_{\nu=5}^{37}Z_\nu R_\nu(\alpha,\beta)\right]$$

式(24)

[0068]Since TCC is a function of the projection pupil K (alpha, beta), the linear approximation to the pupil in the formula 24 shows that it is possible to express TCC by linear approximation. This is attained by substituting the formula 24 for the formula 1. The formula 25 is obtained by this. By stating two or more and the clause of ** being disregarded again, TCC of the formula 25 can be simplified, as shown in the formula 26.

[0069]The wave front W (alpha, beta) is shown by the sum of a Zernike striped polynomial in most cases, as shown in the formula 21. Deployment of Taylor series can express index e^x using the linearity theory of aberration. Deployment of Taylor series is effective about small x, and by former research, when Z_V is less than 0.04 lambda, coincidence good about an aerial image is shown.

Deployment of the Taylor series about e^x is shown in the formula 22. Although it stated two or more and the clause of ** is omitted in the formula 22, this is effective when Z_V is less than 0.04 (it is 0.04^2=0.0016 and can ignore).

$$TCC(m,n,p,q) \cong \iint_{\sqrt{\alpha^2+\beta^2}<\sigma} J_s(\alpha,\beta)K_0\left(\alpha+\frac{m\lambda}{P_xNA},\beta+\frac{n\lambda}{P_yNA}\right)\left[1-i\frac{2\pi}{\lambda}\sum_{v=5}^{37}Z_vR_v\left(\alpha+\frac{m\lambda}{P_xNA},\beta+\frac{n\lambda}{P_yNA}\right)\right]$$

$$\cdot K_0^*\left(\alpha-\frac{p\lambda}{P_xNA},\beta-\frac{q\lambda}{P_yNA}\right)\left[1+i\frac{2\pi}{\lambda}\sum_{v=5}^{37}Z_vR_v\left(\alpha-\frac{p\lambda}{P_xNA},\beta-\frac{q\lambda}{P_yNA}\right)\right]d\alpha d\beta \quad \text{式(25)}$$

$$TCC(m,n,p,q) \cong \iint_{\sqrt{\alpha^2+\beta^2}<\sigma} J_s(\alpha,\beta)K_0\left(\alpha+\frac{m\lambda}{P_xNA},\beta+\frac{n\lambda}{P_yNA}\right)K_0^*\left(\alpha-\frac{p\lambda}{P_xNA},\beta-\frac{q\lambda}{P_yNA}\right)$$

$$\cdot\left[1-i\frac{2\pi}{\lambda}\sum_{v=5}^{37}Z_vR_v\left(\alpha+\frac{m\lambda}{P_xNA},\beta+\frac{n\lambda}{P_yNA}\right)+i\frac{2\pi}{\lambda}\sum_{v=5}^{37}Z_vR_v\left(\alpha-\frac{p\lambda}{P_xNA},\beta-\frac{q\lambda}{P_yNA}\right)\right]d\alpha d\beta \quad \text{式(26)}$$

[0070]As shown in the formula 29, the linear function of TCC_0 and TCC_v can express TCC by specifying un-deviating TCC of the formulas 27 and 28, TCC_0 (m, n, p, q) and the deviation TCC, and TCC_v (m, n, p, q), respectively.

$$TCC_0(m,n,p,q) = \iint_{\sqrt{\alpha^2+\beta^2}<\sigma} J_s(\alpha,\beta)K_0\left(\alpha+\frac{m\lambda}{P_xNA},\beta+\frac{n\lambda}{P_yNA}\right)K_0^*\left(\alpha-\frac{p\lambda}{P_xNA},\beta-\frac{q\lambda}{P_yNA}\right)d\alpha d\beta \quad \text{式(27)}$$

$$TCC_v(m,n,p,q) = -i\frac{2\pi}{\lambda}\iint_{\sqrt{\alpha^2+\beta^2}<\sigma} J_s(\alpha,\beta)K_0\left(\alpha+\frac{m\lambda}{P_xNA},\beta+\frac{n\lambda}{P_yNA}\right) \quad \text{式(28)}$$

$$TCC(m,n,p,q) \cong TCC_0(m,n,p,q)+\sum_{v=5}^{37}Z_v\left[TCC_v(m,n,p,q)+TCC_v^*(-p,-q,-m,-n)\right] \quad \text{式(29)}$$

[0071]Since TCC can be built as linear approximation as shown in the formula 29, J_{opt} can also be written as linear approximation. The linear approximation to J_{opt} is following the methodology about the linear approximation of TCC which described the outline in the formulas 18 and 29 using the formula 8 about J_{opt}, and is called for in the formula 30.

$$J_{opt}(\alpha,\beta,m,n,p,q) \cong J_s(\alpha,\beta)T(m,n)T^*(-p,-q)K_0\left(\alpha+\frac{m\lambda}{P_xNA},\beta+\frac{n\lambda}{P_yNA}\right)K_0^*\left(\alpha-\frac{p\lambda}{P_xNA},\beta-\frac{q\lambda}{P_yNA}\right)$$

$$\cdot\left[1-i\frac{2\pi}{\lambda}\sum_{v=5}^{37}Z_vR_v\left(\alpha+\frac{m\lambda}{P_xNA},\beta+\frac{n\lambda}{P_yNA}\right)+i\frac{2\pi}{\lambda}\sum_{v=5}^{37}Z_vR_v\left(\alpha-\frac{p\lambda}{P_xNA},\beta-\frac{q\lambda}{P_yNA}\right)\right]d\alpha d\beta \quad \text{式(30)}$$

[0072]Subsequently, the formula 30 about J_{opt} can be divided into the sum of non-deviating J_{opt0} and deviation J_{optv} as shown in the formula 33. The definition of J_{opt0} and J_{optv} is shown in the formulas 31 and 32, respectively.

$$J_{opt0}(\alpha,\beta,m,n,p,q)=J_s(\alpha,\beta)K_0\left(\alpha+\frac{m\lambda}{P_xNA},\beta+\frac{n\lambda}{P_yNA}\right)K_0^*\left(\alpha-\frac{p\lambda}{P_xNA},\beta-\frac{q\lambda}{P_yNA}\right)$$

式(31)

$$J_{optv}(\alpha,\beta,m,n,p,q)=-i\frac{2\pi}{\lambda}J_s(\alpha,\beta)K_0\left(\alpha+\frac{m\lambda}{P_xNA},\beta+\frac{n\lambda}{P_yNA}\right)$$

$$\cdot K_0^*\left(\alpha-\frac{p\lambda}{P_xNA},\beta-\frac{q\lambda}{P_yNA}\right)R_v\left(\alpha+\frac{m\lambda}{P_xNA},\beta+\frac{n\lambda}{P_yNA}\right)$$

式(32)

[0073]The formula 32 describes the portion of the illumination shape combined with specific aberration. A coupling amount affects image strength and is useful for an understanding of the sensitivity of the aberration over Lighting Sub-Division. By combining the formulas 31 and 32, J_{opt} can be written as linear approximation.

$$J_{opt}(\alpha,\beta,m,n,p,q)\equiv J_{opt0}(\alpha,\beta,m,n,p,q)+\sum_{v=5}^{37}Z_v\left[J_{optv}(\alpha,\beta,m,n,p,q)+J_{optv}^*(\alpha,\beta,-p,-q,-m,-n)\right]$$

式(33)

[0074]In another mode of this invention, the response to the specific metrics which introduce a weighting factor, for example, contain the depth of focus (DOF), a picture log inclination (ILS), a picture inclination (IS), or aberration sensitivity can be maximized or minimized. As shown in the formula 34, optimal J_{tot} of the formula 15 can be changed so that these weighting factors may be included.

$$J_{tot}(\alpha,\beta)=\sum_m\sum_n\sum_p\sum_q w(\alpha,\beta,m,n,p,q)J_{opt}(\alpha,\beta,m,n,p,q)$$

式(34)

[0075]Generally, photoresist reacts in proportion to the logarithm of the luminous intensity which enters into it. A feature is printed in a resist with higher fidelity as the logarithm of intensity, therefore intensity increases (that is, a resist profile improves and a process window improves). Therefore, it is desirable to make strong logarithmic change (ILS) into the maximum. ILS is defined as the formula 35.

$$ILS\propto\frac{\partial\ln I}{\partial x}=\frac{1}{I}\frac{\partial I}{\partial x}$$

式(35)

[0076]The formula 35 increases further because a strong differential coefficient increases a strong differential coefficient since change is quicker than a strong reciprocal. Intensity can be computed from the formula 3 and the differential coefficient of the intensity to x is defined in the formula 36. By the differential coefficient to x, as shown in the formula 37, weighting function w_x is obtained. Similarly, as shown in the formula 38, weighting function w_y to y can be defined.

$$\frac{\partial I(x,y)}{\partial x}=\sum_m\sum_n\sum_p\sum_q i\frac{2\pi}{P_x}(m+p)e^{ix\left[\frac{2\pi}{P_x}(m+p)\right]}e^{iy\left[\frac{2\pi}{P_y}(n+q)\right]}DOCC(m,n,p,q)$$

$$=\sum_m\sum_n\sum_p\sum_q w_x(m,p)e^{ix\left[\frac{2\pi}{P_x}(m+p)\right]}e^{iy\left[\frac{2\pi}{P_y}(n+q)\right]}DOCC(m,n,p,q)$$

式(36)

$$w_x=i\frac{2\pi}{P_x}(m+p)$$

式(37)

$$w_y=i\frac{2\pi}{P_y}(n+q)$$

式(38)

[0077]Since a pattern feature and an intensity feature are two dimensions, change of the intensity to a position can be shown using the norm of an inclination. The norm of an intensity inclination is defined as the formula 39. By this, we can define the weighting function for computing J_{tot} in the formula 34. The formula 40 defines the weighting function for maximizing a picture log inclination.

$$\|\nabla I\| \Rightarrow w_{NILS} = \sqrt{|w_x|^2 + |w_y|^2} \qquad \text{式(39)}$$

$$w_{ILS}(m,n,p,q) = 2\pi\sqrt{\left(\frac{m+p}{P_x}\right)^2 + \left(\frac{n+q}{P_y}\right)^2} \qquad \text{式(40)}$$

[0078]The formula 40 shows that a weighting function is set to 0, when it is m+p=0 and n+q=0. When it is m+p=0 and n+q=0, these orders do not contribute to image modulation at all, but reflect DC contribution to a picture. w_{ILS} increases as m+p and n+q increase. The weighting of the diffraction order clause of an order with this higher is carried out more greatly, and it shows that the contribution to ILS becomes large.

[0079]If in addition to maximization of ILS ILS is improved and the intensity reaction to a focus is suppressed to the minimum, the depth of focus of a process will become large. A focus is explained by the pupil K (alpha, beta). Although the pupil K (alpha, beta) is shown in the formula 41, the focus is indicated to be z here. The formula 41 can be divided into the 2nd clause. That is, as shown in the formula 42, it is a clause (un-out-of-focus clause) which is independently from the clause (out-of-focus clause) and z depending on z.

$$K(\alpha,\beta) = \underbrace{\left[\frac{1-(\alpha^2+\beta^2)/M^2}{1-(\alpha^2+\beta^2)}\right]^{1/4}}_{\text{obliquity-factor}} \underbrace{exp\left[-i\frac{2\pi}{\lambda}z\sqrt{1-\alpha^2-\beta^2}\right]}_{\text{defocus}} \underbrace{exp\left[-i\frac{2\pi}{\lambda}W(\alpha,\beta)\right]}_{\text{aberrations}} \qquad \text{式(41)}$$

$$K(\alpha,\beta) = \underbrace{K_{nd}(\alpha,\beta)}_{\text{non-defocused}} \underbrace{\exp\left[-i\frac{2\pi}{\lambda}z\sqrt{1-\alpha^2-\beta^2}\right]}_{\text{defocus}} = K_{nd}(\alpha,\beta)K_d(\alpha,\beta) \qquad \text{式(42)}$$

[0080]By setting the differential coefficient of the intensity to z as zero, change of the intensity by the focus z can be suppressed to the minimum. The formula 42 can be substituted for the formulas 1 thru/or 3, and as shown in the formula 43, the cost function f (alpha, beta, z) can be defined. This is a cost function of the intensity image formation clause depending on z.

$$f(\alpha,\beta,z) = K_d\left(\alpha+\frac{m\lambda}{P_xNA},\beta+\frac{n\lambda}{P_yNA}\right)K_d^*\left(\alpha-\frac{p\lambda}{P_xNA},\beta-\frac{q\lambda}{P_yNA}\right) \qquad \text{式(43)}$$

[0081]On the other hand, as for the cost function f (alpha, beta, z), g (alpha, beta, m, n, p, q) is stopped to the minimum, when equal to zero (see the following formulas 44). In the formula 44, since the differential coefficient to z is equal to zero only when the clause of a size is equal to zero, the phase term is removed. When g (alpha, beta, m, n, p, q) is zero, sensitivity [as opposed to a focus in the field (alpha, beta) of the pupil about a given order (m, n, p, q)] is the minimum. These are the most desirable fields of a pupil for building illumination shape. Weighting function w_{focus} (alpha, beta, m, n, p, q) is defined as the formula 45. This weighting function has the sensitivity equal to 1 to a focus in the minimum field, and its sensitivity to a focus is equal to 0 in the No.1 field. Subsequently, by the formula 46, the new weighting function which maximizes ILS through an omnifocal lens can be defined, and illumination shape can be changed using this.

$$g(\alpha,\beta,n,n,p,q)=\frac{\partial}{\partial z}f(\alpha,\beta,z)$$

$$=\left[-i\frac{2\pi}{\lambda}\sqrt{1-\left(\alpha+\frac{m\lambda}{P_xNA}\right)^2-\left(\beta+\frac{n\lambda}{P_yNA}\right)^2}+i\frac{2\pi}{\lambda}\sqrt{1-\left(\alpha-\frac{p\lambda}{P_xNA}\right)^2-\left(\beta-\frac{q\lambda}{P_yNA}\right)^2}\right]$$

式(44)

$$w_{focus}(\alpha,\beta,m,n,p,q)=1-|g(\alpha,\beta,m,n,p,q)|$$

式(45)

$$w(\alpha,\beta,m,n,p,q)=w_{ILS}(m,n,p,q)w_{focus}(\alpha,\beta,m,n,p,q)$$

式(46)

[0082]According to above-mentioned methodology, strong sensitivity can be stopped to the influence of focal, and aberration to the minimum. Since the influence of focal on intensity is suppressed to the minimum, the influence of strong can be suppressed to specific aberration to the minimum. This is desirable about a certain pattern in which high sensitivity is proved to specific aberration. The projection pupil in the formula 19 can be written as non-deviating clause K_0 (alpha, beta) which carried out multiplication by deviation clause K_a (alpha, beta), as shown in the formula 47.

$$K(\alpha,\beta)=K_0(\alpha,\beta)K_a(\alpha,\beta)$$ 式(47)

[0083]The sensitivity of the intensity to specific aberration Z_i can be stopped by setting the differential coefficient of the intensity to Z_i as zero to the minimum. The formula 47 is substituted for the formulas 1 thru/or 3, and by taking a strong differential coefficient, h (alpha, beta, m, n, p, q) in the formula 48 stops aberration sensitivity to the minimum, when equal to zero.

$$\frac{\partial}{\partial Z_i}I(x,y)=0\Rightarrow$$

$$h(\alpha,\beta,m,n,p,q)=K_a\left(\alpha+\frac{m\lambda}{P_xNA},\beta+\frac{n\lambda}{P_yNA}\right)\frac{\partial}{\partial Z_i}K_a^*\left(\alpha-\frac{p\lambda}{P_xNA},\beta-\frac{q\lambda}{P_yNA}\right)$$

$$+\frac{\partial}{\partial Z_i}K_a\left(\alpha+\frac{m\lambda}{P_xNA},\beta+\frac{n\lambda}{P_yNA}\right)K_a^*\left(\alpha-\frac{p\lambda}{P_xNA},\beta-\frac{q\lambda}{P_yNA}\right)=0$$ 式(48)

$$h(\alpha,\beta,m,n,p,q)=\left[R_i\left(\alpha-\frac{p\lambda}{P_xNA},\beta-\frac{q\lambda}{P_yNA}\right)-R_i\left(\alpha+\frac{m\lambda}{P_xNA},\beta+\frac{n\lambda}{P_yNA}\right)\right]=0$$ 式(49)

[0084]It simplifies like the formula 49 and the formula 48 can also be written. In the formula 50, weighting function w_{ab} (alpha, beta, m, n, p, q) is defined, this has sensitivity equal to 1 in the field (alpha, beta) of the minimum pupil to Z_i, and sensitivity is equal to 0 in the No.1 field to Z_i.

$$w_{ab}(\alpha,\beta,m,n,p,q)=1-\frac{1}{2}|h(\alpha,\beta,m,n,p,q)|$$ 式(50)

[0085]Subsequently, in the formula 51, the weighting function which stops the ILS sensitivity to specific aberration Z_i to the minimum can be defined. The ILS sensitivity to specific aberration Z_i can be held down to the formula 52 to the minimum, and the weighting function which maximizes ILS through an omnifocal lens can also be defined as it. The lighting system which has the optimal response to given metrics can be computed by the ability to substitute all of these formulas for the formula 34.

$$w(\alpha,\beta,m,n,p,q)=w_{NILS}(m,n,p,q)w_{ab}(\alpha,\beta,m,n,p,q)$$ 式(51)

$$w(\alpha,\beta,m,n,p,q)=w_{NILS}(m,n,p,q)w_{focus}(\alpha,\beta,m,n,p,q)w_{ab}(\alpha,\beta,m,n,p,q)$$ 式(52)

[0086]Drawing 15 is a schematic view of one example of the lithography device used according to this invention. This equipment contains a radiation system. A radiation system comprises lamp LA (this should just be taken, for example as an excimer laser), and a lighting system. A lighting system can be provided with beam shaping optical system EX, the integrator IN, and condenser CO, for example. A radiation system supplies the projection beam PB of radiation. For example, the radiation system can supply ultraviolet

rays, deep ultraviolet, or extreme-ultraviolet radiation. Generally the radiation system can also supply radiation of soft X ray or other forms.

[0087]The 1st object table or mask table MT holds mask MA. Mask MA contains pattern space C containing the mask pattern for image formation. Since mask table MT is movable to the projection beam PB, it can be irradiated with the portion from which a mask differs. In order to judge whether alignment of the mask is appropriately carried out to the substrate or the wafer W, alignment mask M_1 and M_2 are used.

[0088]Projection system PL projects the projection beam PB on the wafer W. As for the wafer W, including two alignment mask P_1 and P_2, before these start image formation, alignment of them is carried out to mask M_1 and M_2. The wafer W is supported by board table WT, and in order to expose the portion from which the wafer W differs, it can move this table WT to a projection beam. Thus, image formation of the mask pattern C can be carried out on the target part c from which the wafer W differs. In order to make it wafer table WT be certainly in a right location to the position of mask table MT, interference position monitor IF is used.

[0089]Although it related and this invention has been explained to a specific embodiment, this invention is not necessarily limited to the indicated embodiment, and meaning so that various modification and the equal composition which are included in Claims may be included conversely will be understood.

[Translation done.]

DESCRIPTION OF DRAWINGS

[Brief Description of the Drawings]
[Drawing 1]It is a figure of the mutual transmission coefficient function for the accepted image forming system.
[Drawing 2]It is one example of the mask feature by the micro lithography of a brick-wall separation pattern.
[Drawing 3]It is a figure of the diffraction order of the mask feature of drawing 2.
[Drawing 4]It is the map of 4-dimensional optimization illumination shape in which it was computed for the mask feature of drawing 2.
[Drawing 5]It is the initial gray-scale illumination shape (J_{tot}) by which it was computed for the mask feature of drawing 2.
[Drawing 6]It is binary expression of the illumination shape of drawing 5.
[Drawing 7]Analysis of the printed matter of the mask feature of drawing 2 printed with annular illumination shape is shown.
[Drawing 8]Analysis of the printed matter of the mask feature of drawing 2 printed with the optimized ellipse illumination shape is shown.
[Drawing 9]It is the map of 4-dimensional optimization illumination shape in which it was computed for the mask feature of drawing 2 reduced to a 110-nm design basis.
[Drawing 10]It is the initial gray-scale illumination shape by which it was computed for the mask feature of drawing 2 reduced to a 110-nm design basis.
[Drawing 11 a] It is binary expression of the illumination shape of drawing 10 with which the values of sigma differ.
[Drawing 11 b] It is binary expression of the illumination shape of drawing 10 with which the values of sigma differ.
[Drawing 12]It is one example of the mask pattern in which the critical gate and the cell were shown.
[Drawing 13]In order to reduce the pitch number of a pattern, it is a mask pattern of drawing 12 which added the auxiliary feature.
[Drawing 14]The frequency function of the spatial width of drawing 12 and the mask pattern of 13 is compared.
[Drawing 15]It is a schematic view of the equipment for a micro photolithography.

[Translation done.]

* NOTICES *

JPO and INPIT are not responsible for any
damages caused by the use of this translation.

1.This document has been translated by computer. So the translation may not reflect the original precisely.
2.**** shows the word which can not be translated.
3.In the drawings, any words are not translated.

DRAWINGS

[Drawing 1]

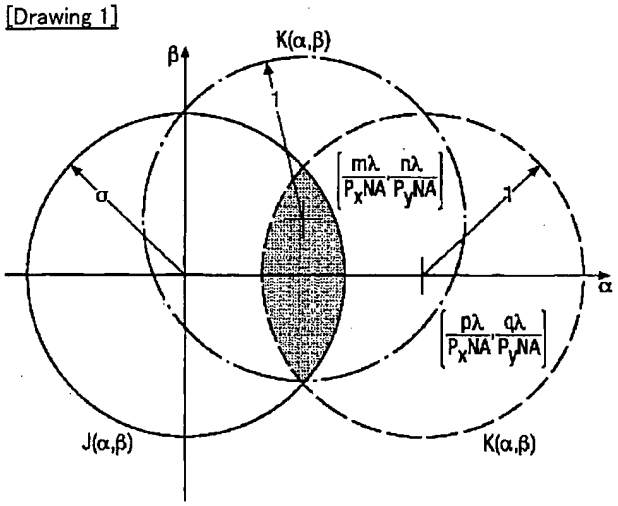

[Drawing 2]

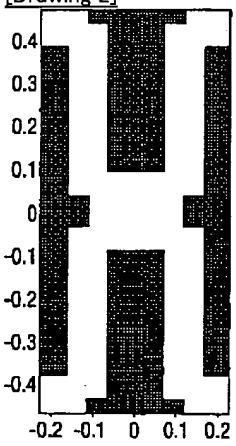

[Drawing 3]

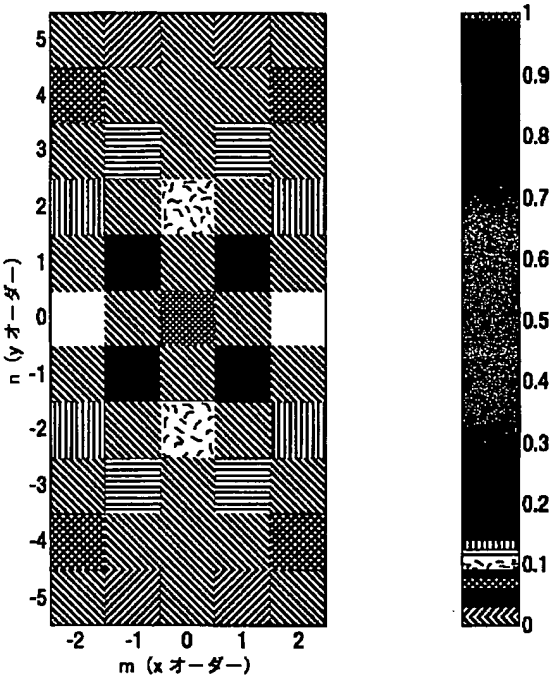

[Drawing 5]

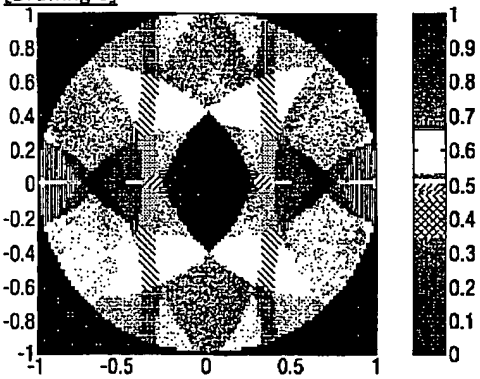

[Drawing 6]

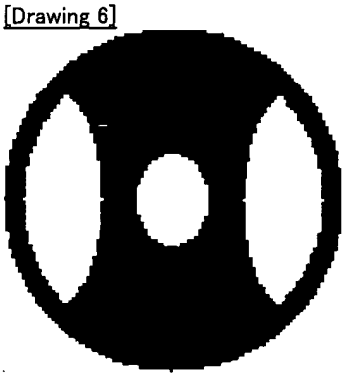

[Drawing 10]

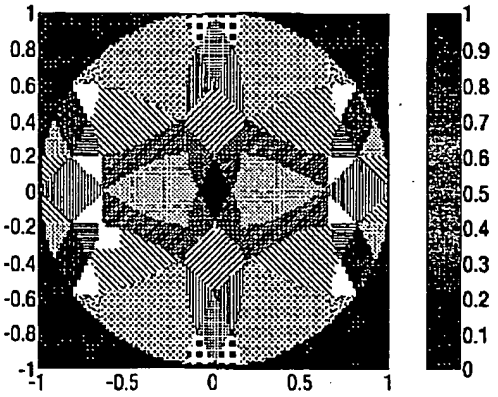

[Drawing 11 a]

[Drawing 11 b]

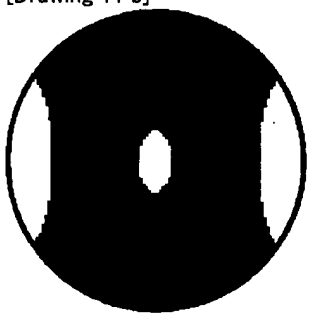

[Drawing 4]

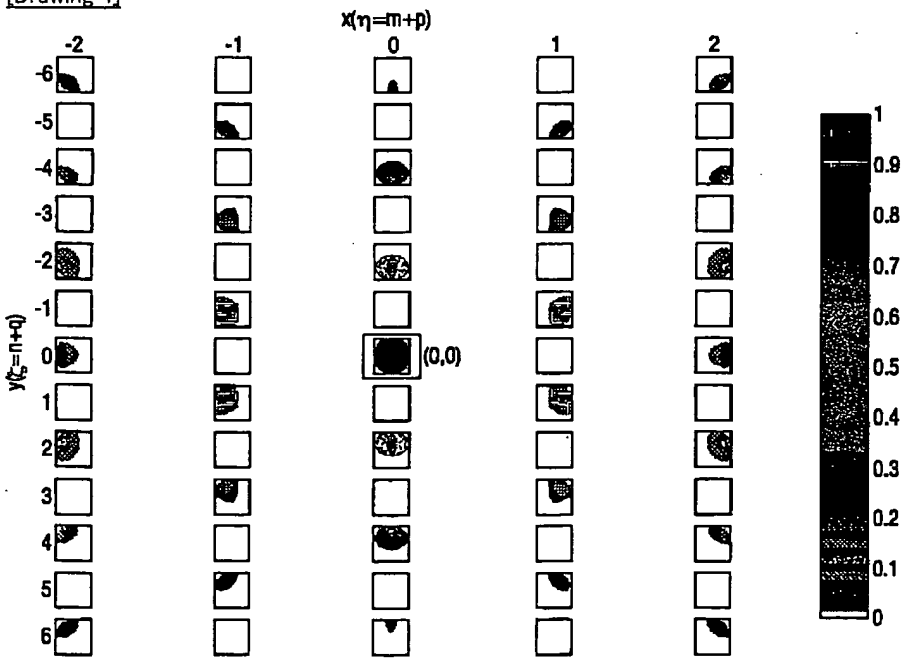

[Drawing 9]

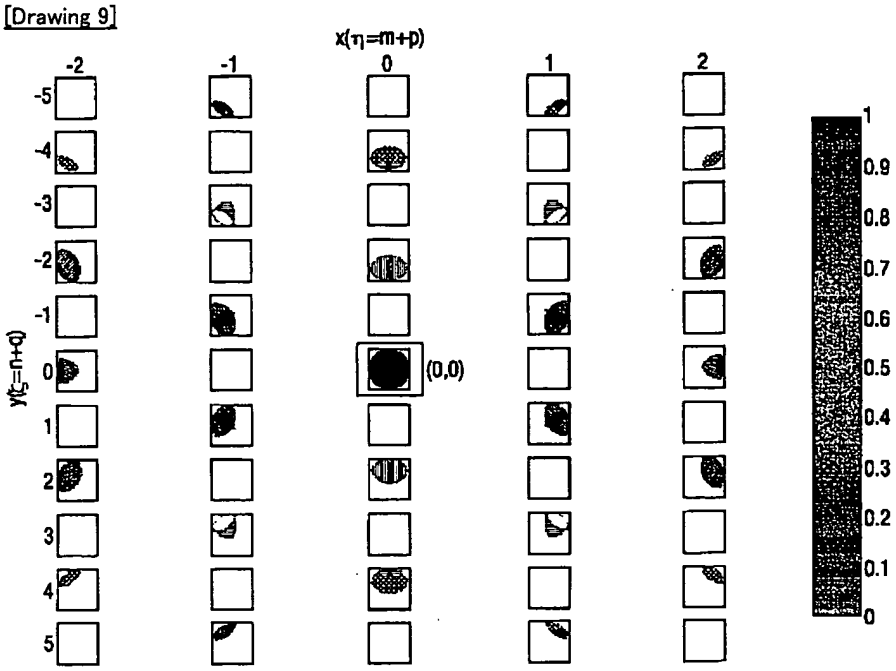

[Drawing 7]

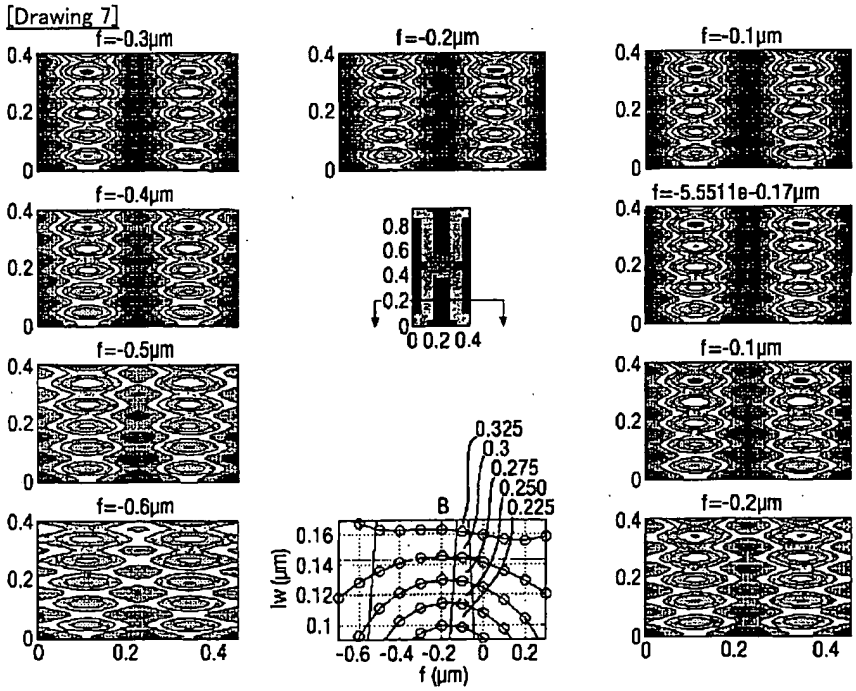

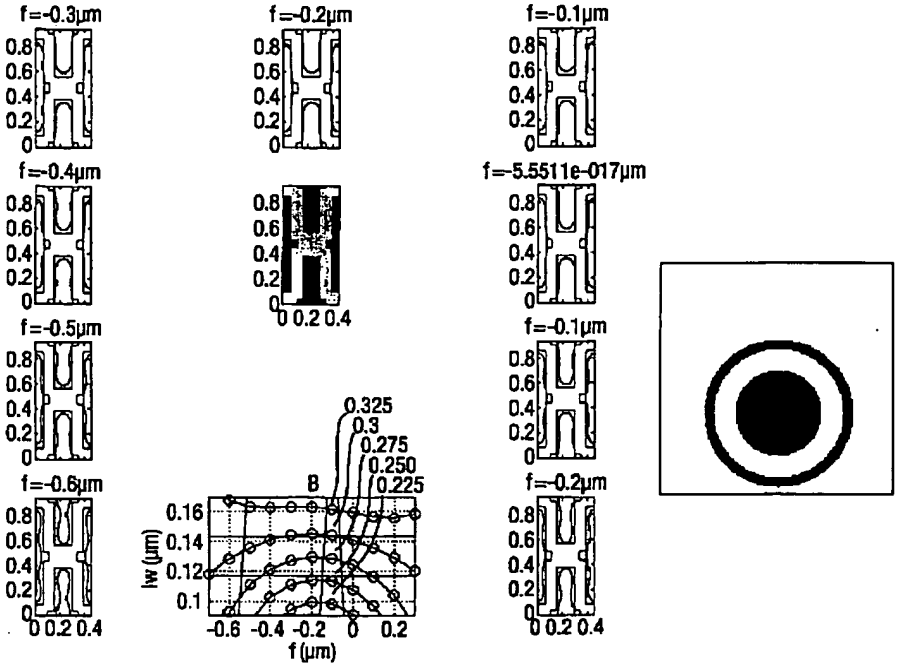
f=-0.3μm
f=-0.2μm
f=-0.1μm
f=-0.4μm
f=-5.5511e-017μm
f=-0.5μm
f=-0.1μm
f=-0.6μm
f=-0.2μm
0.325
0.3
0.275
0.250
0.225
B
lw (μm)
f (μm)

[Drawing 8]

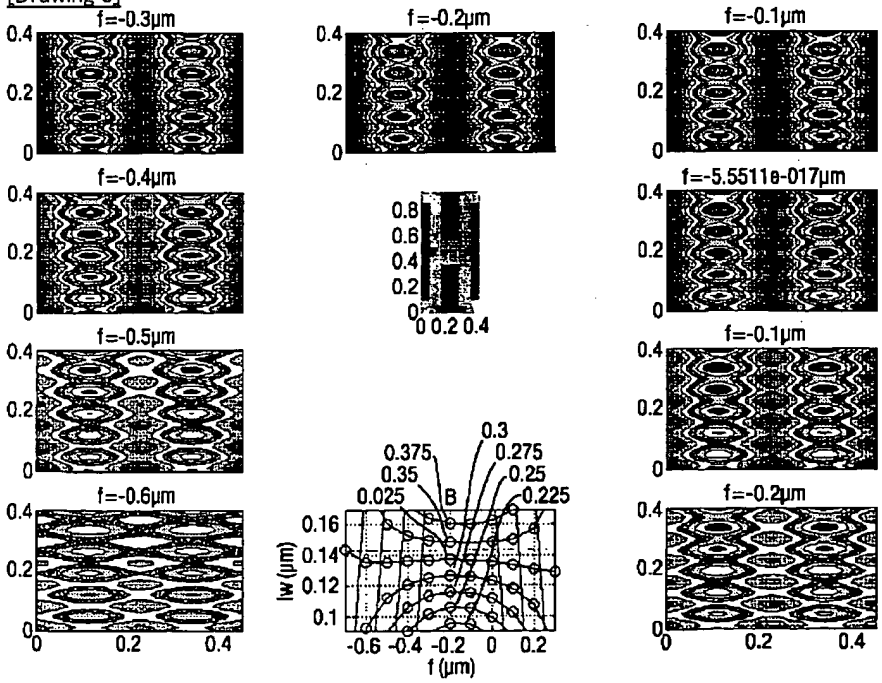
f=-0.3μm
f=-0.2μm
f=-0.1μm
f=-0.4μm
f=-5.5511e-017μm
f=-0.5μm
f=-0.1μm
f=-0.6μm
f=-0.2μm
0.375
0.35
0.025
0.3
0.275
0.25
0.225
B
lw (μm)
f (μm)

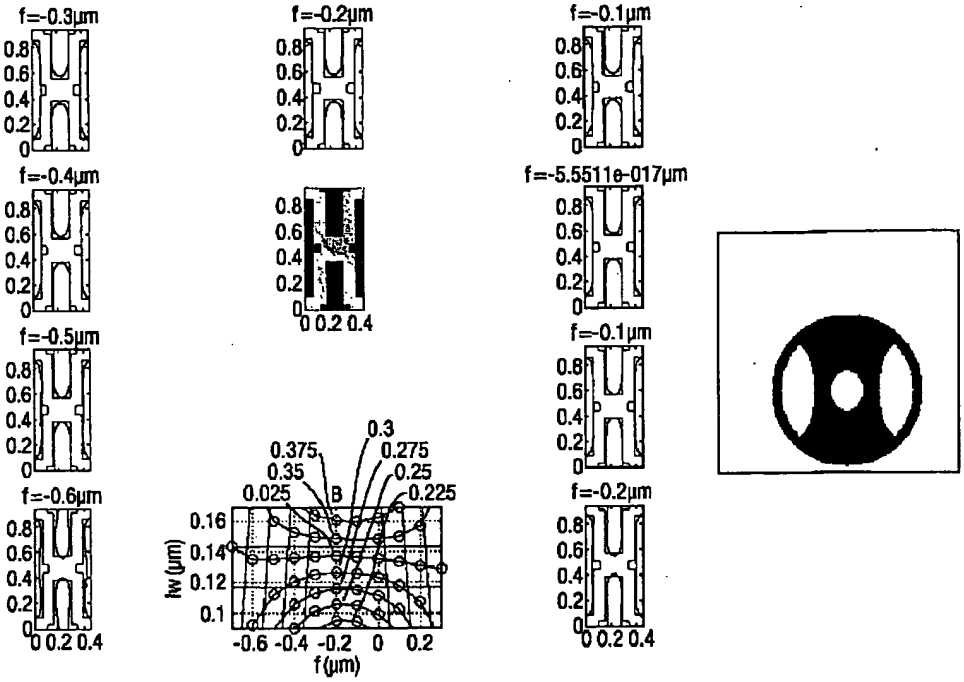

[Drawing 12]

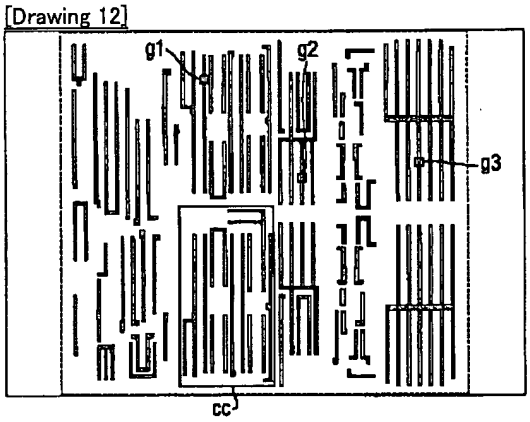

[Drawing 13]

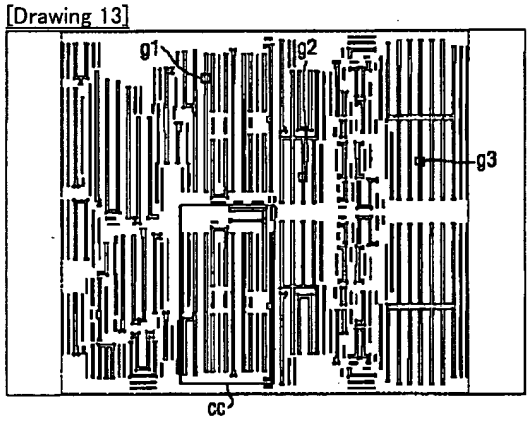

[Drawing 14]

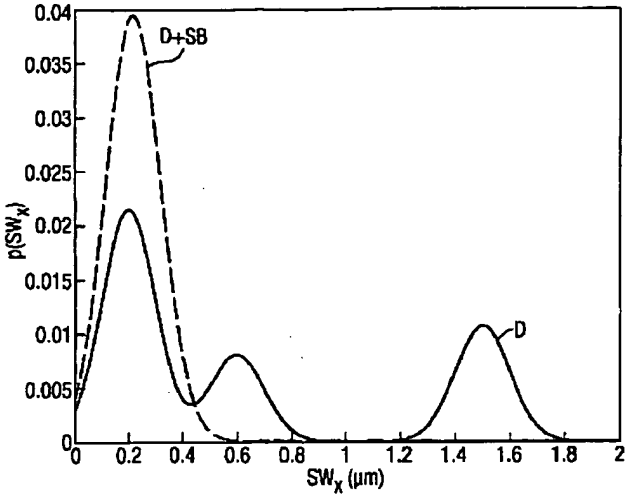

[Drawing 15]

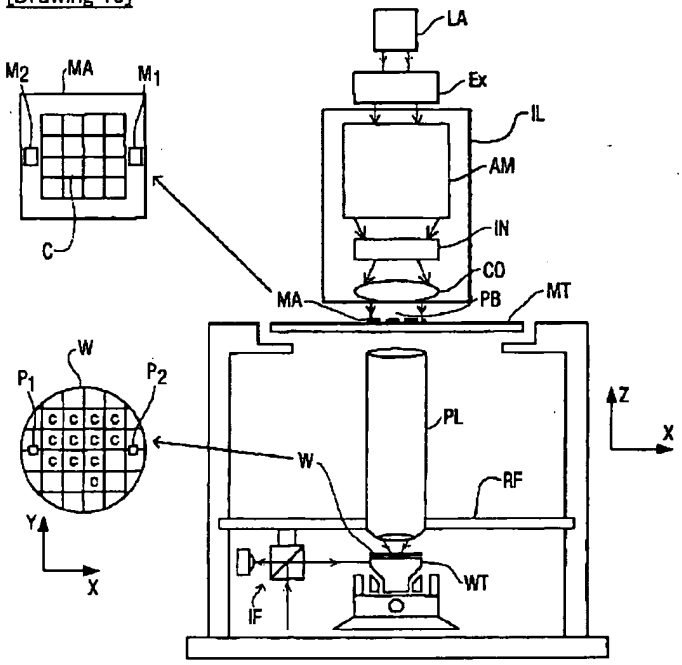

[Translation done.]

(19)日本国特許庁（ＪＰ）　(12)公開特許公報（A）　(11)特許出願公開番号
特開2002－334836
（P2002－334836A）
(43)公開日　平成14年11月22日(2002.11.22)

(51)Int.Cl.'	識別記号	ＦＩ		テーマコード'(参考)
Ｈ０１Ｌ　21/027		Ｇ０３Ｆ　7/20	５２１	５Ｆ０４６
Ｇ０３Ｆ　7/20	５２１	Ｈ０１Ｌ　21/30	５２７	
			５０２Ｇ	

審査請求　未請求　請求項の数16　ＯＬ　外国語出願　（全 72 頁）

(21)出願番号　特願2002－97334(P2002－97334)

(22)出願日　平成14年２月22日(2002.2.22)

(31)優先権主張番号　２７１３０５

(32)優先日　平成13年２月23日(2001.2.23)

(33)優先権主張国　米国（ＵＳ）

(71)出願人　502010332
エイエスエムエル　ネザランドズ　ベスローテン　フエンノートシャップ
オランダ国　フェルトホーフェン、　デルン　1110

(72)発明者　ロバート　ジョン　ソカ
アメリカ合衆国　カリフォルニア、キャンベル、　モンテ　ヴィラ　コート　137

(74)代理人　100066692
弁理士　浅村　皓　（外３名）

Ｆターム(参考)　5F046 BA04 CB17 CB23 DA30 DB05

(54)【発明の名称】　特定のマスク・パターンのための照明の最適化

(57)【要約】
【課題】　選択したパターニング手段のパターンのための照明プロファイルを最適化する方法および装置を提供する。
【解決手段】　マイクロリソグラフィのための方法および装置。この方法および装置は、特定のマスク・パターンの特徴に基づいて照明モードを最適化することを含む。照明は、レチクルの回折オーダーに基づいて適切な照明モードを決定すること、および投影光学系の自己相関によって、最適化される。変調に何の影響ももたない照明パターンの部分を除去することで、余分なＤＣ光を減じることができ、これによって焦点深度を改善する。マスク・パターンの最適化には、サブレゾルーションのフィーチャを追加してピッチを減らし、空間幅の確率密度関数を打ち切ることが含まれる。

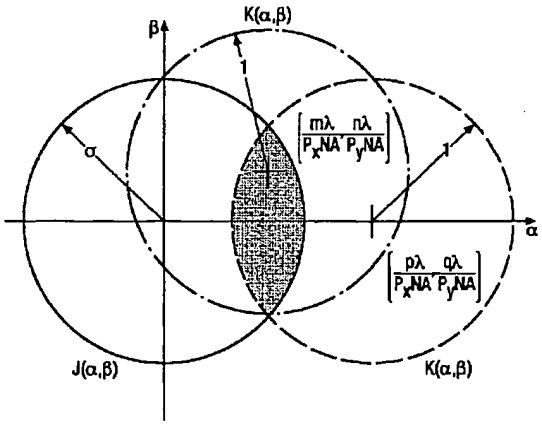

【特許請求の範囲】

【請求項１】　選択したパターニング手段のパターンのための照明プロファイルを最適化する方法であって：照明装置および前記選択したパターニング手段のパターンを含む光学システムのための相互透過係数関数を規定するステップと；前記選択したパターンに基づいて回折オーダーの結像に対する相対的な関連性を求めるステップと；前記相互透過係数から最適化した照明形状を算出し、前記回折オーダーの結像に対する前記相対的な関連性に基づいて前記照明形状の領域に重み付けを行うステップと；を備える照明プロファイルを最適化する方法。

【請求項２】　前記回折オーダーの結像に対する相対的な関連性を求めるステップは、更に、前記選択したマスク・パターンの特徴的なピッチを求めるステップを備える請求項１に記載された方法。

【請求項３】　更に、前記特徴的なピッチを求めることに先立って、前記選択したパターンのクリティカルな領域を識別するステップを備え、前記選択したパターンの前記特徴的なピッチを求めることは、前記クリティカルな領域の前記特徴的なピッチを求めることによって行われる請求項２に記載された方法。

【請求項４】　前記クリティカルな領域を識別するステップは、更に、複数のクリティカルな領域を識別することを含み、前記クリティカルな領域の前記特徴的なピッチを求めることは：識別した各クリティカル領域のピッチを比較することと；前記識別した各クリティカル領域のピッチがほぼ等しい場合、前記クリティカル領域の前記特徴的なピッチを、前記識別した領域のうち１つの前記特徴的なピッチに等しいと判定することと；を含む請求項３に記載された方法。

【請求項５】　更に、焦点深度、ライン端部、画像ログ傾斜（ＩＬＳ）、画像傾斜（ＩＳ）、および収差感度から成る群から選択した、選択された最適化測定基準に基づいて、前記照明装置形状の領域に重み付けを行うことを含む請求項１から４までのいずれか１項に記載された方法。

【請求項６】　複数のクリティカル領域を識別するステップと；前記識別したクリティカル領域の各々のピッチを求めるステップと；前記相互透過係数関数から最適化照明形状を算出し、各クリティカル領域ごとに回折オーダーの結像に対する関連性に基づいてオーダーに重み付けを行うステップと；をさらに備える請求項１または２に記載された方法。

【請求項７】　光近接補正技法によって前記マスク・パターンにおける異なるピッチの合計数を減らすことで、前記選択したパターンを変更するステップをさらに備える、請求項１から６までのいずれか１項に記載された方法。

【請求項８】　前記光近接補正技法によって前記選択したパターンを変更するステップは、更に、前記選択したマスク・パターンにサブレゾルーションのフィーチャを追加することを含む請求項７に記載された方法。

【請求項９】　前記選択したパターンを変更するステップおよび最適化照明形状を算出するステップを繰り返す請求項７に記載された方法。

【請求項１０】　照明プロフィールを最適化するためのコンピュータ・プログラムであって、コンピュータ・システム上で実行された場合、請求項１ないし９のいずれか１項の方法の前記ステップを実行するように前記コンピュータ・システムに命令することを意味するプログラム・コードを備えるコンピュータ・プログラム。

【請求項１１】　ディバイス製造方法であって：

（ａ）放射感知物質の層によって少なくとも部分的に被覆された基板を供給するステップと；

（ｂ）照明システムを用いて放射の投影ビームを供給するステップと；

（ｃ）パターニング手段を用いて前記投影ビームの断面にパターンを与えるステップと；

（ｄ）前記放射感知物質層の対象部分上に前記パターニングした放射ビームを投影するステップと；

を備え、請求項１ないし９のいずれか１項による方法を用いて、ステップ（ｄ）の前に、ステップ（ｂ）において生成した前記投影ビームにおける断面強度分布を、ステップ（ｃ）において用いる前記パターンに適合させるディバイス製造方法。

【請求項１２】　リソグラフィ投影装置であって：放射の投影ビームを供給するための照明システムと；パターニング手段を支持するための支持構造であって、前記パターニング手段が所望のパターンに従って前記投影ビームをパターニングするように機能する、支持構造と；基板を保持するための基板テーブルと；前記基板の対象部分上に前記パターニングしたビームを投影するための投影システムと；を備え、前記装置は、更に：前記照明装置および前記パターニング手段の相互透過係数関数を規定し、前記パターニング手段によって生成した前記パターンに基づいて回折オーダーの結像に対する相対的な関連性を求め、前記相互透過係数関数から最適化した照明形状を算出し、前記回折オーダーの結像に対する前記相対的な関連性に基づいて前記照明形状の領域に重み付けを行う、算出手段と；前記算出手段によって算出した前記照明形状に従って、前記照明システムから射出する前記投影ビームにおける断面強度分布を選択するための選択手段と；を備えるリソグラフィ投影装置。

【請求項１３】　選択したマスク設計を最適化する方法であって：前記選択したマスク設計のクリティカル・フィーチャを識別することと；前記クリティカル・フィーチャの回折オーダーに基づいて最適化した照明プロファイルを求めることと；前記選択したマスク・フィーチャに存在するピッチ数を減らすように選択した光近接補正技法を用いることによって前記選択したマスク設計を変

更することと；を備える選択したマスク設計を最適化する方法。

【請求項１４】　前記光近接補正は、更に、前記選択したマスク設計の空間幅の連続確率密度関数を変更するように選択されたサブレゾルーションのフィーチャを追加して、前記変更した確率密度関数が打ち切りを多く有するようにすることを含む請求項１１に記載された方法。

【請求項１５】　前記最適化した照明プロファイルを求めるステップは、請求項１ないし９のいずれか１項の方法の前記ステップを備える請求項１３または１４に記載された方法。

【請求項１６】　選択したマスク設計を最適化するためのコンピュータ・プログラムであって、コンピュータ上で実行された場合、請求項１３ないし１５のいずれか１項の方法を実行するように前記コンピュータに命令することを意味するプログラム・コードを備えるコンピュータ・プログラム。

【発明の詳細な説明】

【０００１】

【発明の属する技術分野】本発明は、一般に、マイクロリソグラフィ映像法のための方法および装置に関する。更に特定すれば、本発明は、結像している特定のパターンに従って照明の形状を最適化するための装置および方法に関する。

【０００２】

【従来の技術】集積回路および、プログラム可能ゲート・アレイ等の他の微細なフィーチャの製品の製造において、現在、光リソグラフィが用いられている。最も一般的な説明では、リソグラフィ装置は、放射の投影ビームを供給する照明システムと、パターニング手段を保持する支持構造と、基板を支持する基板テーブルと、パターニングしたビームを基板の対象部分上に結像するための投影システム（レンズ）とを含む。

【０００３】パターニング手段という用語は、基板の対象部分に生成されるパターンに対応して、パターニングした断面を入来する放射ビームに与えるために使用可能な装置および構造を指すものとして広く解釈するものとする。また、この文脈において、「光弁」という用語も用いられている。一般に、パターンは、集積回路または他の素子等、対象部分に生成している素子内の特定の機能層に対応する。

【０００４】かかる機構の一例はマスクであり、これは、通常、（可動）マスク・テーブルによって保持される。マスクの概念はリソグラフィにおいて周知であり、これは、２値、交番移相、減衰移相、および様々なハイブリッド・マスク・タイプ等のマスク・タイプを含む。かかるマスクを投影ビーム内に配置すると、マスクに入射する放射は、マスク上のパターンに従って、選択的に透過（透過型マスクの場合）または反射（反射型マスクの場合）する。マスク・テーブルは、入射する投影ビーム内の所望の位置にマスクを確実に保持することができ、更に、所望の場合にはビームに対してマスクを動かすことも確実に可能となる。

【０００５】かかる機構の別の例は、粘弾性制御層および反射面を含むマトリクス・アドレス可能面である。かかる装置の背後にある基本的な原理は、（例えば）反射面のアドレスされた領域が入射光を回折光として反射する一方、アドレスされていない領域が入射光を非回折光として反射することである。適切なフィルタを用いて、反射ビームから前記非回折光を除去し、回折光のみを残すことができる。このようにして、マトリクス・アドレス可能面のアドレッシング・パターンに従って、ビームをパターニングする。プログラム可能ミラー・アレイの代替的な実施形態では、マトリクスに配置した小さなミラーを用いる。適切な局所電界を印加することで、または圧電作動手段を用いることで、各ミラーは、軸を中心にそれぞれ傾けることができる。この場合も、ミラーはマトリクス・アドレス可能であり、アドレスされたミラーが、アドレスされていないミラーとは異なる方向に入来放射ビームを反射させるようになっている。このようにして、マトリクス・アドレス可能ミラーのアドレッシング・パターンに従って、反射ビームをパターニングする。必要なマトリクス・アドレッシングは、適切な電子手段を用いて行うことができる。上述の状況の双方において、パターニング手段は、１つ以上のプログラム可能ミラー・アレイから成るものとすることができる。ここで参照したミラー・アレイに関する更に詳しい情報は、例えば、米国特許第５，２９６，８９１号および第５，５２３，１９３号、およびＰＣＴ特許出願ＷＯ９８／３８５９７号およびＷＯ９８／３３０９６号から得ることができる。これらは、引用により本願にも含まれるものとする。プログラム可能ミラー・アレイの場合、前記支持構造は、フレームまたはテーブルとして具現化し、例えば、必要に応じて固定または可動とすることができる。

【０００６】別の例は、プログラム可能ＬＣＤアレイである。この場合、支持構造はやはり、例えばフレームまたはテーブルとすることができる。かかる構造の一例は、米国特許第５，２２９，８７２号に与えられている。これも引用により本願にも含まれるものとする。

【０００７】簡略化のために、この文書の以降の部分では、いくつかの箇所で、マスクを伴う例を特定して扱うことがある。しかしながら、かかる例で論じる一般的な原理は、上述のパターニング手段の更に広い文脈で理解するものとする。

【０００８】投影システムという用語は、様々なタイプの投影システムを包含する。素人の理解では、「レンズ」とは通常、屈折光学系を意味するが、ここでは、この用語は、例えばカトプトリック系およびカタディオプトリック系を含むように広義で用いる。また、照明シス

テムは、投影ビームを方向付け、整形し、または制御するためにこれらの原理のいずれかに従って動作する素子を含む場合があり、以下では、かかる素子のことも、まとめてまたは単独で「レンズ」と呼ぶことがある。

【０００９】加えて、「ウエハ・テーブル」という用語は、画像を受ける基板がシリコン・ウエハであることを暗に示すことなく用いることができ、リソグラフィ装置によって処理されるあらゆる基板を支持するのに適切なステージを示すことができる。

【００１０】リソグラフィ投影装置は、例えば、集積回路（ＩＣ）の製造において用いることができる。かかる場合、パターニング手段は、ＩＣの個々の層に対応した回路パターンを発生することができ、このパターンを、放射感知物質（レジスト）の層によって被覆されている基板（シリコン・ウエハ）上の対象の部分（１つ以上のダイから成る）上に結像することができる。一般に、単一のウエハは、投影システムによって一度に１つずつ連続的に照射された隣接する対象部分から成るネットワークを含む。マスク・テーブル上のマスクによるパターニングを用いた現在の装置では、２つの異なるタイプの機械を区別することができる。一方のタイプのリソグラフィ投影装置では、各対象部分を照射する際に、一度でマスク・パターン全体を対象部分上に露出する。かかる装置は、一般にウエハ・ステッパと呼ばれる。一般にステップ・アンド・スキャン装置と呼ばれる他方の装置では、各対象部分を照射する際に、投影ビーム下のマスク・パターンを所与の基準方向（「走査」方向）に徐々に走査し、これに同期して、この方向に対して平行または非平行に基板テーブルを走査する。一般に、投影システムはある倍率Ｍ（一般に＜１）を有するので、基板テーブルを走査する速度Ｖは、倍率Ｍに、マスク・テーブルを走査する速度を掛けたものである。ここで述べるリソグラフィ装置に関する更に詳しい情報は、例えば、米国特許第６，０４６，７９２号から得ることができる。この特許は、引用により本願にも含まれるものとする。

【００１１】リソグラフィ投影装置を用いた製造プロセスでは、放射感知物質（レジスト）の層によって少なくとも部分的に被覆された基板上に、（例えばマスク内の）パターンを結像する。この結像ステップに先立って、基板に対して、プライミング、レジスト被覆、およびソフトベーク等の様々な手順を施す場合がある。露光後、基板に対し、露光後ベーク（ＰＥＢ）、現像、ハードベーク、および結像したフィーチャの測定／検査等の他の手順を施す場合がある。この手順の配列は、例えばＩＣのような素子の個々の層をパターニングするための基礎として用いられる。かかるパターニングされた層は、次いで、エッチング、イオン注入（ドーピング）、メタライゼーション、酸化、化学機械的研磨等の様々なプロセスを経る場合がある。これらは全て、個々の層を完成させるためのものである。いくつかの層が必要である場合には、手順全体またはその変形を、新たな各層ごとに繰り返す必要がある。最終的に、基板（ウエハ）上には、素子のアレイが存在することになる。これらの素子は、次いで、ダイシングまたはのこ引き等の技法によって互いに切り離され、そこから個々の素子を、ピン等に接続されたキャリア上に搭載することができる。かかるプロセスに関する更に詳細な情報は、例えば、Ｐｅｔｅｒ ｖａｎ Ｚａｎｔ、McGraw Ｈｉｌｌ ＰｕｂｌｉｓｈｉｎｇＣｏ．１９９７年、ＩＳＢＮ ０－０７－０６７２５０－４の書籍「Ｍｉｃｒｏｃｈｉｐ Ｆａｂｒｉｃａｔｉｏｎ： Ａ Ｐｒａｃｔｉｃａｌ Ｇｕｉｄｅｔｏ Ｓｅｍｉｃｏｎｄｕｃｔｏｒ Ｐｒｏｃｅｓｓｉｎｇ（マイクロチップの製造： 半導体処理のための実用的な手引き）」第３版から得ることができる。この文献は引用により本願にも含まれるものとする。

【００１２】簡略化のために、投影システムを、以降、「レンズ」と呼ぶ場合がある。しかしながら、この用語は、例えば屈折光学部品、反射光学部品、および反射屈折光学系を含む様々なタイプの投影システムを包含するものとして広く解釈するものとする。また、放射システムは、放射の投影ビームを方向付け、整形し、または制御するためにこれらの設計タイプのいずれかに従って動作する構成要素を含むことができ、以下では、かかる構成要素のことを、まとめてまたは単独で「レンズ」と呼ぶ場合がある。更に、リソグラフィ装置は、２つ以上の基板テーブル（および／または２つ以上のマスク・テーブル）を有するタイプのものである場合がある。かかる「多数ステージ」の装置では、平行な追加のテーブルを用いる場合があり、または、１つ以上のテーブル上で準備ステップを実行しながら、１つ以上の他のテーブルを露光のために用いることも可能である。２ステージのリソグラフィ装置は、例えば、米国特許第５，９６９，４４１号およびＷＯ９８／４０７９１号に記載されている。これらは引用により本願にも含まれるものとする。

【００１３】照明システムが、従来のものから環状、四重極、および更に複雑な照明の形状を生成するように発展していくにつれて、現在、制御パラメータの数はいっそう多くなっている。従来の照明パターンでは、光軸を含む円形領域を照明し、このパターンに加える唯一の調整は、外半径（σ_x）を変更することである。環状の照明は、照明される輪を規定するために、内半径（σ_c）を規定する必要がある。多極のパターンでは、制御可能なパラメータ数が増え続ける。例えば、四重極の照明形状では、２つの半径の他に、極の角度αが、選択した内半径と外半径との間の各極によって定められる角度を規定する。

【００１４】同時に、マスク技術も進展している。２値強度マスクは、移相マスクおよび他の高度化したマスクによって取って代わられている。２値マスクは、単に、

所与の点において結像放射を送出、反射、または阻止するが、移相マスクは、一部の放射を減衰させたり、移相を行った後に光を送出もしくは反射させたり、またはその双方を行ったりすることができる。移相マスクは、結像放射の波長またはこれより小さいオーダーのフィーチャを結像するために用いられている。なぜなら、これらの解像度における回折効果は、様々な問題の中でも特に、不十分なコントラストおよびライン端部のエラーを引き起こす恐れがあるからである。

【００１５】様々なタイプの照明形状を用いて、解像度、焦点深度、コントラスト、およびその他の印刷画像の特徴を改善することができる。しかしながら、各照明タイプは、何らかのトレードオフを伴う。例えば、コントラストの改善は、焦点深度を犠牲にして得ることができる。各タイプのマスクは、結像されるパターンにも依存する性能を有する。

【００１６】従来、ウエハ上に所与のパターンを結像する最適な照明モードを選択するために、一連のテスト・ウエハを行き当たりばったりで露光し比較していた。上記のように、最近の照明システムでは、操作可能な変数の数はますます増えている。変数設定の様々な並び替えが増大するにつれて、試行錯誤による照明形状の最適化のコストが極めて大きくなり、照明形状を選択する定量的な方法が必要とされている。

【００１７】先に確認した必要性およびその他に対処するために、本発明は、選択したパターニング手段のパターンのための照明プロファイルを最適化する方法を提供する。この方法は：照明装置および選択したパターニング手段のパターンを含む光学システムのための相互透過係数関数を規定するステップと；選択したパターンに基づいて回折オーダーの結像に対する相対的な関連性を求めるステップと；相互透過係数関数から最適化した照明形状を算出し、回折オーダーの結像に対する相対的な関連性に基づいて照明形状の領域に重み付けを行うステップと；を備える。

【００１８】本発明の別の態様によれば、ディバイス製造方法が提供される。この方法は：

（ａ）放射感知物質の層によって少なくとも部分的に被覆された基板を供給するステップと；

（ｂ）照明システムを用いて放射の投影ビームを供給するステップと；

（ｃ）パターニング手段を用いて投影ビームの断面にパターンを与えるステップと；

（ｄ）放射感知物質層の対象部分上にパターニングした放射ビームを投影するステップと；

を備え、前述の方法を用いて、ステップ（ｄ）の前に、ステップ（ｂ）において生成した投影ビームにおける断面強度分布を、ステップ（ｃ）において用いるパターンに適合させる。

【００１９】本発明の別の態様によれば、リソグラフィ投影装置が提供される。この方法は：放射の投影ビームを供給するための照明システムと；パターニング手段を支持するための支持構造であって、このパターニング手段が所望のパターンに従って投影ビームをパターニングするように機能する、支持構造と；基板を保持するための基板テーブルと；基板の対象部分上にパターニングしたビームを投影するための投影システムと；を備え、この装置は、更に：照明装置および所望のパターンの相互透過係数関数を規定し、パターニング手段によって生成したパターンに基づいて回折オーダーの結像に対する相対的な関連性を求め、相互透過係数関数から最適化した照明形状を算出し、回折オーダーの結像に対する相対的な関連性に基づいて照明形状の領域に重み付けを行う、算出手段と；算出手段によって算出した照明形状に従って、照明システムから射出する投影ビームにおける断面強度分布を選択するための選択手段と；を備える。

【００２０】本発明の更に別の態様によれば、選択したマスク設計を最適化する方法が提供される。この方法は：選択したマスク設計のクリティカル・フィーチャを識別すること；クリティカル・フィーチャの回折オーダーに基づいて最適化した照明プロフィールを求めること；および選択したマスク・フィーチャに存在するピッチ数を減らすように選択した光近接補正技法を用いることによって選択したマスク設計を変更すること；を備える。

【００２１】本発明は、更に、上述の方法を実行するためのコンピュータ・プログラムを提供する。

【００２２】この明細書において、本発明による装置をＩＣの製造に用いることに特に言及することができるが、かかる装置は多くの他の可能な用途を有することは明示的に理解されよう。例えば、これは、集積光学システム、磁気ドメイン・メモリ用の誘導および検出パターン、液晶表示パネル、薄膜磁気ヘッド等の製造に用いることができる。かかる代替的な用途の状況においては、この文書における「レチクル」、「ウエハ」、または「ダイ」という用語のいかなる使用も、より一般的な用語「マスク」、「基板」、および「対象位置」によってそれぞれ置換されるものとして見なされることは、当業者には認められよう。

【００２３】本発明について、例示的な実施形態および添付の図面を参照して、以下で更に説明する。

【００２４】

【発明の実施の形態】本発明は、照明源およびパターンの詳細について考慮して、最初に、（例えばマスクから）基板上へのパターンの結像を数学的にモデリングすることを含む。

【００２５】有限照明源について空中像を算出するためには、主に２つの方法がある。これらの方法は、アッベの公式化およびホプキンズの公式化である。アッベの公式化では、照明形状における各点源が、パターン上に入

射する平面波を生成し、これらの点源の各々がウエハ上に結像される。点源は空間的に非干渉性であるので、ウエハにおける合計強度は、これらの点源の各々によって生成される強度の和である。従って、アッベの公式化では、照明形状での積分は、パターンでの積分の後に行う。

【００２６】ホプキンズの公式化では、積分の順序を変える。すなわち、源での積分を最初に行う。ホプキンズの公式化では、４次元相互透過係数（ＴＣＣ）を規定し、ＴＣＣの逆フーリエ変換が画像の強度となる。ＴＣＣの導出については、例えば、ＢｏｒｎおよびＷｏｌｆのＰｒｉｎｃｉｐｌｅｓ　ｏｆ　Ｏｐｔｉｃｓ（光学の原理）、第６版、５２８ないし５３２ページに説明されている。これは、引用により本願にも含まれるものとする。

【００２７】ＴＣＣは、照明ひとみで乗算した投影ひとみの自己相関である。図１に、３つの重複する円の集合としてＴＣＣを示す。左から右に説明すると、第１の円は、照明ひとみ$J_s(\alpha,\beta)$を表し、ここでαおよびβは照明形状の座標である。後の計算のために、J_sの半径は、例えば、結像に用いるリソグラフィ装置に可能な最大の外半径σ_rに設定することができる。また、実現性の研究を行うため、および更に大きなσ_rの利点を明らかにするために、σ_rを１．０以上に設定することも可能である。

【００２８】中央の円は、（$-m\lambda/P_xNA$，$-n\lambda/P_yNA$）を中心とする投影ひとみK（α，β）を表す。座標系は、λ/NAの因数で正規化されているので、Kの半径は１．０である。右側の円は、同様に投影ひとみを表すが、これは、（$p\lambda/P_xNA$、$q\lambda/P_yNA$）を中心としている。これらの最後の２つの式では、ｍ、ｎ、ｐ、およびｑは別個の回折オーダーに相当し、ＴＣＣが上述のような４次元（４－Ｄ）の式であることが明らかになる。ｘ方向の回折オーダーはｍおよびｐによって表され、ｙ方向の回折オーダーはｎおよびｑによって表される。この説明のためにｘおよびｙ座標を用いるが、以下の式で、座標系を適切に変更して代替的な座標系を使用可能であることは、当業者には理解されよう。

【００２９】４－Ｄの別個の点（ｍ、ｎ、ｐ、ｑ）についてのＴＣＣは、３つの全ての円が重複している陰影を付けた領域の積分である。構造は周期的であると想定されているので、パターンのフーリエ変換は離散的であり、ＴＣＣは離散的である。連続的なパターン画像では、隣接するフィーチャが対象パターンのフーリエ変換に影響を及ぼさなくなるまで、ピッチを長くすることができる。図１のＴＣＣは、数学的に、式１で書き表される。

$$\iint_{\sqrt{\alpha^2+\beta^2}<\sigma} J_s(\alpha,\beta)K\left(\alpha+\frac{m\lambda}{P_xNA},\beta+\frac{n\lambda}{P_yNA}\right)K^*\left(\alpha-\frac{p\lambda}{P_xNA},\beta-\frac{q\lambda}{P_yNA}\right)d\alpha d\beta \qquad \text{式(1)}$$

【００３０】ＴＣＣは、回折オーダー相互係数（ＤＯＣＣ）を規定することで、パターンの効果を含むように拡張することができる。式２にＤＯＣＣを規定する。これは、ＴＣＣにパターンのフーリエ変換係数を乗算することによって得られる。

$$DOCC(m,n,p,q)=T(m,n)T^*(-p,-q)TCC(m,n,p,q) \qquad \text{式(2)}$$

【００３１】更に、ウエハにおける放射強度は、式３に示すように、ＤＯＣＣの逆フーリエ変換によって算出することができる。

$$I(x,y)=\sum_m\sum_n\sum_p\sum_q e^{ix\left[\frac{2\pi}{P_x}(m+p)\right]}e^{iy\left[\frac{2\pi}{P_y}(n+q)\right]}DOCC(m,n,p,q) \qquad \text{式(3)}$$

【００３２】投影光学系は、部分的に低域フィルタとして作用し、これによって回折オーダーが減少するので、算出した画像強度において重要な回折オーダーは小数のみである。結果として、ＴＣＣは帯域限定関数である。必要な最大のｘおよびｙのオーダーを、それぞれ、式４および５に従って算出することができる。各々の場合において、負および正の双方のオーダーが必要である。例えば、ｍは負のm_{max}から正のm_{max}までに及ぶ（$-m_{max}\leqq m\leqq+m_{max}$）。負および正の双方のオーダーが必要であるので、ＴＣＣの大きさは、$2m_{max}+1$掛ける$2n_{max}+1$掛ける$2p_{max}+1$掛ける$2q_{max}+1$である。しかしながら、幸い、ＴＣＣは帯域が限定されているので、全てのパターン回折オーダーを計算する必要はない。ＴＣＣにおいてと同様、ｘ方向ではパターン回折オーダー$-m_{max}\leqq m\leqq+m_{max}$のみ、ｙ方向においてはオーダー$-n_{max}\leqq n\leqq+n_{max}$のみが必要である。

$$f_{x\max} = m_{max} = p_{max} = floor\left[\frac{P_x NA(1+\sigma_o)}{\lambda}\right] \qquad 式(4)$$

$$f_{y\max} = n_{max} = q_{max} = floor\left[\frac{P_y NA(1+\sigma_o)}{\lambda}\right] \qquad 式(5)$$

【0033】式1および2を式3に代入すると、ウエハにおける放射強度についての式6が得られる。式7に示すように、積分の順序を変えることで、すなわち、ホプキンズの公式化でなくアッベの公式化を用いることで、結像に最も影響を与える照明ひとみの部分を求めることができる。式6および7の各々は2行に及ぶことを注記しておく。

$$I(x,y) = \sum_m \sum_n \sum_p \sum_q e^{i\omega\left[\frac{2\pi}{P_x}(m+p)\right]} e^{i\psi\left[\frac{2\pi}{P_y}(n+q)\right]} T(m,n)T^*(-p,-q) \qquad 式(6)$$

$$\cdot \iint_{\sqrt{\alpha^2+\beta^2}<\sigma} J_s(\alpha,\beta)K\left(\alpha+\frac{m\lambda}{P_x NA},\beta+\frac{n\lambda}{P_y NA}\right)K^*\left(\alpha-\frac{p\lambda}{P_x NA},\beta-\frac{q\lambda}{P_y NA}\right)d\alpha d\beta$$

$$I(x,y) = \iint_{\sqrt{\alpha^2+\beta^2}<\sigma} d\alpha d\beta \sum_m \sum_n \sum_p \sum_q e^{i\omega\left[\frac{2\pi}{P_x}(m+p)\right]} e^{i\psi\left[\frac{2\pi}{P_y}(n+q)\right]} \qquad 式(7)$$

$$\cdot J_s(\alpha,\beta)T(m,n)T^*(-p,-q)K\left(\alpha+\frac{m\lambda}{P_x NA},\beta+\frac{n\lambda}{P_y NA}\right)K^*\left(\alpha-\frac{p\lambda}{P_x NA},\beta-\frac{q\lambda}{P_y NA}\right)$$

【0034】αおよびβは照明ひとみの座標を表すので、新たな関数J_{opt}を規定することができる。新たな関数J_{opt}は、所与の回折オーダー（m、n、p、q）に対して照明形状のどの部分（α、β）が用いられているかを示し、式8で書き表される。式8から、これに逆フーリエ係数（e^{ikx}）を乗算し、式9に示すように6個の全ての変数（m、n、p、q、α、β）を合計することで、画像強度を算出することができる。

$$J_{opt}(\alpha,\beta,m,n,p,q) = J_s(\alpha,\beta)T(m,n)T^*(-p,-q)K\left(\alpha+\frac{m\lambda}{P_x NA},\beta+\frac{n\lambda}{P_y NA}\right)K^*\left(\alpha-\frac{p\lambda}{P_x NA},\beta-\frac{q\lambda}{P_y NA}\right)$$

式(8)

$$I(x,y) = \iint_{\sqrt{\alpha^2+\beta^2}<\sigma} d\alpha d\beta \sum_m \sum_n \sum_p \sum_q e^{i\omega\left[\frac{2\pi}{P_x}(m+p)\right]} e^{i\psi\left[\frac{2\pi}{P_y}(n+q)\right]} J_{opt}(\alpha,\beta,m,n,p,q)$$

式(9)

【0035】明らかになるであろうが、J_{opt}は6次元の関数であり、従って、これを照明形状に適用することは難しい。照明形状のどの部分が画像形成にとって重要であるかを最良に求めるためには、6個の変数のうちいくつかを除去することが望ましい。

【0036】m＋pおよびn＋qについて逆変換を取ることで、空中像強度I（x，y）を求める。m＋p＝n＋q＝0である場合、空中像強度は変調されていない。照明最適化の目標の1つは、変調に及ぼす影響がほとんど無いか全く無い照明形状の部分を除去することなので、m＋p＝n＋q＝0となる照明形状の部分を除去することができる。これらの部分を除去し、画像形成にとって重要な照明形状の部分を更に視覚化するために、変数の変換によって、6次元のJ_{opt}関数（4回折オーダ

ー）の変数のうち２つを除去し、それを４次元関数（２回折オーダー）に変換する。この４次元関数をJ_{opt-2D}と呼ぶ。式１０および１１をＩ（ｘ，ｙ）についての式９に代入することで、式１２を得ることができる。

$$\eta = m + p \Rightarrow p = \eta - m \qquad \text{式(10)}$$

$$\xi = n + q \Rightarrow q = \xi - n \qquad \text{式(11)}$$

$$I(x,y) = \iint_{\sqrt{\alpha^2+\beta^2}<\sigma} d\alpha d\beta \sum_{\eta=-2f_{x\max}}^{+2f_{x\max}} \sum_{\xi=-2f_{y\max}}^{+2f_{y\max}} e^{i\left[\frac{2\pi}{P_x}\eta\right]} e^{i\left[\frac{2\pi}{P_y}\xi\right]} \underbrace{\sum_{m=-f_{x\max}}^{+f_{x\max}} \sum_{n=-f_{y\max}}^{+f_{y\max}} J_{opt}(\alpha,\beta,m,n,\eta-m,\xi-n)}_{J_{opt-2D}(\alpha,\beta,\eta,\xi)} \qquad \text{式(12)}$$

【００３７】式１２では、J_{opt-2D}は、式１０および１１に従って変数を変換した後、ｍおよびｎについてのJ_{opt}の和と見ることができる。更に、式８を式１２に代入することで、J_{opt-2D}を式１３におけるように表すことができ、強度Ｉ（ｘ，ｙ）を、式１４におけるようにJ_{opt-2D}の関数として書くことができる。

$$J_{opt-2D}(\alpha,\beta,\eta,\xi) = J_s(\alpha,\beta) \sum_{m=-f_{x\max}}^{+f_{x\max}} \sum_{n=-f_{y\max}}^{+f_{y\max}} T(m,n) T^*[-(\eta-m),-(\xi-n)] \qquad \text{式(13)}$$

$$\cdot K\left(\alpha + \frac{m\lambda}{P_x NA}, \beta + \frac{n\lambda}{P_y NA}\right) K^*\left(\alpha - (\eta-m)\frac{\lambda}{P_x NA}, \beta - (\xi-n)\frac{\lambda}{P_y NA}\right)$$

$$I(x,y) = \iint_{\sqrt{\alpha^2+\beta^2}<\sigma} d\alpha d\beta \sum_{\eta=-2f_{x\max}}^{+2f_{x\max}} \sum_{\xi=-2f_{y\max}}^{+2f_{y\max}} e^{i\left[\frac{2\pi}{P_x}\eta\right]} e^{i\left[\frac{2\pi}{P_y}\xi\right]} J_{opt-2D}(\alpha,\beta,\eta,\xi) \qquad \text{式(14)}$$

【００３８】関数J_{opt-2D}は、値を求めると、各回折オーダーごとに重要な照明形状の部分を示す。J_{opt-2D}は、各回折オーダーＴ（ｍ，ｎ）によって重み付けされるので、大きい回折オーダーは、空中像に及ぼす影響が大きくなる。

【００３９】特定のパターンについて最適な照明形状のための開始点を、J_{tot}と示すことができ、これは、式１５に示すように、ηおよびξについてJ_{opt-2D}を合計し、J_{opt-2D}（α，β，η＝０、ξ＝０）を減算することで求められる。式１５では、η＝０およびξ＝０の場合、空中像は変調されておらず、J_{opt-2D}（α，β，η＝０、ξ＝０）成分は、ゼロのオーダーまたはＤＣ光を表す。結像に寄与しない照明内の点によって、ＤＣ光の全量は増大する。増大したＤＣ光は変調を引き起こさないので、これは大して有益ではなく、更に、結果として焦点深度が浅くなる恐れがある。

【００４０】このため、J_{tot}による照明形状はＤＣ光の量を最小限に抑え、結果としてプロセス・ウインドウが改善する。式J_{tot}を用いて、照明装置のどの部分が画像形成にとって重要性が高いか（または重要性が低いか）を示すことができる。

$$J_{tot}(\alpha,\beta) = \left[\sum_{\eta=-2f_{x\max}}^{+2f_{x\max}} \sum_{\xi=-2f_{y\max}}^{+2f_{y\max}} \left|J_{opt-2D}(\alpha,\beta,\eta,\xi)\right|\right] - \left|J_{opt-2D}(\alpha,\beta,0,0)\right| \qquad \text{式(15)}$$

【００４１】照明形状およびパターンは結合されるので、光近接補正（ＯＰＣ）を変更すると回折オーダーに影響を与え、従ってJ_{tot}に影響を与える。結果として、当業者には理解されようが、ＯＰＣエンジンおよび照明エンジンによる処理の繰り返しを用いて、初期照明形状J_{tot}およびパターンに対する変更を何度か行わなければならない。更に、パターンおよび照明形状は、特定の結像基準（焦点深度（ＤＯＦ）、ライン端部（ＥＯＬ）、収差に対する感度等）を最適化するようにも調節する必要があり、これは最適化ソフトウエアによって行うことができる。しかしながら、最適な照明形状に最大の影響を与えるのは、ＯＰＣフィーチャではなく、全体としてのパターンであるので、J_{tot}は最適な初期照明形状であり、照明形状およびパターンに関する繰り返しの最適化のために最も速く収束することになる。

【００４２】初期照明形状J_{tot}は、０ないし１の範囲の連続的な強度値を有するグレー・スケール照明形状によって表すことができる。回折光学素子（ＤＯＥ）によって、またはディザリングを行ったクロムめっきを施した水晶板を用いることで、かかるグレー・スケール照明

形状を生成することができる。グレー・スケール照明形状が可能でないか、または好ましくない場合は、グレー・スケールに閾値を適用することで、照明装置プロファイルを０および１のみに強制することができる。この場合、閾値を超える値は１に切り上げて、閾値未満の値は０に切り捨てる。任意の閾値を適用することができ、または、プロセス・ウインドウをシミュレートすることで、もしくは試運転を繰り返すことで、最適な閾値を見出すことができる。

【００４３】例１：　先に概説したJ_{tot}を算出するための技法を、れんが壁分離パターンに適用した。１５０ｎｍのパターンを１３０ｎｍおよび１１０ｎｍ設計基準に縮小し、開口数（ＮＡ）が０．８のステップ・アンド・スキャン・リソグラフィ・システムにより結像した。図２に、１３０ｎｍ設計基準の分離パターンを示す。

【００４４】図３に、このマスク・フィーチャの回折オーダーの大きさを示す。図３では、最大のオーダーは、（０，０）オーダーまたはＤＣ背景光である。結像に最も寄与したオーダーは、（±２，０）オーダーであり、れんが壁パターンにおける縦方向のれんがを表す。他の重要なオーダーは（±１，±１）であり、クリアな領域を表し、分離パターンの端部を規定する。また、これより高いオーダーは、各ラインの端部等の２次元構造を規定するのに役立つ。回折パターンが一定でないので、オーダーによってＤＯＣＣにおける重み付け係数が変化し、これは、マスク・パターンが照明の方法に影響を与えることを示唆している。

【００４５】図３における回折オーダー係数Ｔ（ｍ，ｎ）を式１３に代入して、J_{opt-2D}を算出することができる。これを図４に示す。図４からわかるように、J_{opt-2D}に対する最大の寄与は、（η＝０、ξ＝０）オーダーである。（０，０）オーダーは、結像に寄与せず、ＤＯＦを浅くする。式１５が示すように、この（０，０）オーダーを、合計照明J_{tot}から減算することができる。（０，０）オーダーを考慮しないと、最大の寄与は（η＝±２、ξ＝０）回折オーダーであり、これは、ｘ方向に沿った分離ラインの形成を表す。大きく、かつ分離ラインの端部を規定する別の成分は、（η＝±１、ξ＝±１）回折オーダーである。（０，±２）回折オーダーはやや小さいが、これより大きいオーダーは、レンズのη＝０およびξ＝±２の領域において結合する。また、これらの領域は、ライン端部を規定するのに役立つ。ＤＯＣＣの手法は、画像形成を改善するためにどのように照明ひとみをサンプリングするかを示し、れんが壁分離パターンの結像を理解するために有効な方法である。

【００４６】式１５を用いて、１３０ｎｍ設計基準のれんが壁パターンの照明ひとみを算出することができる。これを図５に示す。図５は、画像形成にとって最も重要な領域はｘ軸に沿った照明形状の外側部分であることを示している。これらの外側部分は、楕円ダイポールを形成する。これらの楕円ダイポール要素に加えて、照明ひとみの中心は、画像形成に大きく寄与する。上記のように、照明ひとみは、グレー・スケールまたは２値照明プロフィールで実施することができる。

【００４７】用いる装置に応じて、グレー・スケール照明が可能である場合がある。グレー・スケール照明とは、制御可能な照明強度を意味し、照明形状の少なくとも所与の部分について、０から１までの正規化レベルを選択することができる。例えば、かかる照明強度の制御は、照明システムにおける回折光学素子（ＤＯＥ）を用いて行うことができる。この場合、例えば、照明形状は、図５に示すように実施することができる。しかしながら、理論上算出され図５に見られる局所スパイクの一部は、上述のように、投影光学系の結果として照明情報を低域フィルタで沪波した後に除去される。従って、照明形状を設計する場合、沪波されるスパイクは無視するものとする。

【００４８】２値照明形状を用いる場合、すなわち、照明装置の強度に２値のみ（０または１）が可能である場合、照明形状の各点に０または１の値を割り当てるための基礎として、閾値を選択しなければならない。例えば、０．８の閾値を選択した場合、０．８を超える照明装置の強度値は１に切り上げられ、０．８未満の値は０に切り捨てられる。所望の場合は、他の閾値を適用することも可能である。

【００４９】例２：２値の手法にグレー・スケールを用いて、０．８８の最大外半径σを想定して、同じれんが壁分離パターンについて２値照明形状を設計し、図６に示す。

【００５０】次いで、図６の最適化された照明形状の性能を、ＮＡ＝０．８およびλ＝２４８ｎｍのステップ・アンド・スキャン・リソグラフィ装置上の２値マスクについてシミュレートし、環状照明のシミュレートした性能と比較した。このシミュレーションでは、開口数が０．７を超えたので、ベクトル（薄膜）結像レジスト・モデルを用いた。このモデルでは、レジストは、屈折率ｎ＝１．７６－ｊ０．０１１６）を有するタイプの４００ｎｍの厚さであり、ｎ＝１．５７７－ｊ３．５８８のポリシリコン物質の上のｎ＝１．４５－ｊ０．３を有する別のタイプの６６ｎｍの上にある。図７および８に、環状照明（σ_{in}＝０．５８およびσ_{out}＝０．８８）ならびに最適化した照明装置（σ_{out}＝０．８８）の結果をそれぞれ示す。図７および８の双方において、分離領域の中央における断面の結果およびトップダウンのシミュレーション結果を示す。これらの図では、レジストを介した強度を平均化することによって、空中像閾値からＢｏｓｓｕｎｇプロットＢを算出し、結果として得られた線幅ｌｗを、閾値の強度について、焦点ｆに対してグラフ化する。この技法は、ＤＯＦを厚さのロスとして過

剰予測する傾向があり、レジスト・プロファイルの傾斜は考慮されていない。おそらく、少なくとも厚さのロスを算出するレジスト・モデルが必要であろう。図の各々において、トップダウンの結果は、Ｂｏｓｓｕｎｇプロットで算出したような最適な閾値（最適な照射量）での実線の曲線として描かれている。これらのシミュレートした閾値の画像を、点線の直線で示す実際のマスク・データと比較する。

【００５１】図７には、環状照明（σ_{in}＝０．５８およびσ_{out}＝０．８８）を用いた０．８のＮＡでの２値マスク・フィーチャについて、１３０ｎｍ設計基準のれんが壁分離パターンのシミュレーション結果を示す。この環状設定は、－０．４μｍから０．０μｍ焦点まで、約０．４μｍのＤＯＦを有する。レジストのコントラストは、全焦点を通じて低く、低コントラストのレジストによって結像することができる。しかしながら、この低強度のコントラストでは、マスク誤差増大ファクタ（ＭＥＥＦ）が大きく、露出ラチチュード（ＥＬ）が小さい。また、図７におけるトップダウンの画像は、ライン端部（ＥＯＬ）の短縮が約２０ｎｍであることを示しているが、これは、１３０ｎｍ設計基準についてわずかにラインを延長して固定することができる。しかしながら、設計基準が縮小し続けると、延長したラインが他のフィーチャと衝突する恐れがあるので、ラインの延長はもはや実行可能でない。従って、照明によってＥＯＬを固定することが望ましい。

【００５２】図８では、１３０ｎｍ設計基準のれんが壁分離パターンについてのシミュレーション結果を、０．８のＮＡで、図６の最適化２値照明形状を用いて、２値マスク・フィーチャについて図示している。最適な照明形状は、－０．４５μｍから＋０．１５μｍ焦点まで、約０．６μｍのＤＯＦを有する。図８の断面画像を図７のものと比較すると、最適化した照明形状は、環状の照明に比べて、全焦点を通じてコントラストが大きい。この大きなコントラストは、環状照明に比べて最適化照明形状についてのＭＥＥＦが小さく、最適化照明形状のための露出ラチチュードが大きいことを示唆する。この最適化照明形状の別の利点は、環状照明に比べて、ライン端部の性能が改善されていることである。図８のトップダウン画像は、この最適化照明形状が、パターン上のラインを延長することなくＥＯＬを維持可能であることを示し、これは、より大胆な設計基準の縮小のために好都合である。

【００５３】例３：　図７および８における２値マスク（ＢＩＭ）についての結果を、クロムレス・マスク（ＣＬＭ）についてのシミュレーション結果と比較した。当業者に既知の方法で、ソフトウエア・シミュレーションの実験結果から、クロムレスれんが壁分離パターンを設計した。クロムレス技術は、軸はずれ照明によって得られるＤＯＦの改善から十分な恩恵を受けるように、（０，０）オーダーの光を必要とする。シミュレーションからの実験結果によって、（０，０）オーダーの光の必要性が裏付けられる。このために、分離層にディザリングを行うか、またはハーフトーンとしなければならない。ハーフトーンのピッチは、ディザリングを行った方向の第１のオーダーが投影ひとみに入らないように選択すれば良い。この例では、$\lambda/[NA(1+\sigma_{out})]$未満のピッチで、垂直方向にラインにディザリングを行った。しかしながら、ディザリングのデューティ・サイクルは、最適なＤＯＦおよびパターン忠実度のために、（０，０）オーダーの光の量を最適化するように調整しなければならない。ＣＬＭのためのシミュレーション結果では、ハーフトーン・ピッチは、５０％のデューティ・サイクルで１５５ｎｍであった（７７．５ｎｍのクロム・アイランド）。このピッチでは、（０，±１）オーダーが投影ひとみに入ることがほぼ妨げられる。しかしながら、このデューティ・サイクルは、コンピュータ支援設計ツールによってＤＯＦを最大にするように調整しなければならない。

【００５４】例４：　１３０ｎｍ設計基準層についてのシミュレーション結果を、１５５ｎｍハーフトーン・ピッチおよび５０％デューティ・サイクルのＣＬＭについて図示した。０．８のＮＡおよび環状照明（σ_{in}＝０．５８およびσ_{out}＝０．８８）により、λ＝２４８ｎｍの装置で、ＣＬＭを露光した。この環状設定のＣＬＭは、ＤＯＦが０．５μｍであった（－０．４μｍ焦点から＋０．１μｍ焦点）。環状照明のＣＬＭは、環状照明のＢＩＭに比べて、ＤＯＦが大きく、全焦点を通じてコントラストが優れていた。これは、ＣＬＭの性能がＢＩＭマスクよりも優れていたことを示す。トップダウン・シミュレーションの結果は、ＣＬＭによるＥＯＬ性能が理論的にはＢＩＭによるＥＯＬ性能よりも優れていること、および、ＣＬＭはＢＩＭに比べてコンタクト・ホールのランディング領域をより十分に規定することもできたことを示した。

【００５５】例５：　１３０ｎｍれんが壁分離パターン分離層についてのシミュレーション結果を、０．８のＮＡおよび図６に示す最適化楕円ダイポールのλ＝２４８ｎｍの装置について図示した。これらの結果を、１５５ｎｍハーフトーン・ピッチおよび５０％のデューティ・サイクルを有する前の例で用いたＣＬＭレチクルと同一のレチクルを用いてシミュレートした。この最適化照明形状で露光したＣＬＭは、０．７μｍのＤＯＦ（－０．５μｍから＋０．２μｍ）を有し、４０％の改善であった。Ｂｏｓｓｕｎｇプロットは、同焦点強度が約０．２１であることを示していた。加えて、正確な線幅の大きさとなるようにレチクルを調整し、更に性能を改善するために、モデルに基づくＯＰＣ手法を適用することができた。線幅を補正するには、例えば、バイアスをかけること、およびハーフトーン・デューティ・サイクルの変

更を行えば良い。トップダウン・シミュレーション結果は、ＣＬＭがコンタクトのランディング領域を規定することができ、ＣＤの均一性を維持することができることを示していた。この楕円照明形状によって、くびれおよび他の線幅の不一致が低減した。更に、ＣＬＭレチクルは、ＤＯＦを改善するようにバイアスをかけることができ、この結果、ＥＯＬ性能が改善するはずである。更に、モデルに基づくＯＰＣは、ＥＯＬを更に補正することができるはずである。

【００５６】例６：　１１０ｎｍ設計基準の分離層について、図２のマスク・パターンを用いて、式１３および１５により、最適化照明形状を生成した。照明ひとみのサンプリングを視覚化するために、J_{opt-2D}を図９に図示し、ｘオーダー（$\eta=m+p$）を水平方向に、ｙオーダー（$\xi=n+q$）を垂直方向に示す。１３０ｎｍ設計基準についての図４と同様に、図１１の１１０ｎｍ設計基準に対する最大の寄与は、（$\eta=0$、$\xi=0$）オーダーである。この（０，０）オーダーの光は、ＤＯＦにとって有害であり、式１５に示すように、J_{tot}において除去される。また、図９は、（±２、０）オーダーでなく（±１、±１）オーダーが、照明形状の最適化に対して最大の寄与となることを示す。これは、ＮＡ＝０．８の２４８ｎｍの装置では１１０ｎｍ設計基準は積極的すぎるという事実のためであり、この解像度を達成するためには、わずかに高いＮＡが好ましい。分離線幅を規定するために最も寄与するオーダーは、（±２、０）オーダーである。しかしながら、（±２、０）オーダーは、照明形状の遠方縁部にあり（$0.8<\sigma<1.0$）、これは、σが１であると、この波長における１１０ｎｍ設計基準の実施を改善可能であることを示している。

【００５７】式１５および図９の結果を用いて、図１０に、１１０ｎｍれんが壁分離層についての最適化照明形状を示す。図１０は、画像形成に最も寄与する照明形状領域が、照明形状の中央の小部分および遠方縁部であることを示している。図１１ａに、この照明形状の１つの可能な実施態様を図示する。２４８ｎｍ装置を用いて更に積極的な設計基準を印刷し、投影開口数の制限を課すためには、図１１ｂに示すように、σを１．０とし、小さいセクタ（σのリング幅は０．２）を有する照明形状を用いる。

【００５８】本発明の実施態様は、クリティカルなセルまたは特定のゲートの選択を含む。次いで、これらのクリティカル・フィーチャを処理して、上述のようにJ_{tot}を求める。セクション１では、照明形状はパターンに依存することが示された。従って、クリティカル・フィーチャについてピッチに著しい差が無い場合、全てのクリティカル・フィーチャについて、プロセス・ウインドウを最適化する単一の照明形状を生成することができる。図１２に、クリティカル・ゲートg_1、g_2、g_3およびクリティカル・セルｃｃを有する回路の１例を示す。これらのタグ付きのクリティカル・フィーチャの回折オーダーを算出することができ、すでに述べた理論を用いることで、最適化照明形状を算出することができる。最適化照明形状を算出した後、プロセス・ウインドウを算出し、他の照明形状によるプロセス・ウインドウと比較することができる。

【００５９】照明／パターンの相互作用を最適化する別の方法は、散乱バーによってパターン設計を変更することである。散乱バーは、ＡＳＩＣまたは論理設計についての半連続関数からピッチを打ち切る。散乱バーを配した後、ピッチは少なくなる。これは、シミュレーション・ソフトウエアにおいて、０．６１λ／ＮＡのエッジ間分離で散乱バーを配置することで実証することができる。図１３では、複数の散乱バーを加えることで図１２の設計を変更している。次いで、この変更した設計について、照明形状を最適化することができる。次いで、散乱バーを有する設計について最適化した照明形状のプロセス・ウインドウ性能を、散乱バーを有することなく最適化した照明形状のプロセス・ウインドウと比較することができる。散乱バーを有する設計はピッチを打ち切るので、散乱バーと最適化した軸はずれ照明（ＯＡＩ）との組み合わせは、最大の可能ＤＯＦプロセス・ウインドウを有する。

【００６０】照明形状の最適化を実施するための別の概念は、空間幅（ＳＷ）の考慮に基づいた散乱バーの配置によるものである。散乱バーは、ルールに基づくＯＰＣによって配置する。このルールは、空間幅によって規定することができる。シミュレーション・ソフトウエアを用いて、散乱バーを有しない場合および散乱バーを有する場合の空間幅の確率密度関数（ｐｄｆ）を算出することができるはずである。次いで、式１６に示すようにJ_{opt-2D}を変更することでｐｄｆを考慮して、照明を最適化することができる。垂直のラインおよび水平のラインが無限であると想定すると、回折オーダーＴ（ｍ，ｎ）を算出することも可能である。式１７において、ｍおよびｎの関数として回折オーダーを算出する。ここでｗは線幅であり、τはレチクルの強度透過率、ならびに、$P_x=SW_x+w$および$P_y=SW_y+w$は、それぞれｘおよびｙ方向におけるピッチである。

$$J_{opt-2D}(\alpha,\beta,\eta,\xi)=$$

$$J_s(\alpha,\beta)\sum_{m=-fx_{max}}^{+fx_{max}}\sum_{n=-fy_{max}}^{+fy_{max}}\int\int dP_x dP_y pdf(Px)pdf(Py)T(m,n)T^*[-(\eta-m),-(\xi-n)]$$

$$\cdot K\left(\alpha+\frac{m\lambda}{P_x NA},\beta+\frac{n\lambda}{P_y NA}\right)K^*\left(\alpha-(\eta-m)\frac{\lambda}{P_x NA},\beta-(\xi-n)\frac{\lambda}{P_y NA}\right)$$

式(16)

【0061】式17は、4つの式の行列であり、提示の順に、m＝n＝0、m＝0、n≠0、m≠0、n＝0、およびm≠0、n≠0である。

$$T(m,n)=\begin{cases}1-w\left(1+\sqrt{\tau}\right)\left(\frac{1}{P_x}+\frac{1}{P_y}\right)+\frac{w^2}{P_x P_y}\left(1+\sqrt{\tau}\right)^2\\ \left[1-\frac{w}{P_x}\left(1+\sqrt{\tau}\right)\right]\left(1+\sqrt{\tau}\right)\left(\frac{P_y}{\pi n}\right)\sin\left(n\frac{\pi w}{P_y}\right)\\ \left[1-\frac{w}{P_y}\left(1+\sqrt{\tau}\right)\right]\left(1+\sqrt{\tau}\right)\left(\frac{P_x}{\pi m}\right)\sin\left(m\frac{\pi w}{P_x}\right)\\ \left(1+\sqrt{\tau}\right)^2\left(\frac{P_x}{\pi m}\right)\sin\left(m\frac{\pi w}{P_x}\right)\left(\frac{P_y}{\pi n}\right)\sin\left(n\frac{\pi w}{P_y}\right)\end{cases}$$

式(17)

【0062】一部のピッチは他のものほど重要でないことが示唆されるため、ｐｄｆによって最適照明形状を算出すると、いくつかの問題が生じる。ｐｄｆにおいて全てのゲートがクリティカルであると見なされる場合、重み付け係数によってｐｄｆを変更しなければならない。この重み付け係数は、ｗｆ（Ｐｘ）と呼ぶピッチの関数である。この重み付け係数により、全てのクリティカルなピッチを同一に扱い、ｗｆ（Ｐｘ）・ｐｄｆ（Ｐｘ）＝1となるようにしなければならない。式16におけるｐｄｆ（Ｐｘ）をｗｆ（Ｐｘ）・ｐｄｆ（Ｐｘ）によって置換することで、この重み付け係数を式16に追加するものとする。ピッチの全てがクリティカルである場合、重み付け係数は、最適化を決定するために役立たず、（パターンの）設計を変更することなく最適化照明形状を生成することは難しい。

【0063】この問題に対する1つの解決策は、上述の散乱バーを加えて設計を変更することである。散乱バーは、分離されたフィーチャについてピッチを小さくするのに役立つ。一旦、設計に散乱バーを加えたならば、以前分離したフィーチャは、密集したフィーチャとして作用する傾向がある。このため、散乱バーは、連続的なｐｄｆから更に離散的なｐｄｆまでピッチを打ち切る。図14は、散乱バーを適用した場合および適用していない場合の、ｙ方向（すなわち「垂直」方向）に配向したフィーチャを有する論理パターンについての一例のｐｄｆである。図14は、ｘ（水平）軸上に垂直ゲート空間幅（μｍ）を示す。散乱バーを有しない変更されていない設計Ｄでは、０．２、０．６、および１．５μｍの空間幅において、ｐｄｆに3つの別個の隆起がある。散乱バーを配置した後、Ｄ＋ＳＢでは、ピッチ数が減って、空間幅のほとんどが０．２μｍの密集したピッチにあるようになっている。このｐｄｆの変更によって、照明形状を最適化することが可能な確率が高くなる。

【0064】水平（ｘ軸）および垂直のフィーチャの双方を有する設計についての全体的な照明形状は、水平および垂直の照明形状の和である。垂直フィーチャについて照明形状をσ_{cx}に集中させ、水平フィーチャについてσ_{cy}に集中させる場合、

$$\sqrt{2}\,\sigma_{cx}\leqq 1\ \text{かつ}\ \sqrt{2}\,\sigma_{cy}\leqq 1$$

であるならば、最適照明形状は、「従来の」四重極照明形状である。その他の場合、このタイプの分析は、結果として、４５度回転した四極照明形状となる。

【0065】ここに提示し5照明技法は、収差を考慮するように拡張することができる。収差を含むことで、オペレータは、照明形状のどの部分が収差に結合するかを決定することができる。結合量は、収差に対する画像強度の感度に直接関連する。この結合を理解することで、設計の収差感度を最小限に抑えるように照明形状を変更することができる場合がある。

【0066】スカラ結像についての投影ひとみＫ（α，β）は、傾斜ファクタ、焦点はずれ、およびゼルニケ多項式によって表される波面の指数関数を含む。このスカラ結像ひとみを式18に示す。このひとみは、更に、2つの部分に分割することができる。すなわち、非逸脱ひとみK_0（α，β）および逸脱ひとみ（波面の指数関数）であり、これらの2つの部分は式19に示すように共に乗算する。

$$K(\alpha,\beta)=\underbrace{\left[\frac{1-\left(\alpha^2+\beta^2\right)/M^2}{1-\left(\alpha^2+\beta^2\right)}\right]^{1/4}}_{obliquity-factor}\underbrace{exp\left[-i\frac{2\pi}{\lambda}z\sqrt{1-\alpha^2-\beta^2}\right]}_{defocus}\underbrace{exp\left[-i\frac{2\pi}{\lambda}W(\alpha,\beta)\right]}_{aberrations}$$

式(18)

$$K(\alpha,\beta)=\underbrace{K_0(\alpha,\beta)}_{unaberrated}\underbrace{\exp\left[-i\frac{2\pi}{\lambda}W(\alpha,\beta)\right]}_{aberrations}$$

式(19)

ここで、

$$K_0(\alpha,\beta)=\underbrace{\left[\frac{1-\left(\alpha^2+\beta^2\right)/M^2}{1-\left(\alpha^2+\beta^2\right)}\right]^{1/4}}_{obliquity-factor}\underbrace{\exp\left[-i\frac{2\pi}{\lambda}z\sqrt{1-\alpha^2-\beta^2}\right]}_{defocus}$$

式(20)

$$W(\alpha,\beta)=\sum_{v=5}^{37}Z_vR_v(\alpha,\beta)$$

式(21)

$$e^x=1+x+\frac{x^2}{2!}+\frac{x^3}{3!}+\ldots\cong 1+x$$

式(22)

【0067】式22から、波面を線形の近似として書くことができる。これを式23に示す。式23を式22に代入することで、式24により、投影ひとみK（α，β）についての線形近似を算出することができる。

$$\exp\left[-i\frac{2\pi}{\lambda}W(\alpha,\beta)\right]\cong 1-i\frac{2\pi}{\lambda}W(\alpha,\beta)=1-i\frac{2\pi}{\lambda}\sum_{v=5}^{37}Z_vR_v(\alpha,\beta)$$

式(23)

$$K(\alpha,\beta)\cong K_0(\alpha,\beta)\left[1-i\frac{2\pi}{\lambda}\sum_{v=5}^{37}Z_vR_v(\alpha,\beta)\right]$$

式(24)

【0068】TCCは投影ひとみK（α，β）の関数であるので、式24におけるひとみに対する線形近似は、線形近似によってTCCを表すことが可能であることを示している。これは、式24を式1に代入することで達成される。これによって式25が得られる。再び、2以上のべきの項を無視することで、式25のTCCを式26に示すように簡略化することができる。

【0069】波面W（α，β）は、式21に示すように、ゼルニケ縞多項式の和によって示されることが最も多い。収差の線形理論を用いて、指数e^xを、テイラー級数の展開によって表すことができる。テイラー級数の展開は、小さいxについては有効であり、以前の研究によって、Z_vが0．04λ未満の場合、空中像について良好な一致が示されている。式22に、e^xについてのテイラー級数の展開を示す。式22では、2以上のべきの項を切り捨てているが、これは、Z_vが0．04未満である場合に有効である（$0.04^2=0.0016$であり、無視することができる）。

$$TCC(m,n,p,q)\cong \iint_{\sqrt{\alpha^2+\beta^2}<\sigma} J_s(\alpha,\beta)K_0\left(\alpha+\frac{m\lambda}{P_xNA},\beta+\frac{n\lambda}{P_yNA}\right)\left[1-i\frac{2\pi}{\lambda}\sum_{v=5}^{37}Z_vR_v\left(\alpha+\frac{m\lambda}{P_xNA},\beta+\frac{n\lambda}{P_yNA}\right)\right]$$

$$\cdot K_0^*\left(\alpha-\frac{p\lambda}{P_xNA},\beta-\frac{q\lambda}{P_yNA}\right)\left[1+i\frac{2\pi}{\lambda}\sum_{v=5}^{37}Z_vR_v\left(\alpha-\frac{p\lambda}{P_xNA},\beta-\frac{q\lambda}{P_yNA}\right)\right]d\alpha d\beta$$

式(25)

$$TCC(m,n,p,q)\cong \iint_{\sqrt{\alpha^2+\beta^2}<\sigma} J_s(\alpha,\beta)K_0\left(\alpha+\frac{m\lambda}{P_xNA},\beta+\frac{n\lambda}{P_yNA}\right)K_0^*\left(\alpha-\frac{p\lambda}{P_xNA},\beta-\frac{q\lambda}{P_yNA}\right)$$

$$\cdot\left[1-i\frac{2\pi}{\lambda}\sum_{v=5}^{37}Z_vR_v\left(\alpha+\frac{m\lambda}{P_xNA},\beta+\frac{n\lambda}{P_yNA}\right)+i\frac{2\pi}{\lambda}\sum_{v=5}^{37}Z_vR_v\left(\alpha-\frac{p\lambda}{P_xNA},\beta-\frac{q\lambda}{P_yNA}\right)\right]d\alpha d\beta$$

式(26)

【0070】式27および28の非逸脱TCC、TCC_0(m，n，p，q)、および逸脱TCC、TCC_v(m，n，p，q)をそれぞれ規定することで、式29に示すように、TCC_0およびTCC_vの線形関数によってTCCを表すことができる。

$$TCC_0(m,n,p,q)=\iint_{\sqrt{\alpha^2+\beta^2}<\sigma} J_s(\alpha,\beta)K_0\left(\alpha+\frac{m\lambda}{P_xNA},\beta+\frac{n\lambda}{P_yNA}\right)K_0^*\left(\alpha-\frac{p\lambda}{P_xNA},\beta-\frac{q\lambda}{P_yNA}\right)d\alpha d\beta$$

式(27)

$$TCC_v(m,n,p,q)=-i\frac{2\pi}{\lambda}\iint_{\sqrt{\alpha^2+\beta^2}<\sigma} J_s(\alpha,\beta)K_0\left(\alpha+\frac{m\lambda}{P_xNA},\beta+\frac{n\lambda}{P_yNA}\right)$$

式(28)

$$TCC(m,n,p,q)\equiv TCC_0(m,n,p,q)+\sum_{v=5}^{37}Z_v\left[TCC_v(m,n,p,q)+TCC_v^*(-p,-q,-m,-n)\right]$$

式(29)

【0071】式29に示すように線形近似としてTCCを構築することができるので、J_{opt}も線形近似として書くことができる。J_{opt}に対する線形近似は、J_{opt}についての式8を用い、式18および29に概要を記したようなTCCの線形近似についての方法論に従うことで、式30において求められる。

$$J_{opt}(\alpha,\beta,m,n,p,q)\equiv J_s(\alpha,\beta)T(m,n)T^*(-p,-q)K_0\left(\alpha+\frac{m\lambda}{P_xNA},\beta+\frac{n\lambda}{P_yNA}\right)K_0^*\left(\alpha-\frac{p\lambda}{P_xNA},\beta-\frac{q\lambda}{P_yNA}\right)$$

$$\cdot\left[1-i\frac{2\pi}{\lambda}\sum_{v=5}^{37}Z_vR_v\left(\alpha+\frac{m\lambda}{P_xNA},\beta+\frac{n\lambda}{P_yNA}\right)+i\frac{2\pi}{\lambda}\sum_{v=5}^{37}Z_vR_v\left(\alpha-\frac{p\lambda}{P_xNA},\beta-\frac{q\lambda}{P_yNA}\right)\right]d\alpha d\beta$$

式(30)

【0072】次いで、J_{opt}についての式30を、式33に示すように、非逸脱J_{opt0}および逸脱J_{optv}の和に分割することができる。式31および32に、J_{opt0}およびJ_{optv}の定義をそれぞれ示す。

$$J_{opt0}(\alpha,\beta,m,n,p,q)=J_s(\alpha,\beta)K_0\left(\alpha+\frac{m\lambda}{P_xNA},\beta+\frac{n\lambda}{P_yNA}\right)K_0^*\left(\alpha-\frac{p\lambda}{P_xNA},\beta-\frac{q\lambda}{P_yNA}\right)$$

式(31)

$$J_{optv}(\alpha,\beta,m,n,p,q)=-i\frac{2\pi}{\lambda}J_s(\alpha,\beta)K_0\left(\alpha+\frac{m\lambda}{P_xNA},\beta+\frac{n\lambda}{P_yNA}\right)$$

$$\cdot K_0^*\left(\alpha-\frac{p\lambda}{P_xNA},\beta-\frac{q\lambda}{P_yNA}\right)R_v\left(\alpha+\frac{m\lambda}{P_xNA},\beta+\frac{n\lambda}{P_yNA}\right)$$

式(32)

【0073】式32は、特定の収差に結合する照明形状の部分を記述する。結合量は、画像強度に影響を与え、照明に対する収差の感度の理解に役立つ。式31および32を組み合わせることで、J_{opt}を線形近似として書くことができる。

$$J_{opt}(\alpha,\beta,m,n,p,q)\cong J_{opt0}(\alpha,\beta,m,n,p,q)+\sum_{v=5}^{37}Z_v\left[J_{optv}(\alpha,\beta,m,n,p,q)+J_{optv}^*(\alpha,\beta,-p,-q,-m,-n)\right]$$

式(33)

【0074】本発明の別の態様では、重み付け係数を導入して、例えば、焦点深度（ＤＯＦ）、画像ログ傾斜（ＩＬＳ）、画像傾斜（ＩＳ）、または収差感度を含む特定の測定基準に対する応答を最大化または最小化することができる。式34に示すように、これらの重み付け係数を含むように式15の最適なJ_{tot}を変更することができる。

$$J_{tot}(\alpha,\beta)=\sum_m\sum_n\sum_p\sum_q w(\alpha,\beta,m,n,p,q)J_{opt}(\alpha,\beta,m,n,p,q)$$

式(34)

【0075】一般に、フォトレジストは、それに入射する光の強度の対数に比例して反応する。強度、従って強度の対数が増大するにつれて、フィーチャは、より高い忠実度でレジスト内に印刷される（すなわち、レジスト・プロファイルが改善し、プロセス・ウインドウが改善する）。従って、強度の対数変化（ＩＬＳ）を最大とすることが望ましい。式35に、ＩＬＳを定義する。

$$ILS\propto\frac{\partial\ln I}{\partial x}=\frac{1}{I}\frac{\partial I}{\partial x}$$

式(35)

【0076】強度の導関数は強度の逆数よりも変化が速いので、強度の導関数を増大させることで式35は更に増大する。強度は式3から算出可能であり、xに対する強度の導関数は式36において定義される。xに対する導関数によって、式37に示すように、重み付け関数w_xが得られる。同様に、式38に示すように、yに対する重み付け関数w_yを定義することができる。

$$\frac{\partial I(x,y)}{\partial x}=\sum_m\sum_n\sum_p\sum_q i\frac{2\pi}{P_x}(m+p)e^{ix\left[\frac{2\pi}{P_x}(m+p)\right]}e^{iy\left[\frac{2\pi}{P_y}(n+q)\right]}DOCC(m,n,p,q)$$

$$=\sum_m\sum_n\sum_p\sum_q w_x(m,p)e^{ix\left[\frac{2\pi}{P_x}(m+p)\right]}e^{iy\left[\frac{2\pi}{P_y}(n+q)\right]}DOCC(m,n,p,q)$$

式（３６）

$$w_x=i\frac{2\pi}{P_x}(m+p)$$

式（３７）

$$w_y=i\frac{2\pi}{P_y}(n+q)$$

式（３８）

【００７７】パターン・フィーチャおよび強度フィーチャは２次元であるので、傾斜のノルムを用いて、位置に対する強度の変化を示すことができる。式３９に、強度傾斜のノルムを定義する。これによって、我々は、式３４におけるJ_{tot}を算出するための重み付け関数を定義することができる。式４０によって、画像ログ傾斜を最大化するための重み付け関数を定義する。

$$\|\nabla I\|\Rightarrow w_{NILS}=\sqrt{|w_x|^2+|w_y|^2}$$

式（３９）

$$w_{ILS}(m,n,p,q)=2\pi\sqrt{\left(\frac{m+p}{P_x}\right)^2+\left(\frac{n+q}{P_y}\right)^2}$$

式（４０）

【００７８】式４０は、ｍ＋ｐ＝０およびｎ＋ｑ＝０である場合、重み付け関数が０になることを示す。ｍ＋ｐ＝０およびｎ＋ｑ＝０である場合、これらのオーダーは、画像変調に何ら寄与せず、画像に対するＤＣ寄与を反映する。更に、ｍ＋ｐおよびｎ＋ｑが増大するにつれて、w_{ILS}が増大する。これは、より高いオーダーの回折オーダー項は、より大きく重み付けされ、ＩＬＳに対する寄与が大きくなることを示している。

【００７９】ＩＬＳの最大化に加え、ＩＬＳが改善されて焦点に対する強度反応が最小限に抑えられると、プロセスの焦点深度が大きくなる。焦点は、ひとみＫ（α，β）によって説明される。ひとみＫ（α，β）を式４１に示すが、ここで、焦点はｚと示している。式４１は、２つの項に分割することができる。すなわち、式４２に示すように、ｚに依存する項（焦点はずれ項）およびｚから独立している項（非焦点はずれ項）である。

$$K(\alpha,\beta)=\underbrace{\left[\frac{1-(\alpha^2+\beta^2)/M^2}{1-(\alpha^2+\beta^2)}\right]^{1/4}}_{obliquity-factor}\underbrace{exp\left[-i\frac{2\pi}{\lambda}z\sqrt{1-\alpha^2-\beta^2}\right]}_{defocus}\underbrace{exp\left[-i\frac{2\pi}{\lambda}W(\alpha,\beta)\right]}_{aberrations}$$

式（４１）

$$K(\alpha,\beta)=\underbrace{K_{nd}(\alpha,\beta)}_{non-defocused}\underbrace{\exp\left[-i\frac{2\pi}{\lambda}z\sqrt{1-\alpha^2-\beta^2}\right]}_{defocus}=K_{nd}(\alpha,\beta)K_d(\alpha,\beta)$$

式（４２）

【００８０】ｚに対する強度の導関数をゼロに設定することで、焦点ｚによる強度の変動を最小限に抑えることができる。式４２を式１ないし３に代入して、式４３に示すように、費用関数ｆ（α，β，ｚ）を定義することができる。これは、ｚに依存する強度結像項の費用関数である。

$$f(\alpha,\beta,z)=K_d\left(\alpha+\frac{m\lambda}{P_xNA},\beta+\frac{n\lambda}{P_yNA}\right)K_d^*\left(\alpha-\frac{p\lambda}{P_xNA},\beta-\frac{q\lambda}{P_yNA}\right)$$

式（４３）

【００８１】一方、費用関数ｆ（α，β，ｚ）は、ｇ（α，β，ｍ，ｎ，ｐ，ｑ）がゼロに等しい場合、最小

限に抑えられる（以下の式４４を参照）。式４４では、大きさの項がゼロに等しい場合にのみ、ｚに対する導関数がゼロに等しいので、位相項が除去されている。ｇ（α，β，ｍ，ｎ，ｐ，ｑ）がゼロである場合、所与のオーダー（ｍ，ｎ，ｐ，ｑ）についてのひとみの領域（α，β）は、焦点に対する感度が最小である。これらは、照明形状を構築するための、ひとみの最も望ましい領域である。式４５に、重み付け関数w_{focus}（α，β，ｍ，ｎ，ｐ，ｑ）を定義する。この重み付け関数は、焦点に対する感度が最低の領域では１に等しく、焦点に対する感度が最高の領域では０に等しい。次いで、式４６によって、全焦点を通じてＩＬＳを最大化する新たな重み付け関数を定義し、これを用いて、照明形状を変更することができる。

$$g(\alpha,\beta,n,n,p,q)=\frac{\partial}{\partial z}f(\alpha,\beta,z)$$

$$=\left[-i\frac{2\pi}{\lambda}\sqrt{1-\left(\alpha+\frac{m\lambda}{P_xNA}\right)^2-\left(\beta+\frac{n\lambda}{P_yNA}\right)^2}+i\frac{2\pi}{\lambda}\sqrt{1-\left(\alpha-\frac{p\lambda}{P_xNA}\right)^2-\left(\beta-\frac{q\lambda}{P_yNA}\right)^2}\right]$$

式（４４）

$$w_{focus}(\alpha,\beta,m,n,p,q)=1-|g(\alpha,\beta,m,n,p,q)|$$

式（４５）

$$w(\alpha,\beta,m,n,p,q)=w_{ILS}(m,n,p,q)w_{focus}(\alpha,\beta,m,n,p,q)$$

式（４６）

【００８２】上述の方法論によって、焦点の影響、収差に対して、強度の感度を最小限に抑えることができる。強度に対する焦点の影響が最小限に抑えられるので、特定の収差に対して強度の影響を最小限に抑えられる。これは、特定の収差に対して高い感度が実証されている何らかのパターンについて望ましい。式１９における投影ひとみは、式４７に示すように、逸脱項K_a（α，β）によって乗算した非逸脱項K_0（α，β）として書くことができる。

$$K(\alpha,\beta)=K_0(\alpha,\beta)K_a(\alpha,\beta)$$

式（４７）

【００８３】特定の収差Z_iに対する強度の感度は、Z_iに対する強度の導関数をゼロに設定することで、最小限に抑えることができる。式４７を式１ないし３に代入し、強度の導関数を取ることで、式４８におけるｈ（α，β，ｍ，ｎ，ｐ，ｑ）がゼロに等しい場合、収差感度を最小限に抑える。

$$\frac{\partial}{\partial Z_i}I(x,y)=0\Rightarrow$$

$$h(\alpha,\beta,m,n,p,q)=K_a\left(\alpha+\frac{m\lambda}{P_xNA},\beta+\frac{n\lambda}{P_yNA}\right)\frac{\partial}{\partial Z_i}K_a^*\left(\alpha-\frac{p\lambda}{P_xNA},\beta-\frac{q\lambda}{P_yNA}\right)$$

$$+\frac{\partial}{\partial Z_i}K_a\left(\alpha+\frac{m\lambda}{P_xNA},\beta+\frac{n\lambda}{P_yNA}\right)K_a^*\left(\alpha-\frac{p\lambda}{P_xNA},\beta-\frac{q\lambda}{P_yNA}\right)=0 \qquad \text{式（４８）}$$

$$h(\alpha,\beta,m,n,p,q)=\left[R_i\left(\alpha-\frac{p\lambda}{P_xNA},\beta-\frac{q\lambda}{P_yNA}\right)-R_i\left(\alpha+\frac{m\lambda}{P_xNA},\beta+\frac{n\lambda}{P_yNA}\right)\right]=0 \qquad \text{式（４９）}$$

【００８４】式４８は、式４９のように簡略化して書くことも可能である。式５０において重み付け関数w_{ab}（α，β，ｍ，ｎ，ｐ，ｑ）を定義し、これはZ_iに対して感度が最低のひとみの領域（α，β）では１に等しく、Z_iに対して感度が最高の領域では０に等しい。

$$w_{ab}(\alpha,\beta,m,n,p,q)=1-\frac{1}{2}|h(\alpha,\beta,m,n,p,q)| \qquad \text{式（５０）}$$

【００８５】次いで、式５１において、特定の収差Z_iに対するＩＬＳ感度を最小限に抑える重み付け関数を定義することができる。更に、式５２に、特定の収差Z_iに対するＩＬＳ感度を最小限に抑え、全焦点を通じてＩＬＳを最大化する重み付け関数も定義することができる。これらの式のいずれも式３４に代入して、所与の測定基準に対する最適な応答を有する照明装置を算出することができる。

$$w(\alpha,\beta,m,n,p,q)=w_{NILS}(m,n,p,q)w_{ab}(\alpha,\beta,m,n,p,q) \quad \text{式(51)}$$

$$w(\alpha,\beta,m,n,p,q)=w_{NILS}(m,n,p,q)w_{focus}(\alpha,\beta,m,n,p,q)w_{ab}(\alpha,\beta,m,n,p,q) \quad \text{式(52)}$$

【0086】図15は、本発明に従って用いられるリソグラフィ装置の1例の概略図である。この装置は、放射システムを含む。放射システムは、ランプLA（これは、例えばエキシマ・レーザとすれば良い）と、照明システムとから成る。照明システムは、例えば、ビーム整形光学系EX、積分器IN、および集光レンズCOを備えることができる。放射システムは、放射の投影ビームPBを供給する。例えば、放射システムは、紫外線、深紫外線、または超紫外線放射を供給することができる。また、一般に、放射システムは、軟X線または他の形態の放射を供給することも可能である。

【0087】第1の物体テーブルまたはマスク・テーブルMTが、マスクMAを保持する。マスクMAは、結像対象のマスク・パターンを含むパターン領域Cを含む。マスク・テーブルMTは、投影ビームPBに対して移動することができるので、マスクの異なる部分を照射することが可能である。マスクが基板またはウエハWと適切に位置合わせされているか否かを判定するために、位置合わせマスクM_1およびM_2を用いる。

【0088】投影システムPLが、投影ビームPBをウエハW上に投影する。ウエハWは、2枚の位置合わせマスクP_1およびP_2を含み、これらは、結像を開始する前にマスクM_1およびM_2と位置合わせされる。ウエハWは、基板テーブルWTによって支持され、このテーブルWTは、ウエハWの異なる部分を露光するために投影ビームに対して移動することができる。このようにして、マスク・パターンCを、ウエハWの異なる対象部分c上に結像することができる。ウエハ・テーブルWTがマスク・テーブルMTの位置に対して確実に正しい位置にあるようにするために、干渉位置モニタIFを用いる。

【0089】本発明について、特定の実施形態に関連付けて説明してきたが、本発明は開示した実施形態に限定されるわけではなく、逆に、特許請求の範囲内に含まれる様々な変形および均等の構成を包含するよう意図することは理解されよう。

【図面の簡単な説明】

【図1】一般化した画像形成システムのための相互透過係数関数の図である。

【図2】れんが壁分離パターンのマイクロリソグラフィによるマスク・フィーチャの1例である。

【図3】図2のマスク・フィーチャの回折オーダーの図である。

【図4】図2のマスク・フィーチャのための算出された最適化4次元照明形状のマップである。

【図5】図2のマスク・フィーチャのための算出された初期グレー・スケール照明形状（J_{tot}）である。

【図6】図5の照明形状の2値表現である。

【図7】環状照明形状によって印刷した図2のマスク・フィーチャの印刷物の分析を示す。

【図8】最適化した楕円照明形状によって印刷した図2のマスク・フィーチャの印刷物の分析を示す。

【図9】110nm設計基準に縮小した図2のマスク・フィーチャのための算出された最適化4次元照明形状のマップである。

【図10】110nm設計基準に縮小した図2のマスク・フィーチャのための算出された初期グレー・スケール照明形状である。

【図11a】σの値が異なる図10の照明形状の2値表現である。

【図11b】σの値が異なる図10の照明形状の2値表現である。

【図12】クリティカル・ゲートおよびセルを示したマスク・パターンの1例である。

【図13】パターンのピッチ数を減らすために補助フィーチャを加えた図12のマスク・パターンである。

【図14】図12および13のマスク・パターンの空間幅の確率密度関数を比較する。

【図15】マイクロフォトリソグラフィのための装置の概略図である。

【図1】

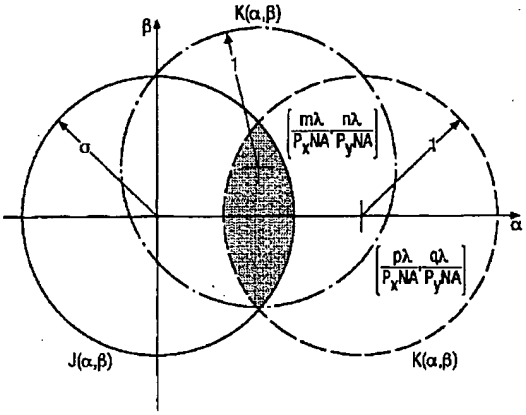

【図2】

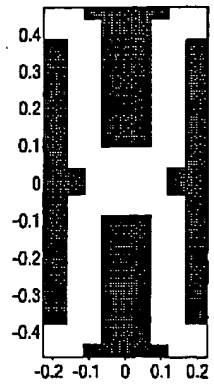

【図6】

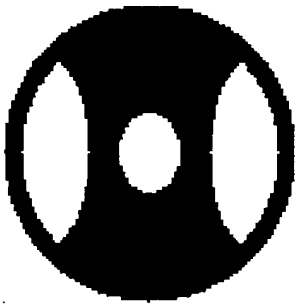

【図11a】

【図3】

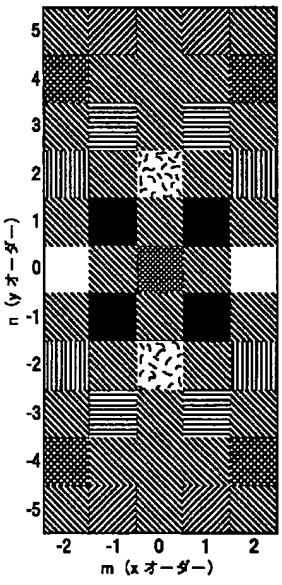

【図5】

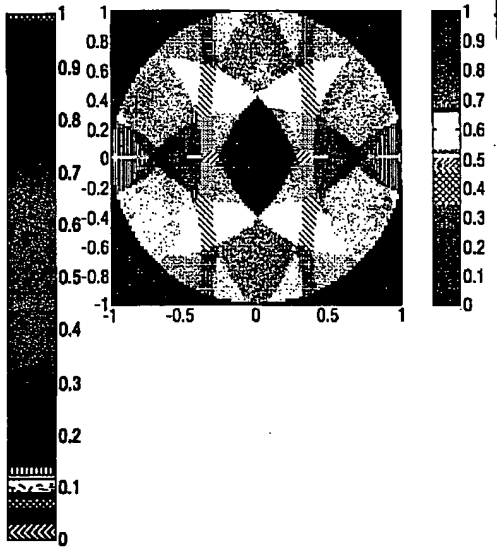

【図10】

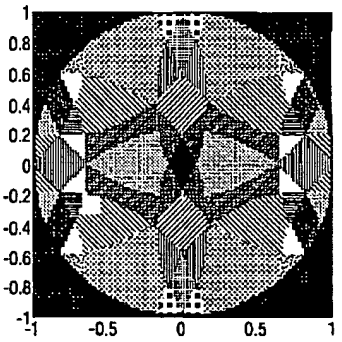

【図11b】

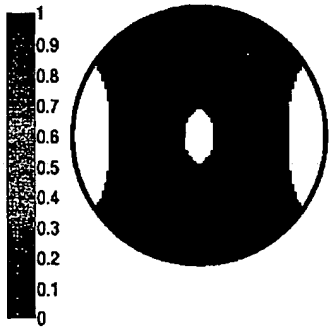

【図4】

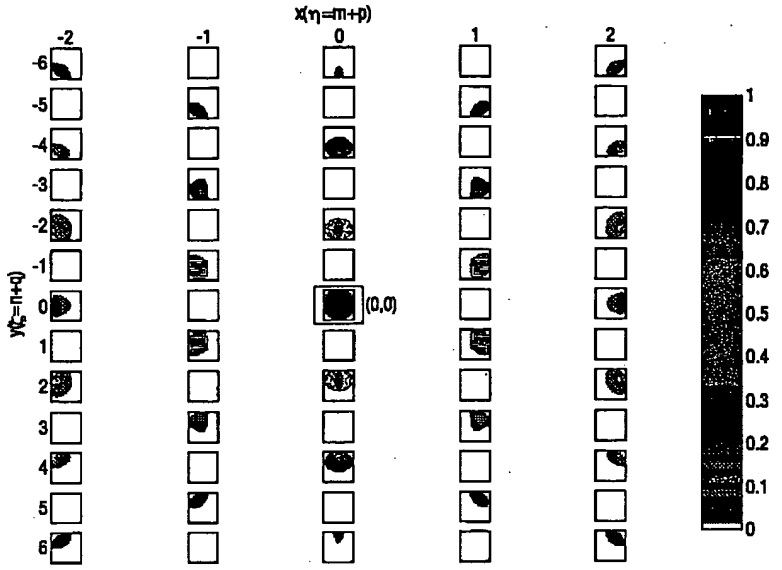
x(η=m+p)
-2
-1
0
1
2
y(ξ=n+q)
-6
-5
-4
-3
-2
-1
0
1
2
3
4
5
6
(0,0)
1
0.9
0.8
0.7
0.6
0.5
0.4
0.3
0.2
0.1
0

【図9】

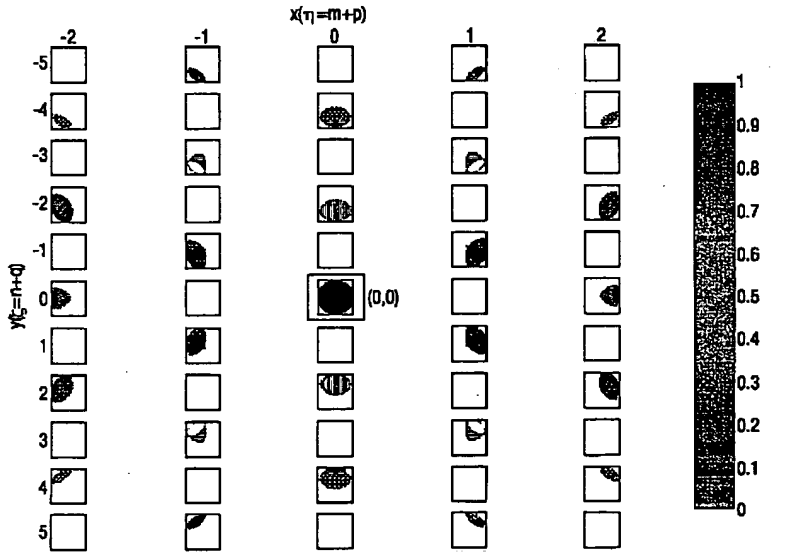
x(η=m+p)
-2
-1
0
1
2
y(ξ=n+q)
-5
-4
-3
-2
-1
0
1
2
3
4
5
(0,0)
1
0.9
0.8
0.7
0.6
0.5
0.4
0.3
0.2
0.1
0

【図7】

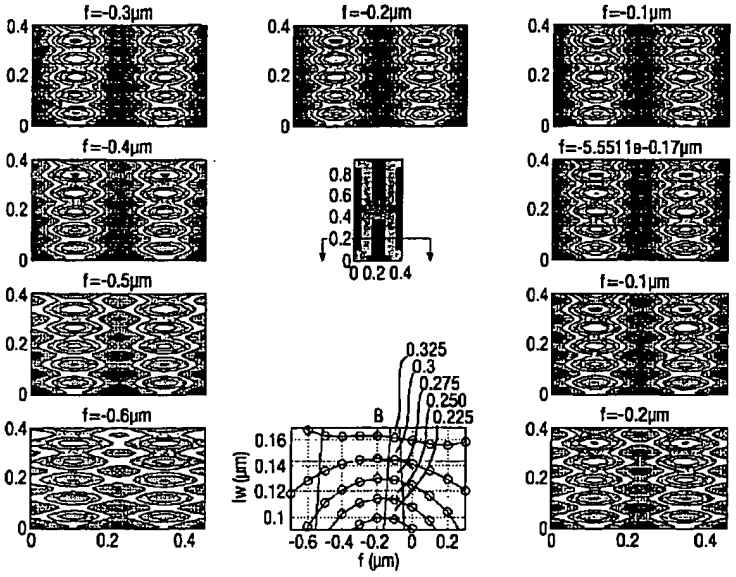
f=-0.3μm
f=-0.2μm
f=-0.1μm
f=-0.4μm
f=-5.5511e-0.17μm
f=-0.5μm
f=-0.1μm
f=-0.6μm
f=-0.2μm
B
0.325
0.3
0.275
0.250
0.225
lw (μm)
f (μm)

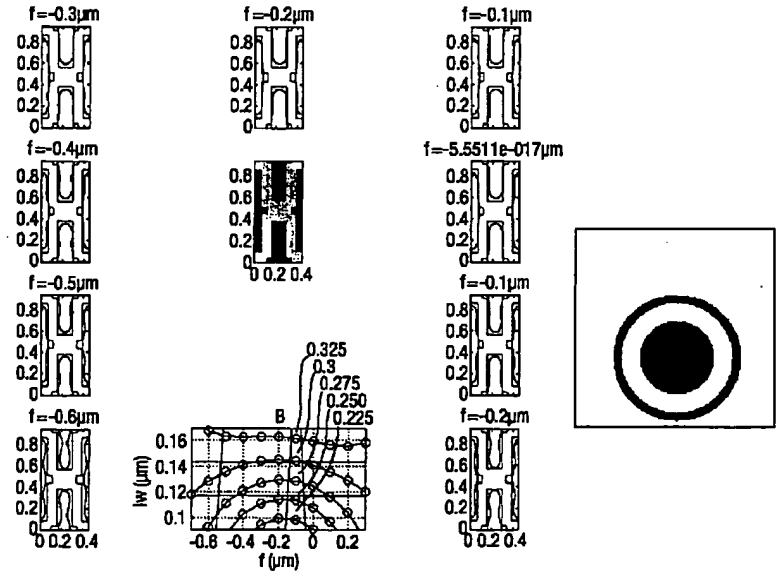
f=-0.3μm
f=-0.2μm
f=-0.1μm
f=-0.4μm
f=-5.5511e-017μm
f=-0.5μm
f=-0.1μm
f=-0.6μm
f=-0.2μm
B
0.325
0.3
0.275
0.250
0.225
lw (μm)
f (μm)

【図8】

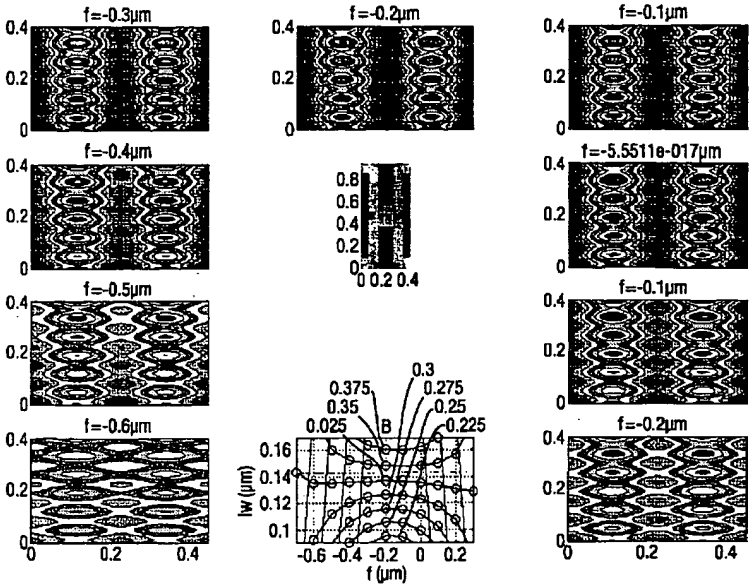
f=-0.3μm
f=-0.2μm
f=-0.1μm
f=-0.4μm
f=-5.5511e-017μm
f=-0.5μm
f=-0.1μm
f=-0.6μm
f=-0.2μm
0.3
0.375
0.275
0.35
0.25
0.025
B
0.225
lw (μm)
f (μm)

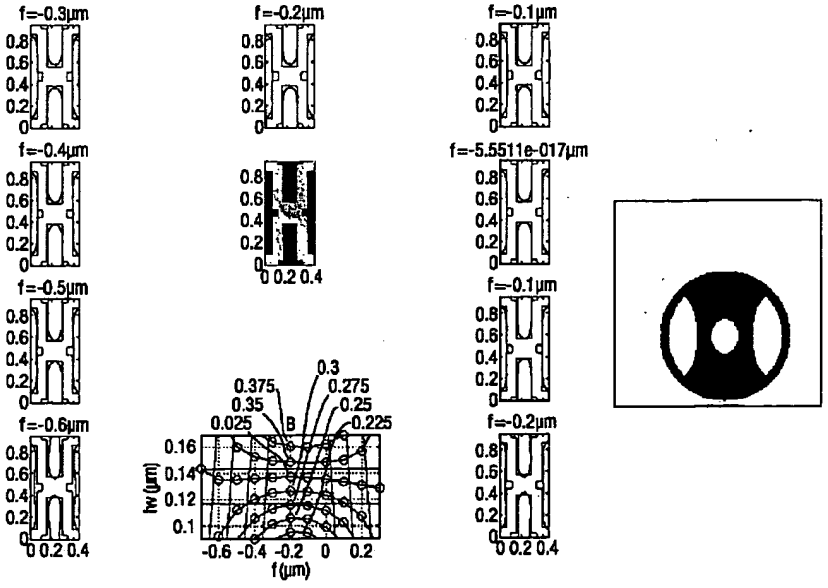
f=-0.3μm
f=-0.2μm
f=-0.1μm
f=-0.4μm
f=-5.5511e-017μm
f=-0.5μm
f=-0.1μm
f=-0.6μm
f=-0.2μm
0.3
0.375
0.275
0.35
0.25
0.025
B
0.225
lw (μm)
f (μm)

【図12】

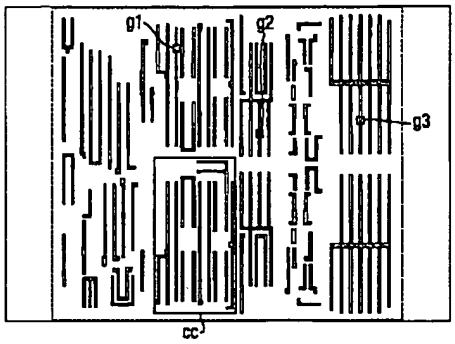

【図13】

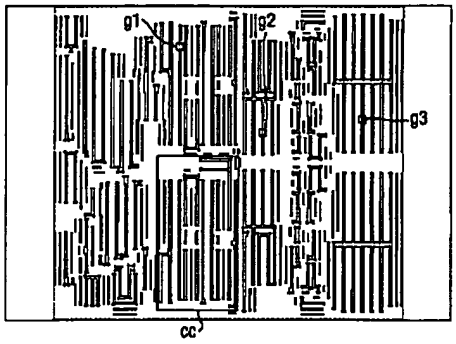

【図14】

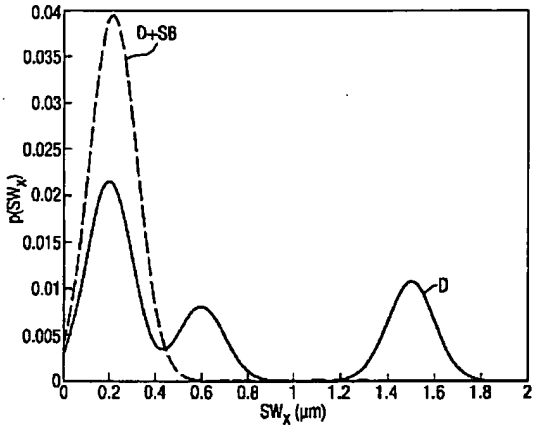

【図15】

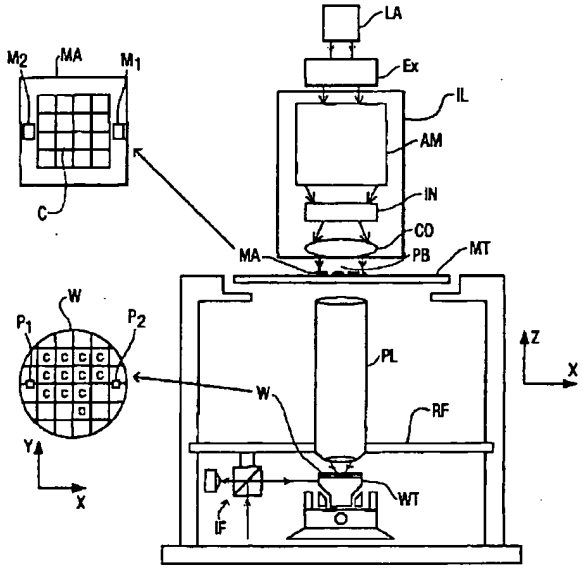

【外国語明細書】

1 Title of Invention

ILLUMINATION OPTIMIZATION FOR SPECIFIC MASK PATTERNS

2 Claims

1. A method of optimizing an illumination profile for a selected patterning means pattern, comprising the steps of:

defining a transmission cross coefficient function for an optical system including an illuminator and the selected patterning means pattern;

determining relative relevance to imaging of diffraction orders based on the selected pattern; and

calculating an optimized illumination configuration from the transmission cross coefficient function, weighting regions of the illumination configuration based on the relative relevance to imaging of the diffraction orders.

2. A method as in claim 1, wherein the step of determining relative relevance to imaging of diffraction orders further comprises the step of:

determining a characteristic pitch of the selected mask pattern.

3. A method as in claim 2, further comprising the steps of:

identifying a critical region of the selected pattern prior to determining the characteristic pitch,

wherein determining the characteristic pitch for the selected pattern is performed by determining the characteristic pitch for the critical region.

4. A method as in claim 3, wherein the step of identifying a critical region further comprises identifying a plurality of critical regions and wherein determining the characteristic pitch for the critical region includes:

comparing a pitch of each identified critical region; and

if the pitch of each identified region is substantially equal, determining the characteristic pitch for the critical region to be equal to the characteristic pitch of one of the identified regions.

5. A method as in any one of the preceding claims, further comprising weighting regions of the illuminator configuration based on a selected optimized metric selected from the group consisting of depth of focus, end-of-line, image log slope (ILS), image slope (IS), and aberration sensitivity.

6. A method as in claim 1 or 2, further comprising the steps of:

identifying a plurality of critical regions;

determining a pitch of each of the identified critical regions; and

calculating optimized illumination configurations from the transmission cross coefficient function, weighing orders based on relevance to imaging of diffraction orders for each critical region, and

wherein calculating an optimized illumination configuration further comprises calculating a composite optimized illumination configuration based on the calculated optimized illumination configuration for each critical region.

7. A method as in any one of the preceding claims, further comprising the steps of:

modifying the selected pattern by optical proximity correction techniques to reduce a total number of different pitches in the mask pattern.

8. A method as in claim 7, wherein the step of modifying the selected pattern by optical proximity correction techniques further comprises addition of sub-resolution features to the selected mask pattern.

9. A method as in claim 7, wherein the steps of modifying the selected pattern and calculating an optimized illumination configuration steps are iterated.

10. A computer program for optimizing an illumination profile comprising program code means that, when executed on a computer system, instruct the computer system to carry out the steps of the method of any one of claims 1 to 9.

11. A device manufacturing method comprising the steps of:

(a) providing a substrate that is at least partially covered by a layer of radiation-sensitive material;

(b) providing a projection beam of radiation using an illumination system;

(c) using patterning means to endow the projection beam with a pattern in its cross-section;

(d) projecting the patterned beam of radiation onto a target portion of the layer of radiation-sensitive material, wherein, prior to step (d), the cross-sectional intensity distribution in the projection beam produced in step (b) is tailored to the pattern employed in step (c) using a method according to any one of claims 1 to 9.

12. A lithographic projection apparatus comprising:

- an illumination system for providing a projection beam of radiation;

- a support structure for supporting patterning means, the patterning means serving to pattern the projection beam according to a desired pattern;

- a substrate table for holding a substrate;

- a projection system for projecting the patterned beam onto a target portion of the substrate,

wherein the apparatus additionally comprises:

- calculating means, for defining a transmission cross coefficient function for the illuminator and the patterning means, determining relative relevance to imaging of diffraction orders based on the pattern produced by the patterning means, and calculating an optimized illumination configuration from the transmission cross coefficient function, weighing regions of the illumination configuration based on the relative relevance to imaging of the diffraction orders; and

- selecting means, for selecting the cross-sectional intensity distribution in the projection beam exiting the illumination system in accordance with the illumination configuration calculated by the said calculating means.

13. A method of optimizing a selected mask design comprising:

identifying critical features of the selected mask design;

determining an optimized illumination profile based on diffraction orders of the critical features; and

modifying the selected mask design by use of optical proximity correction techniques which are selected to reduce a number of pitches present in the selected mask design.

14. A method as in claim 11 wherein the optical proximity correction further comprises addition of sub-resolution features selected to modify a continuous probability density function of the space width of the selected mask design such that the modified probability density function has an increased discretization.

15. A method as in claim 13 or 14 wherein said step of determining an optimized illumination profile comprises the steps of the method of any one of claims 1 to 9.

16. A computer program for optimizing a selected mask design comprising program code means that, when executed on a computer, instruct the computer to carry out the method of any one of claims 13 to 15.

3 Detailed Description of Invention

This invention relates generally to a method and apparatus for microlithographic imaging. More particularly, it relates to an apparatus and method for optimizing an illumination configuration according to the specific pattern being imaged.
Optical lithography systems are in current use in the manufacture of integrated circuits and other fine featured products such as programmable gate arrays. In a most general description, a lithography apparatus includes an illumination system which provides a projection beam of radiation, a support structure which holds a patterning means, a substrate table which holds a substrate, and a projection system (lens) for imaging the patterned beam onto a target portion of the substrate.

The term patterning means should be broadly interpreted as referring to devices and structures that can be used to endow an incoming radiation beam with a patterned cross-section, corresponding to a pattern that is to be created in a target portion of a substrate; the term "light valve" has also been used in this context. Generally, the pattern will correspond to a particular functional layer in a device being created in the target portion, such as an integrated circuit or other device.

One example of such a device is a mask, which is generally held by a (movable) mask table. The concept of a mask is well known in lithography, and it includes mask types such as binary, alternating phase-shift, and attenuated phase-shift, as well as various hybrid mask types. Placement of such a mask in the projection beam causes selective transmission (in the case of a transmissive mask) or reflection (in the case of a reflective mask) of the radiation impinging on the mask, according to the pattern on the

mask. The mask table ensures that the mask can be held at a desired position in the incoming projection beam, and that it can be moved relative to the beam if so desired.

Another example of such a device is a matrix-addressable surface having a viscoelastic control layer and a reflective surface. The basic principle behind such an apparatus is that (for example) addressed areas of the reflective surface reflect incident light as diffracted light, whereas unaddressed areas reflect incident light as undiffracted light. Using an appropriate filter, the said undiffracted light can be filtered out of the reflected beam, leaving only the diffracted light behind; in this manner, the beam becomes patterned according to the addressing pattern of the matrix-addressable surface. An alternative embodiment of a programmable mirror array employs a matrix arrangement of tiny mirrors, each of which can be individually tilted about an axis by applying a suitable localized electric field, or by employing piezoelectric actuation means. Once again, the mirrors are matrix-addressable, such that addressed mirrors will reflect an incoming radiation beam in a different direction to unaddressed mirrors; in this manner, the reflected beam is patterned according to the addressing pattern of the matrix-addressable mirrors. The required matrix addressing can be performed using suitable electronic means. In both of the situations described hereabove, the patterning means can comprise one or more programmable mirror arrays. More information on mirror arrays as here referred to can be gleaned, for example, from United States Patents US 5,296,891 and US 5,523,193, and PCT patent applications WO 98/38597 and WO 98/33096, which are incorporated herein by reference. In the case of a programmable mirror array, the said support structure may be embodied as a frame or table, for example, which may be fixed or movable as required.

Another example is a programmable LCD array, in which case the support structure can again be a frame or table, for example. An example of such a construction is given in United States Patent US 5,229,872, which is incorporated herein by reference.

For purposes of simplicity, the rest of this text may, at certain locations, specifically direct itself to examples involving a mask; however, the general principles discussed in such instances should be seen in the broader context of the patterning means as hereabove set forth.

The term projection system encompasses various types of projection systems. Though "lens" in a layperson's understanding usually connotes only refractive optics, herein this term is used broadly to include catoptric and catadioptric systems, for example. The illumination system may also include elements operating according to any of these principles for directing, shaping or controlling the projection beam, and such elements may also be referred to below, collectively or singularly, as a "lens".

Additionally, the term "wafer table" may be used without implying that the substrate receiving the image is a silicon wafer, but may rather indicate a stage suited for support of any substrate to be processed by the lithography apparatus.

Lithographic projection apparatus can be used, for example, in the manufacture of integrated circuits (ICs). In such a case, the patterning means may generate a circuit pattern corresponding to an individual layer of the IC, and this pattern can be imaged onto a target portion (comprising one or more dies) on a substrate (silicon wafer) that has been coated with a layer of radiation-sensitive material (resist). In general, a single wafer will contain a network of adjacent target portions that are successively irradiated via the projection system, one at a time. In current apparatus, employing patterning by a mask on a mask table, a distinction can be made between two different types of machine. In one type of lithographic projection apparatus, each target portion is irradiated by exposing the entire mask pattern onto the target portion at once; such an apparatus is commonly referred to as a wafer stepper. In an alternative apparatus — commonly referred to as a step-and-scan apparatus — each target portion is irradiated by progressively scanning the mask pattern under the projection beam in a given reference direction (the "scanning" direction) while synchronously scanning the substrate table parallel or anti-parallel to this direction. Since, in general, the projection system will have a magnification factor M (generally < 1), the speed V at which the substrate table is scanned will be a factor M times that at which the mask table is scanned. More information with regard to lithographic devices as here described can be gleaned, for example, from US 6,046,792, incorporated herein by reference.

In a manufacturing process using a lithographic projection apparatus, a pattern (e.g. in a mask) is imaged onto a substrate that is at least partially covered by a layer of radiation-sensitive material (resist). Prior to this imaging step, the substrate may undergo various procedures, such as priming, resist coating and a soft bake. After exposure, the substrate may be subjected to other procedures, such as a post-exposure bake (PEB), development, a hard bake and measurement/inspection of the imaged

features. This array of procedures is used as a basis to pattern an individual layer of a device, e.g. an IC. Such a patterned layer may then undergo various processes such as etching, ion-implantation (doping), metallization, oxidation, chemo-mechanical polishing, etc., all intended to finish off an individual layer. If several layers are required, then the whole procedure, or a variant thereof, will have to be repeated for each new layer. Eventually, an array of devices will be present on the substrate (wafer). These devices are then separated from one another by a technique such as dicing or sawing, whence the individual devices can be mounted on a carrier, connected to pins, etc. Further information regarding such processes can be obtained, for example, from the book "Microchip Fabrication: A Practical Guide to Semiconductor Processing", Third Edition, by Peter van Zant, McGraw Hill Publishing Co., 1997, ISBN 0-07-067250-4, incorporated herein by reference.

For the sake of simplicity, the projection system may hereinafter be referred to as the "lens"; however, this term should be broadly interpreted as encompassing various types of projection system, including refractive optics, reflective optics, and catadioptric systems, for example. The radiation system may also include components operating according to any of these design types for directing, shaping or controlling the projection beam of radiation, and such components may also be referred to below, collectively or singularly, as a "lens". Further, the lithographic apparatus may be of a type having two or more substrate tables (and/or two or more mask tables). In such "multiple stage" devices the additional tables may be used in parallel, or preparatory steps may be carried out on one or more tables while one or more other tables are being used for exposures. Dual stage lithographic apparatus are described, for example, in US 5,969,441 and WO 98/40791, incorporated herein by reference.

As illumination systems have evolved from producing conventional to annular, and on to quadrupole and more complicated illumination configurations, the control parameters have concurrently become more numerous. In a conventional illumination pattern, a circular area including the optical axis is illuminated, the only adjustment to the pattern being to alter the outer radius (σ_r). Annular illumination requires the definition of an inner radius (σ_c) in order to define the illuminated ring. For multipole

patterns, the number of parameters which can be controlled continues to increase. For example in a quadrupole illumination configuration, in addition to the two radii, a pole angle α defines the angle subtended by each pole between the selected inner and outer radii.

Concurrently, mask technology has been evolving as well. Binary intensity masks have given way to phase-shifted masks and other advanced designs. While a binary mask simply transmits, reflects or blocks imaging radiation at a given point, a phase-shifted mask may attenuate some radiation or it may transmit or reflect the light after imparting a phase shift, or both. Phase-shifted masks have been used in order to image features which are on the order of the imaging radiation's wavelength or smaller, since diffraction effects at these resolutions can cause poor contrast and end-of-line errors, among other problems.

The various types of illumination configurations can be used to provide improvements in resolution, depth of focus, contrast and other characteristics of the printed image. However, each illumination type has certain tradeoffs. For example, improved contrast may come at the expense of depth of focus; each type of mask has a performance which is dependent on the pattern to be imaged as well.

Conventionally, in order to select the optimum illumination mode for a given pattern to be imaged onto a wafer, a series of test wafers has been exposed and compared on a hit-or-miss basis. As noted above, modern illumination systems have ever increasing numbers of variables which can be manipulated. As the various permutations of variable settings increase, the cost of trial and error optimization of illumination configurations becomes very large and quantitative methods of selecting illumination configurations are needed.

To provide for the above identified needs and others, the present invention provides a method of optimizing an illumination profile for a selected patterning means pattern, comprising the steps of:

defining a transmission cross coefficient function for an optical system including an illuminator and the selected patterning means pattern;

determining relative relevance to imaging of diffraction orders based on the selected pattern; and

calculating an optimized illumination configuration from the transmission cross coefficient function, weighting regions of the illumination configuration based on the relative relevance to imaging of the diffraction orders.

According to another aspect of the present invention there is provided a device manufacturing method comprising the steps of:

(a) providing a substrate that is at least partially covered by a layer of radiation-sensitive material;

(b) providing a projection beam of radiation using an illumination system;

(c) using patterning means to endow the projection beam with a pattern in its cross-section;

(d) projecting the patterned beam of radiation onto a target portion of the layer of radiation-sensitive material, wherein, prior to step (d), the cross-sectional intensity distribution in the projection beam produced in step (b) is tailored to the pattern employed in step (c) using a method as described above.

According to another aspect of the present invention there is provided a lithographic projection apparatus comprising:

- an illumination system for providing a projection beam of radiation;

- a support structure for supporting patterning means, the patterning means serving to pattern the projection beam according to a desired pattern;

- a substrate table for holding a substrate;

- a projection system for projecting the patterned beam onto a target portion of the substrate,

wherein the apparatus additionally comprises:

- calculating means, for defining a transmission cross coefficient function for the illuminator and the desired pattern, determining relative relevance to imaging of diffraction orders based on the pattern produced by the patterning means, and calculating an optimized illumination configuration from the transmission cross

coefficient function, weighing regions of the illumination configuration based on the relative relevance to imaging of the diffraction orders; and

- selecting means, for selecting the cross-sectional intensity distribution in the projection beam exiting the illumination system in accordance with the illumination configuration calculated by the calculating means.

According to a yet another aspect of the present invention there is provided a method of optimizing a selected mask design comprising:

identifying critical features of the selected mask design;

determining an optimized illumination profile based on diffraction orders of the critical features; and

modifying the selected mask design by use of optical proximity correction techniques which are selected to reduce a number of pitches present in the selected mask design.

The present invention further provides computer programs for carrying out the methods described above.

Although specific reference may be made in this text to the use of the apparatus according to the invention in the manufacture of ICs, it should be explicitly understood that such an apparatus has many other possible applications. For example, it may be employed in the manufacture of integrated optical systems, guidance and detection patterns for magnetic domain memories, liquid-crystal display panels, thin-film magnetic heads, etc. The skilled artisan will appreciate that, in the context of such alternative applications, any use of the terms "reticle", "wafer" or "die" in this text should be considered as being replaced by the more general terms "mask", "substrate" and "target portion", respectively.

The present invention will be described further below with reference to exemplary embodiments and the accompanying drawings, in which:

The present invention involves first mathematically modeling the imaging of the pattern onto the substrate (e.g. from a mask), taking into account the illumination source and the pattern details.

There are two primary methods for calculating the aerial image for a finite illumination source. These methods are Abbe's formulation and Hopkins's formulation. In Abbe's formulation, each point source in the illumination configuration produces a plane wave incident onto the pattern, and each of these point sources is imaged onto the wafer. Since the source is spatially incoherent, the total intensity at the wafer is the summation of the intensity produced by each of these point sources. Therefore, in Abbe's formulation, the integration over the illumination configuration is performed after the integration over the pattern.

In Hopkins's formulation, the order of integration is switched, i.e., the integration over the source is performed first. In Hopkins's formulation, a four dimensional transmission cross coefficient (TCC) is defined, and the image intensity is the inverse Fourier transform of the TCC. A derivation of the TCC is described, for example, in Born and Wolf, Principles of Optics, 6th Ed., pp. 528-532, herein incorporated by reference.

The TCC is the autocorrelation of the projection pupil multiplied by the illumination pupil. The TCC is shown in Figure 1 as a set of three overlapping circles. From left to right, the first circle represents the illumination pupil $J_s(\alpha,\beta)$ where α and β are coordinates of the illumination configuration. For the purposes of the following calculations, the radius of J_s may be, for example, set to the maximum allowable outer σ_r for the lithography apparatus which will be used for imaging. It is also possible to set σ_r to 1.0 or larger in order to perform feasibility studies and to determine the benefits of a larger σ_r.

The central circle represents the projection pupil, $K(\alpha,\beta)$ that is centered at $(-m\lambda/P_xNA, -n\lambda/P_yNA)$. The coordinate systems are normalized by a factor of λ/NA so that the radius of K is 1.0. The circle on the right likewise represents the projection pupil; however, it is centered at $(p\lambda/P_xNA, q\lambda/P_yNA)$. In these last two expressions, m,n,p, and q correspond to discrete diffraction orders and it becomes clear that the TCC is a four dimensional (4-D) equation as described above. The diffraction orders in the x-direction are represented by m and p and the diffraction orders in the y-direction are represented by n and q. Though for purposes of this description, x and y coordinates are

used, one skilled in the art understands that alternate coordinate systems could be used with appropriate changes of coordinate systems in the following equations.

The TCC for a 4-D discrete point (m,n,p,q) is the integral of the shaded area where all three circles overlap. Since the structure is assumed to be periodic, the Fourier transform of the pattern is discrete and the TCC is discrete. For a continuous pattern image, the pitch can be increased until an adjacent feature has no influence on the Fourier transform of the pattern of interest. The TCC in Figure 1 is described mathematically in Equation 1.

$$TCC(m,n,p,q) = \iint_{\sqrt{\alpha^2+\beta^2}<\sigma} J_s(\alpha,\beta)K\left(\alpha+\frac{m\lambda}{P_xNA},\beta+\frac{n\lambda}{P_yNA}\right)K^*\left(\alpha-\frac{p\lambda}{P_xNA},\beta-\frac{q\lambda}{P_yNA}\right)d\alpha d\beta \qquad \text{Eqn. 1}$$

The TCC may be expanded to include the effects of the pattern by defining diffraction order cross coefficients (DOCC). The DOCC are defined in Equation 2 which is derived from the multiplication of the TCC by the Fourier transform coefficients of the pattern.

$$DOCC(m,n,p,q) = T(m,n)T^*(-p,-q)TCC(m,n,p,q) \qquad \text{Eqn. 2}$$

Further, the radiation intensity at the wafer may be calculated by the inverse Fourier transform of the DOCC, as shown in Eqn. 3.

$$I(x,y) = \sum_m \sum_n \sum_p \sum_q e^{ix\left[\frac{2\pi}{P_x}(m+p)\right]} e^{iy\left[\frac{2\pi}{P_y}(n+q)\right]} DOCC(m,n,p,q) \qquad \text{Eqn. 3}$$

The projection optical system acts in part as a low pass filter, which reduces the diffraction orders so that only a few of the diffraction orders are important to the calculated image intensity. As a result, the TCC is a band limited function. The maximum necessary x and y orders can be calculated according to Equations 4 and 5

respectively. In each case, both the negative and positive orders are necessary, for example m extends from negative m_{max} to positive m_{max}.($-m_{max} \le m \le +m_{mmax}$). Since both negative and positive orders are needed, the size of the TCC is $2m_{max}+1$ by $2n_{max}+1$ by $2p_{max}+1$ by $2q_{max}+1$. Fortunately, however, because the TCC is band limited, it is not necessary to calculate all the pattern diffraction orders. Like in the TCC, only pattern diffraction orders $-m_{max} \le m \le +m_{max}$ in the x direction and orders $-n_{max} \le n \le +n_{max}$ in the y direction are needed.

$$f_{x\,max} = m_{max} = p_{max} = floor\left[\frac{P_x NA(1+\sigma_o)}{\lambda}\right] \qquad \text{Eqn. 4}$$

$$f_{y\,max} = n_{max} = q_{max} = floor\left[\frac{P_y NA(1+\sigma_o)}{\lambda}\right] \qquad \text{Eqn. 5}$$

Substituting Equations 1 and 2 into Equation 3 gives Equation 6 for the radiation intensity at the wafer. By switching the order of integration, as shown in Equation 7, that is, by using Abbe's formulation rather than Hopkins's, the portions of the illumination pupil which are most influential on imaging may be determined. Note that each of Equations 6 and 7 extends across two lines.

$$I(x,y) = \sum_m \sum_n \sum_p \sum_q e^{i\left[\frac{2\pi}{P_x}(m+p)\right]} e^{i\left[\frac{2\pi}{P_y}(n+q)\right]} T(m,n)T^*(-p,-q) \qquad \text{Eqn. 6}$$

$$\cdot \iint_{\sqrt{\alpha^2+\beta^2}<\sigma} J_s(\alpha,\beta)K\left(\alpha+\frac{m\lambda}{P_x NA},\beta+\frac{n\lambda}{P_y NA}\right)K^*\left(\alpha-\frac{p\lambda}{P_x NA},\beta-\frac{q\lambda}{P_y NA}\right)d\alpha d\beta$$

$$I(x,y)=\iint_{\sqrt{\alpha^2+\beta^2}<\sigma} d\alpha d\beta \sum_m \sum_n \sum_p \sum_q e^{i\left[\frac{2\pi}{P_x}(m+p)\right]x} e^{i\left[\frac{2\pi}{P_y}(n+q)\right]y} \quad \text{Eqn. 7}$$

$$\cdot J_s(\alpha,\beta)T(m,n)T^*(-p,-q)K\left(\alpha+\frac{m\lambda}{P_xNA},\beta+\frac{n\lambda}{P_yNA}\right)K^*\left(\alpha-\frac{p\lambda}{P_xNA},\beta-\frac{q\lambda}{P_yNA}\right)$$

Since α and β represent illumination pupil coordinates, a new function, J_{opt}, may be defined. The new function J_{opt} indicates which part of the illumination configuration (α,β) is being used for a given diffraction order (m,n,p,q) and is expressed in Equation 8. From Equation 8, the image intensity can be calculated by multiplying it by the inverse Fourier coefficient ($e^{i\alpha x}$) and summing over all 6 variables (m,n,p,q,α,β) as shown in Equation 9.

$$J_{opt}(\alpha,\beta,m,n,p,q)=J_s(\alpha,\beta)T(m,n)T^*(-p,-q)K\left(\alpha+\frac{m\lambda}{P_xNA},\beta+\frac{n\lambda}{P_yNA}\right)K^*\left(\alpha-\frac{p\lambda}{P_xNA},\beta-\frac{q\lambda}{P_yNA}\right)$$

Eqn. 8

$$I(x,y)=\iint_{\sqrt{\alpha^2+\beta^2}<\sigma} d\alpha d\beta \sum_m \sum_n \sum_p \sum_q e^{i\left[\frac{2\pi}{P_x}(m+p)\right]x} e^{i\left[\frac{2\pi}{P_y}(n+q)\right]y} J_{opt}(\alpha,\beta,m,n,p,q) \quad \text{Eqn. 9}$$

As will be appreciated, J_{opt} is a six dimensional function and it is therefore difficult to apply it to the illumination configuration. In order to best determine which portions of the illumination configuration are significant to image formation, it is desirable to eliminate a few of the six variables.

The aerial image intensity, I(x,y), is found by taking an inverse transform over m+p and n+q. When m+p=n+q=0, there is no modulation in the aerial image intensity.

Since one of the goals of illumination optimization is to eliminate parts of the illumination configuration that have little or no influence on modulation, those portions of the illumination configuration for which m+p = n+q = 0 may be eliminated. In order to eliminate these parts and to better visualize the illumination configuration portions significant to image formation, a transformation of variables will eliminate two of the variables in the six dimensional J_{opt} function (four diffraction orders) and convert it into a four dimensional function (two diffraction orders). The four dimensional function is called $J_{opt\text{-}2D}$. By substituting Equations 10 and 11 into Equation 9 for I(x,y), Equation 12 may be derived.

$$\eta = m + p \Rightarrow p = \eta - m \qquad \text{Eqn. 10}$$

$$\xi = n + q \Rightarrow q = \xi - n \qquad \text{Eqn. 11}$$

$$I(x,y) = \iint_{\sqrt{\alpha^2+\beta^2}<\sigma} d\alpha d\beta \sum_{\eta=-2f_{x\max}}^{+2f_{x\max}} \sum_{\xi=-2f_{y\max}}^{+2f_{y\max}} e^{ix\left[\frac{2\pi}{P_x}\eta\right]} e^{iy\left[\frac{2\pi}{P_y}\xi\right]} \underbrace{\sum_{m=-f_{x\max}}^{+f_{x\max}} \sum_{n=-f_{y\max}}^{+f_{y\max}} J_{opt}(\alpha,\beta,m,n,\eta-m,\xi-n)}_{J_{opt\text{-}2D}(\alpha,\beta,\eta,\xi)} \qquad \text{Eqn. 12}$$

In Equation 12, $J_{opt\text{-}2D}$ can be seen to be the summation of J_{opt} over m and n after the transformation of variables according to Equations 10 and 11. By further substituting Equation 8 into Equation 12, $J_{opt\text{-}2D}$ may be expressed as in Equation 13 and the intensity, I(x,y), can be written as a function of $J_{opt\text{-}2D}$ as in Equation 14.

$$J_{opt-2D}(\alpha,\beta,\eta,\xi) = J_s(\alpha,\beta) \sum_{m=-f_{x\max}}^{+f_{x\max}} \sum_{n=-f_{y\max}}^{+f_{y\max}} T(m,n)T^*[-(\eta-m),-(\xi-n)] \qquad \text{Eqn. 13}$$

$$\cdot K\left(\alpha + \frac{m\lambda}{P_x NA}, \beta + \frac{n\lambda}{P_y NA}\right) K^*\left(\alpha - (\eta-m)\frac{\lambda}{P_x NA}, \beta - (\xi-n)\frac{\lambda}{P_y NA}\right)$$

$$I(x,y)=\iint_{\sqrt{\alpha^2+\beta^2}<\sigma} d\alpha d\beta \sum_{\eta=-2f_{x\max}}^{+2f_{x\max}} \sum_{\xi=-2f_{y\max}}^{+2f_{y\max}} e^{ix\left[\frac{2\pi}{P_x}\eta\right]} e^{iy\left[\frac{2\pi}{P_y}\xi\right]} J_{opt-2D}(\alpha,\beta,\eta,\xi) \qquad \text{Eqn. 14}$$

The function, $J_{opt\text{-}2D}$, when evaluated, shows those portions of the illumination configuration that are important for each diffraction order. Since $J_{opt\text{-}2D}$ is weighted by each diffraction order, T(m,n), large diffraction orders will have a greater influence on the aerial image.

A starting point for the best illumination configuration for a particular pattern may be denoted J_{tot} and is found by summing $J_{opt\text{-}2D}$ over η and ξ and subtracting $J_{opt\text{-}2D}(\alpha,\beta,\eta=0,\xi=0)$ as shown in Equation 15. In Equation 15, when $\eta=0$ and $\xi=0$ there is no modulation in the aerial image and the $J_{opt\text{-}2D}(\alpha,\beta,\eta=0,\xi=0)$ component represents zero order or DC light. Points in the illumination that do not contribute to imaging increase the overall amount of DC light. Since the increased DC light causes no modulation it is not of great benefit, and moreover it can result in a reduction in depth of focus.

Thus, an illumination configuration in accordance with J_{tot} minimizes the amount of DC light and results in an improved process window. The equation J_{tot} can be used to show which parts of the illuminator are more significant (or less significant) to image formation.

$$J_{tot}(\alpha,\beta)=\left[\sum_{\eta=-2f_{x\max}}^{+2f_{x\max}} \sum_{\xi=-2f_{y\max}}^{+2f_{y\max}} \left|J_{opt-2D}(\alpha,\beta,\eta,\xi)\right|\right]-\left|J_{opt-2D}(\alpha,\beta,0,0)\right| \qquad \text{Eqn. 15}$$

Since the illumination configuration and pattern are coupled, optical proximity correction (OPC) changes influence the diffraction orders, which therefore influences J_{tot}. Consequently, modifications to the starting illumination configuration, J_{tot}, and the pattern should be performed a few times using iterations of processing with an OPC engine and an illumination engine, as will be understood by one skilled in the art.

Furthermore, the pattern and illumination configuration also need to be adjusted to optimize a particular imaging criteria (depth of focus (DOF), end of line (EOL), aberration sensitivity, etc.) which may be performed with optimization software. However, since the pattern as a whole, rather than the OPC features, has the largest impact on the optimal illumination configuration, J_{tot} is the best initial illumination configuration to lead to the fastest convergence for optimizing iterations over the illumination configuration and pattern.

The starting illumination configuration, J_{tot}, may be represented by a gray scale illumination configuration having continuous values of intensity over a 0 to 1 range. It is possible to create such a gray scale illumination configuration with a diffractive optical element (DOE) or by using a quartz plate with dithered chromium plating. If a gray scale illumination configuration is not possible or preferred, the illuminator profile can be forced to be only 0 and 1 by applying a threshold to the gray scale, in which values above the threshold are rounded up to 1 and values below the threshold are rounded down to 0. An arbitrary threshold can be applied, or an optimal threshold may be found through simulating the process window, or by repeated test runs.

Example 1: The technique for calculating J_{tot} outlined above was applied to a brick wall isolation pattern. A 150nm pattern was shrunk to 130nm and 110nm design rules and imaged with a step and scan lithography system having a numerical aperture (NA) of 0.8. The isolation pattern for the 130nm design rule is shown in Figure 2.

The magnitudes of the diffraction orders of this mask feature are plotted in Figure 3. In Figure 3, the largest order is the (0,0) order or the DC background light. The orders that contribute the most to imaging are the (±2,0) orders and represent the vertical bricks in the brick wall pattern. The other significant order is the (±1,±1) which represents the clear areas and defines the end of the isolation pattern. The higher orders also help to define two dimensional structures such as the end of each line. Since the diffraction orders are not constant, the orders change the weighting coefficients in the DOCC, which implies that the mask pattern influences the illumination strategy.

The diffraction order coefficients T(m,n) in Figure 3 can be substituted into Equation 13 to calculate J_{opt-2D} and are plotted in Figure 4. As can be seen from Figure

4, the largest contribution to J_{opt-2D} is the (η=0,ξ=0) order. The (0,0) order does not contribute to imaging and decreases the DOF. As Equation 15 shows, this (0,0) order can be subtracted from the total illumination, J_{tot}. Not considering the (0,0) order, the largest contribution is the (η=±2,ξ=0) diffraction order, which represents the formation of the isolation lines along the x-direction. Another component that is large and defines the end of the isolation lines is the (η=±1,ξ=±1) diffraction order. Although the (0,±2) diffraction order is rather small, higher orders combine in the η=0 and ξ=±2 region of the lens. These regions also help to define the end of line. The DOCC approach shows how the illumination pupil is sampled for improved image formation and is an effective method for understanding imaging of the brick wall isolation pattern.

Using Equation 15, the illumination pupil of the brick wall pattern for the 130nm design rule can be calculated and is shown in Figure 5. Figure 5 shows that the most significant areas for image formation are the outer portions of the illumination configuration along the x-axis. These outer portions form an elliptical dipole. In addition to these elliptical dipole elements, the center of the illumination pupil has a large contribution to image formulation. As noted above, the illumination pupil can be implemented in gray scale or binary illumination profiles.

Depending on the apparatus being used, gray scale illumination may be possible. By gray scale illumination is meant controllable illumination intensity for which a normalized level ranging from 0 to 1 may be selected for at least given portions of the illumination configuration. For example, such control over illumination intensity may be produced by use of a diffractive optical element (DOE) in the illumination system. In this case, for example, the illumination configuration can be implemented as shown in Figure 5. However, some of the local spikes which are calculated in theory and seen in Figure 5 will be removed after low pass filtering of the illumination information as a result of the projection optics, as discussed above. Therefore, when designing an illumination configuration, spikes which will be filtered should be ignored.

If a binary illumination configuration is used, i.e., only binary values for intensity of the illuminator are allowed (0 or 1), a threshold value should be chosen as a basis for assigning values of 0 or 1 to each point on the illumination configuration. For

example, if a threshold of 0.8 is chosen, illuminator intensity values above 0.8 are rounded up to 1 and values below 0.8 are rounded down to 0. Other threshold values may be applied as desired.

Example 2: Using the gray scale to binary approach, a binary illumination configuration for the same brick wall isolation pattern was designed assuming a maximum outer σ of 0.88 and is shown in Figure 6.

The performance of the optimized illumination configuration in Figure 6 was then simulated for binary mask on a step and scan photolithography apparatus having NA=0.8 and λ=248nm and compared to the simulated performance of annular illumination. In the simulation, the vector (thin-film) imaging resist model was used since the numerical aperture was above 0.7. In this model, the resist is 400nm thickness of a type having a refractive index n=1.76-j0.0116), over 66nm of another type having n=1.45-j0.3 on top of a polysilicon material having n=1.577-j3.588. The results with the annular illumination (σ_{in}=0.58 and of σ_{out}=0.88) and with the optimized illuminator (σ_{out}=0.88) are shown in Figures 7 and 8, respectively. In both Figures 7 and 8, cross section results in the middle of the isolation region and top down simulation results are shown. In the Figures, the Bossung plot B from aerial image threshold is calculated by averaging the intensity through the resist, and the resultant linewidth, lw, is plotted versus focus, f, for a threshold intensity. This technique tends to over predict the DOF as thickness loss and resist profile slope is not taken into consideration. A resist model that at least calculates thickness loss is probably necessary. In each of the figures, the top down results are plotted as solid, curved lines at the best threshold (best dose) as calculated by the Bossung plot. These simulated threshold images are compared to actual mask data shown in dashed, straight lines.

Simulation results for the 130nm design rule brick wall isolation pattern are plotted in Figure 7 for a binary mask feature with NA of 0.8 using annular illumination (σ_{in}=0.58 and of σ_{out}=0.88). This annular setting has approximately 0.4μm of DOF from -0.4μm to 0.0μm focus. The contrast of the resist is low through focus, and can be imaged with a low contrast resist. However, at this low intensity contrast, the mask error enhancement factor (MEEF) is large and the exposure latitude (EL) is small. The

top down images in Figure 7 also show that there is approximately 20nm of end of line (EOL) shortening, which can be fixed by extending the line slightly for the 130nm design rule. However, as the design rule continues to shrink, extending the line is no longer feasible as the extended line may conflict with other features. Therefore, it is desirable to fix the EOL with the illumination.

In Figure 8, simulation results for the 130nm design rule brick wall isolation pattern are plotted for a binary mask feature with NA of 0.8 and using the optimized binary illumination configuration in FIG. 6. The optimal illumination configuration has approximately 0.6μm DOF from -0.45μm to +0.15μm focus. In comparing the cross section images in Figure 8 to those in Figure 7, the optimized illumination configuration has a larger contrast through focus as compared to annular illumination. This larger contrast implies that the MEEF for the optimized illumination configuration is lower compared to annular illumination and that the exposure latitude for the optimized illumination configuration is higher. Another benefit of the optimized illumination configuration is the improved line end performance as compared to annular illumination. The top down images in Figure 8 show that the optimized illumination configuration is capable of maintaining the EOL without extending the line on the pattern, which is advantageous for more aggressive design rule shrinks.

Example 3: The results in Figures 7 and 8 for binary mask (BIM) were compared to simulation results for chromeless mask (CLM). A chromeless brick wall isolation pattern was designed from experimental results of software simulation in a manner known to those skilled in the art. The chromeless technology requires (0,0) order light so as to fully benefit from the DOF improvement produced by off axis illumination. Experimental results from the simulation confirm the need for (0,0) order light for which purpose the isolation layer should be dithered or half toned. The half tone pitch may be chosen such that the first order in the dithered direction does not fall into the projection pupil. In the example, the lines were dithered in the vertical direction with pitch less than $\lambda/[NA(1+\sigma_{out})]$. The dithering duty cycle however should be tuned to optimize the amount of (0,0) order light for best DOF and pattern fidelity. In the simulation results for CLM the half tone pitch was 155nm with 50% duty cycle (77.5nm

chrome islands). This pitch substantially prevented the (0,±1) orders from entering the projection pupil; however, this duty cycle should be tuned to maximum DOF with computer aided design tools.

Example 4: Simulation results for the 130nm design rule layer were plotted for a CLM with 155nm halftone pitch and 50% duty cycle. The CLM was exposed on a λ=248nm apparatus with NA of 0.8 and annular illumination (σ_{in}=0.58 and σ_{out}=0.88). The CLM with this annular setting had 0.5μm DOF (-0.4μm focus to +0.1μm focus). The CLM with annular illumination had greater DOF and better contrast through focus as compared to BIM with annular illumination. This indicates that the CLM performed better than the BIM mask. The top down simulation results indicated that the EOL performance with CLM is theoretically better than the EOL performance with BIM and that the CLM was also able to better define the contact hole landing area as compared to BIM.

Example 5: Simulation results for 130nm brick wall isolation pattern isolation layer were plotted for λ=248nm apparatus with NA of 0.8 and the optimized elliptical dipole shown in Figure 6. These results were simulated with a reticle identical to the CLM reticle used in the preceding example, which has a 155nm halftone pitch and 50% duty cycle. The CLM exposed with this optimized illumination configuration had 0.7μm DOF (-0.5μm to +0.2μm), an improvement of 40%. The Bossung plots indicated that the isofocal intensity was around 0.21. A model based OPC approach could additionally be applied in order to tune the reticle to size at the correct linewidth, providing further improvements in performance. The linewidth may be corrected, for example, by biasing and by modifying the half tone duty cycle. The top down simulation results indicated that CLM was able to define the contact landing region and was able to maintain CD uniformity. Necking and other linewidth inconsistencies were reduced with this elliptical illumination configuration. Furthermore, the CLM reticle could be biased to improve the DOF, and consequently the EOL performance should improve. Furthermore, model based OPC should be able to correct the EOL further.

Example 6: Using the mask pattern of Figure 2 for a 110nm design rule isolation layer, an optimized illumination configuration was generated with Equations

13 and 15. In order to visualize sampling of the illumination pupil, $J_{opt\text{-}2D}$ is plotted in Figure 9, showing x orders (η=m+p) horizontally and y orders (ξ=n+q) vertically. As in Figure 4 for the 130nm design rule, the largest contribution to 110nm design rule in Figure 11 is the (η=0, ξ=0) order. This (0,0) order light is detrimental to the DOF and is eliminated in J_{tot} as indicated in Equation 15. Figure 9 also shows that the (±1,±1) orders are the largest contributors to the illumination configuration optimization rather than the (±2,0) order. This is due to the fact that 110nm design rule is too aggressive for the 248nm apparatus with NA=0.8, as slightly higher NA is preferred to achieve this resolution. The orders that contribute most to defining the isolation linewidth are the (±2,0) orders. The (±2,0) orders, however, are at the far edge of the illumination configuration ($0.8<\sigma<1.0$), which indicates that σ of 1 may provide improvement to implement the 110nm design rule at this wavelength.

Using Equation 15 and the results in Figure 9, the optimized illumination configuration for the 110nm brick wall isolation layer is shown in Figure 10. Figure 10 shows that the illumination configuration areas that contribute most to image formation are a small portion in the center and far edges of the illumination configuration. One possible implementation of this illumination configuration is plotted in Figure 11a. In order to use 248nm apparatus to print more aggressive design rules and push the limit of the projection numerical aperture, an illumination configuration with σ of 1.0, as shown in Figure 11b, and with small sectors (σ ring width of 0.2) may be used.

An implementation of the present invention includes selection of cells or particular gates that are critical. These critical features are then processed to determine J_{tot} as described above. In Section 1, it was shown that the illumination configuration is pattern dependent. Therefore, if the pitch does not differ significantly for the critical features, it is possible to create a single illumination configuration which optimizes the process window for all the critical features. In Figure 12, an example of a circuit with critical gates g_1, g_2, g_3 and a critical cell cc is shown. The diffraction orders of these tagged critical features can be calculated, and by using the theory already described, the optimized illumination configuration can be calculated. After calculating the optimized

illumination configuration the process window can be calculated and compared to the process window with other illumination configurations.

Another method of optimizing illumination/pattern interaction is to modify the pattern design with scattering bars. Scattering bars discretize the pitch from a semi-continuous function for an ASIC or logic design. After placing scattering bars, there are fewer pitches. This can be demonstrated in simulation software by placing the scattering bars with an edge-to-edge separation of $0.61\lambda/NA$. In Figure 13, the design in Figure 12 has been modified by adding a plurality of scattering bars. The illumination configuration can then be optimized for the modified design. The process window performance of an illumination configuration optimized for a design with scattering bars can then be compared to the process window of an illumination configuration optimized without scattering bars. Since a design with scattering bars discretizes the pitch, the combination of scattering bars with optimized off axis illumination (OAI) will have the largest possible DOF process window.

Another concept for implementing illumination configuration optimization is through the placing of scattering bars based on space width (SW) considerations. A scattering bar is placed through rule based OPC which rules may be defined by the space width. With simulation software, it should be possible to calculate the probability density function (pdf) of the space width without scattering bars and with scattering bars. The illumination can than be optimized by considering the pdf by modifying $J_{opt\text{-}2D}$ as shown in Equation 16. Assuming that the vertical lines and horizontal lines are infinite, it is also possible to calculate the diffraction orders T(m,n). In Equation 17, the diffraction orders are calculated as a function of m and n where w is the line width, τ is the intensity transmittance of the reticle, and $P_x=SW_x+w$ and $P_y=SW_y+w$ are the pitches in the x and y directions, respectively.

$$J_{opi-2D}(\alpha,\beta,\eta,\xi) =$$
$$J_s(\alpha,\beta)\sum_{m=-fx_{max}}^{+fx_{max}}\sum_{n=-fy_{max}}^{+fy_{max}}\int\int dP_x dP_y pdf(Px)pdf(Py)T(m,n)T^*[-(\eta-m),-(\xi-n)]$$

$$\bullet K\left(\alpha+\frac{m\lambda}{P_x NA},\beta+\frac{n\lambda}{P_y NA}\right)K^*\left(\alpha-(\eta-m)\frac{\lambda}{P_x NA},\beta-(\xi-n)\frac{\lambda}{P_y NA}\right) \qquad \text{Eqn. 16}$$

Equation 17 is a matrix of four equations for which, in order of presentation, m=n=0; m=0, n≠0; m≠0, n=0; and m≠0, n≠0.

$$T(m,n) = \begin{cases} 1 - w\left(1+\sqrt{\tau}\right)\left(\frac{1}{P_x}+\frac{1}{P_y}\right) + \frac{w^2}{P_x P_y}\left(1+\sqrt{\tau}\right)^2 \\ \left[1-\frac{w}{P_x}\left(1+\sqrt{\tau}\right)\right]\left(1+\sqrt{\tau}\right)\left(\frac{P_y}{\pi n}\right)\sin\left(n\frac{\pi w}{P_y}\right) \\ \left[1-\frac{w}{P_y}\left(1+\sqrt{\tau}\right)\right]\left(1+\sqrt{\tau}\right)\left(\frac{P_x}{\pi m}\right)\sin\left(m\frac{\pi w}{P_x}\right) \\ \left(1+\sqrt{\tau}\right)^2\left(\frac{P_x}{\pi m}\right)\sin\left(m\frac{\pi w}{P_x}\right)\left(\frac{P_y}{\pi n}\right)\sin\left(n\frac{\pi w}{P_y}\right) \end{cases} \qquad \text{Eqn. 17}$$

Calculating the optimal illumination configuration with the pdf can present some problems as it implies that some pitches are not as important as others. If all the gates in the pdf are considered to be critical, the pdf should be modified by a weighting factor. This weighting factor is a function of pitch called wf(Px). With this weighting factor, all the critical pitches should be treated the same such that wf(Px)•pdf(Px)=1. This weighting factor should be added to Equation 16 by replacing pdf(Px) in Equation 16 with wf(Px)•pdf(Px). In the case that all of the pitches are critical, the weighting factors will not help to resolve the optimization and it is difficult to create an optimized illumination configuration without modifying the (pattern) design.

One solution to this problem is to modify the design by adding scattering bars as discussed above. Scattering bars help to reduce pitches for isolated features. Once scattering bars are added to the design, the previously isolated features tend to act like

dense features. Thus, scattering bars discretize the pitch from a continuous pdf to a more discrete pdf. Figure 14 is an example pdf for a logic pattern with features oriented in the y-direction (i.e. "vertical" direction) in which scattering bars have and have not been applied. Figure 14 shows vertical gate space widths (μm) on the x (horizontal) axis. For the unmodified design, D, without scattering bars, there are three discrete humps in the pdf at space widths of 0.2, 0.6 and 1.5μm. After the placement of scattering bars, D+SB, the number of pitches has been reduced such that most of the space widths are at dense pitches of 0.2μm. With this change to the pdf, it is more likely that an illumination configuration can be optimized.

The total illumination configuration for a design with both horizontal (x-direction) and vertical features is the sum of horizontal and vertical illumination configurations. If the illumination configuration is concentrated at σ_{cx} for the vertical features and is concentrated at σ_{cy} for the horizontal features, the optimal illumination configuration will be a "conventional" quadrupole illumination configuration provided that $\sqrt{2}\sigma_{cx} \le 1$ and that $\sqrt{2}\sigma_{cy} \le 1$. Otherwise, this type of analysis will result in a four pole illumination configuration that has been rotated 45°.

The illumination technique presented herein may be extended to account for aberrations. Including aberrations allows an operator to determine which part of the illumination configuration couples to the aberration. The amount of coupling is directly related to sensitivity of the image intensity to the aberration. By understanding this coupling, it may be possible to modify the illumination configuration to minimize the aberration sensitivity of a design.

The projection pupil, $K(\alpha,\beta)$, for scalar imaging contains the obliquity factor, defocus, and the exponential of the wavefront represented by the Zernike polynomials. This scalar imaging pupil is shown in Equation 18. This pupil can further be divided into two parts, the unaberrated pupil $K_0(\alpha,\beta)$ and the aberrated pupil (the exponential of the wavefront); these two parts are multiplied together as shown in Equation 19.

$$K(\alpha,\beta)=\underbrace{\left[\frac{1-(\alpha^2+\beta^2)/M^2}{1-(\alpha^2+\beta^2)}\right]^{1/4}}_{obliquity\text{-}factor}\underbrace{exp\left[-i\frac{2\pi}{\lambda}z\sqrt{1-\alpha^2-\beta^2}\right]}_{defocus}\underbrace{exp\left[-i\frac{2\pi}{\lambda}W(\alpha,\beta)\right]}_{aberrations}$$

Eqn. 18

$$K(\alpha,\beta)=\underbrace{K_0(\alpha,\beta)}_{unaberrated}\underbrace{\exp\left[-i\frac{2\pi}{\lambda}W(\alpha,\beta)\right]}_{aberrations}$$

Eqn. 19

where

$$K_0(\alpha,\beta)=\underbrace{\left[\frac{1-(\alpha^2+\beta^2)/M^2}{1-(\alpha^2+\beta^2)}\right]^{1/4}}_{obliquity\text{-}factor}\underbrace{\exp\left[-i\frac{2\pi}{\lambda}z\sqrt{1-\alpha^2-\beta^2}\right]}_{defocus}$$

Eqn. 20

$$W(\alpha,\beta)=\sum_{\nu=5}^{37}Z_\nu R_\nu(\alpha,\beta)$$

Eqn. 21

$$e^x=1+x+\frac{x^2}{2!}+\frac{x^3}{3!}+\ldots\cong 1+x$$

Eqn. 22

From Equation 22, the wavefront can be written as a linear approximation, which is shown in Equation 23. By substituting Equation 23 into Equation 22, the linear approximation for the projection pupil, K(α,β), can be calculated with Equation 24.

$$\exp\left[-i\frac{2\pi}{\lambda}W(\alpha,\beta)\right]\cong 1-i\frac{2\pi}{\lambda}W(\alpha,\beta)=1-i\frac{2\pi}{\lambda}\sum_{\nu=5}^{37}Z_\nu R_\nu(\alpha,\beta)$$

Eqn. 23

$$K(\alpha,\beta) \cong K_0(\alpha,\beta)\left[1 - i\frac{2\pi}{\lambda}\sum_{v=5}^{37} Z_v R_v(\alpha,\beta)\right] \qquad \text{Eqn. 24}$$

Since the TCC is a function of the projection pupil, K(α,β), the linear approximation to the pupil in Equation 24 implies that the TCC can be represented by a linear approximation. This is accomplished by substituting Equation 24 into Equation 1, which results in Equation 25. Once again by neglecting the terms of power 2 or greater, the TCC in Equation 25 can be simplified as shown in Equation 26.

The wavefront, W(α,β), is most often denoted by the summation of Zernike fringe polynomials as shown in Equation 21. Using the linear theory of aberrations, the exponential, e^x, can be represented by a Taylor series expansion. The Taylor series expansion is valid for small x, and previous work has shown good agreement for aerial images when Z_v is less than 0.04λ. The Taylor series expansion for e^x is shown in Equation 22. In Equation 22, terms of power 2 or greater have been dropped, which is valid provided that Z_v is less than 0.04 (0.04^2=0.0016 and is negligible).

$$TCC(m,n,p,q) \cong \iint_{\sqrt{\alpha^2+\beta^2}<\sigma} J_s(\alpha,\beta) K_0\left(\alpha+\frac{m\lambda}{P_x NA},\beta+\frac{n\lambda}{P_y NA}\right)\left[1 - i\frac{2\pi}{\lambda}\sum_{v=5}^{37} Z_v R_v\left(\alpha+\frac{m\lambda}{P_x NA},\beta+\frac{n\lambda}{P_y NA}\right)\right]$$

$$\cdot K_0^*\left(\alpha-\frac{p\lambda}{P_x NA},\beta-\frac{q\lambda}{P_y NA}\right)\left[1 + i\frac{2\pi}{\lambda}\sum_{v=5}^{37} Z_v R_v\left(\alpha-\frac{p\lambda}{P_x NA},\beta-\frac{q\lambda}{P_y NA}\right)\right] d\alpha d\beta \qquad \text{Eqn. 25}$$

$$TCC(m,n,p,q) \cong \iint_{\sqrt{\alpha^2+\beta^2}<\sigma} J_s(\alpha,\beta) K_0\left(\alpha+\frac{m\lambda}{P_x NA},\beta+\frac{n\lambda}{P_y NA}\right) K_0^*\left(\alpha-\frac{p\lambda}{P_x NA},\beta-\frac{q\lambda}{P_y NA}\right)$$

$$\cdot\left[1 - i\frac{2\pi}{\lambda}\sum_{v=5}^{37} Z_v R_v\left(\alpha+\frac{m\lambda}{P_x NA},\beta+\frac{n\lambda}{P_y NA}\right) + i\frac{2\pi}{\lambda}\sum_{v=5}^{37} Z_v R_v\left(\alpha-\frac{p\lambda}{P_x NA},\beta-\frac{q\lambda}{P_y NA}\right)\right] d\alpha d\beta \qquad \text{Eqn. 26}$$

By defining the unaberrated TCC, $TCC_0(m,n,p,q)$, and the aberrated TCC, $TCC_v(m,n,p,q)$, in Equations 27 and 28, respectively, the TCC can be represented by a linear function of TCC_0 and TCC_v as shown in Equation 29.

$$TCC_0(m,n,p,q)=\iint_{\sqrt{\alpha^2+\beta^2}<\sigma} J_s(\alpha,\beta)K_0\left(\alpha+\frac{m\lambda}{P_xNA},\beta+\frac{n\lambda}{P_yNA}\right)K_0^*\left(\alpha-\frac{p\lambda}{P_xNA},\beta-\frac{q\lambda}{P_yNA}\right)d\alpha d\beta$$

Eqn. 27

$$TCC_v(m,n,p,q)=-i\frac{2\pi}{\lambda}\iint_{\sqrt{\alpha^2+\beta^2}<\sigma} J_s(\alpha,\beta)K_0\left(\alpha+\frac{m\lambda}{P_xNA},\beta+\frac{n\lambda}{P_yNA}\right) \qquad \text{Eqn. 28}$$

$$TCC(m,n,p,q)\cong TCC_0(m,n,p,q)+\sum_{v=5}^{37}Z_v\left[TCC_v(m,n,p,q)+TCC_v^*(-p,-q,-m,-n)\right]$$

Eqn. 29

Since the TCC can be constructed as a linear approximation as shown in Equation 29, J_{opt} can also be written as a linear approximation. The linear approximation to J_{opt} is derived in Equation 30 by using Equation 8 for J_{opt} and by following the methodology for the linear approximation of the TCC as outlined in Equations 18 through 29.

$$J_{opt}(\alpha,\beta,m,n,p,q)\cong J_s(\alpha,\beta)T(m,n)T^*(-p,-q)K_0\left(\alpha+\frac{m\lambda}{P_xNA},\beta+\frac{n\lambda}{P_yNA}\right)K_0^*\left(\alpha-\frac{p\lambda}{P_xNA},\beta-\frac{q\lambda}{P_yNA}\right)$$

$$\cdot\left[1-i\frac{2\pi}{\lambda}\sum_{v=5}^{37}Z_vR_v\left(\alpha+\frac{m\lambda}{P_xNA},\beta+\frac{n\lambda}{P_yNA}\right)+i\frac{2\pi}{\lambda}\sum_{v=5}^{37}Z_vR_v\left(\alpha-\frac{p\lambda}{P_xNA},\beta-\frac{q\lambda}{P_yNA}\right)\right]d\alpha d\beta$$

Eqn. 30

Equation 30 for J_{opt} can then be divided into a summation of the unaberrated J_{opt0} with the aberrated J_{optv} as shown in Equation 33. The definition of J_{opt0} and J_{optv} are shown in Equations 31 and 32, respectively.

$$J_{opt0}(\alpha,\beta,m,n,p,q)=J_s(\alpha,\beta)K_0\left(\alpha+\frac{m\lambda}{P_xNA},\beta+\frac{n\lambda}{P_yNA}\right)K_0^*\left(\alpha-\frac{p\lambda}{P_xNA},\beta-\frac{q\lambda}{P_yNA}\right)$$

Eqn. 31

$$J_{optv}(\alpha,\beta,m,n,p,q)=-i\frac{2\pi}{\lambda}J_s(\alpha,\beta)K_0\left(\alpha+\frac{m\lambda}{P_xNA},\beta+\frac{n\lambda}{P_yNA}\right)$$

Eqn. 32

$$\cdot K_0^*\left(\alpha-\frac{p\lambda}{P_xNA},\beta-\frac{q\lambda}{P_yNA}\right)R_v\left(\alpha+\frac{m\lambda}{P_xNA},\beta+\frac{n\lambda}{P_yNA}\right)$$

Equation 32 describes the portion of the illumination configuration which couples to a particular aberration. The amount of coupling affects the image intensity and helps to provide an understanding of aberration sensitivity to illumination. By combining Equations 31 and 32, J_{opt} can be written as a linear approximation.

$$J_{opt}(\alpha,\beta,m,n,p,q)\cong J_{opt0}(\alpha,\beta,m,n,p,q)+\sum_{v=5}^{37}Z_v\left[J_{optv}(\alpha,\beta,m,n,p,q)+J_{optv}^*(\alpha,\beta,-p,-q,-m,-n)\right]$$

Eqn. 33

In another aspect of the present invention, weighting factors can be introduced to maximize or to minimize a response to a particular metric including, for example, depth of focus (DOF), image log slope (ILS), image slope (IS), or aberration sensitivity. The optimal J_{tot} of Equation 15 can be modified to include these weighting factors as shown in Equation 34.

$$J_{tot}(\alpha,\beta)=\sum_m\sum_n\sum_p\sum_q w(\alpha,\beta,m,n,p,q)J_{opt}(\alpha,\beta,m,n,p,q) \qquad \text{Eqn. 34}$$

In general, photoresists react in proportion to the logarithm of the intensity of the light impinging thereon. As the intensity, and therefore the logarithm of the intensity, increases, the feature will be printed into the resist with better fidelity (i.e. improved resist profile and improved process window). Therefore, it is desirable to maximize the logarithmic change in intensity (ILS). The ILS is defined in Equation 35.

$$ILS \propto \frac{\partial \ln I}{\partial x} = \frac{1}{I}\frac{\partial I}{\partial x} \qquad \text{Eqn. 35}$$

Since the derivative of the intensity changes faster than the inverse of intensity, Equation 35 will increase more by increasing the derivative of the intensity. The intensity can be calculated from Equation 3 and the derivative of the intensity with respect to x is defined in Equation 36. The derivative with respect to x results in the weighting function, w_x, as shown in Equation 37. Likewise, a weighting function w_y can be defined with respect to y as shown in Equation 38.

$$\frac{\partial I(x,y)}{\partial x} = \sum_m \sum_n \sum_p \sum_q i\frac{2\pi}{P_x}(m+p)e^{ix\left[\frac{2\pi}{P_x}(m+p)\right]}e^{iy\left[\frac{2\pi}{P_y}(n+q)\right]}DOCC(m,n,p,q)$$

$$= \sum_m \sum_n \sum_p \sum_q w_x(m,p)e^{ix\left[\frac{2\pi}{P_x}(m+p)\right]}e^{iy\left[\frac{2\pi}{P_y}(n+q)\right]}DOCC(m,n,p,q) \qquad \text{Eqn. 36}$$

$$w_x = i\frac{2\pi}{P_x}(m+p) \qquad \text{Eqn. 37}$$

$$w_y = i\frac{2\pi}{P_y}(n+q) \qquad \text{Eqn. 38}$$

Since pattern features and intensity features are two dimensional, the norm of the gradient may be used to indicate the change in intensity with respect to position. The norm of the intensity gradient is defined in Equation 39. This allows us to define a weighting function to calculate J_{tot} in Equation 34. The weighting function to maximize the image log slope is defined by Equation 40.

$$\|\nabla I\| \Rightarrow w_{NILS} = \sqrt{|w_x|^2 + |w_y|^2} \qquad \text{Eqn. 39}$$

$$w_{ILS}(m,n,p,q) = 2\pi\sqrt{\left(\frac{m+p}{P_x}\right)^2 + \left(\frac{n+q}{P_y}\right)^2} \qquad \text{Eqn. 40}$$

Equation 40 shows that when m+p=0 and n+q=0, the weighting function becomes 0. When m+p=0 and n+q=0, these orders contribute nothing to image modulation and reflect DC contributions to the image. Furthermore, w_{ILS} increases as m+p and n+q increase. This implies that higher order diffraction order terms are more highly weighted and contribute more to ILS.

In addition to maximizing ILS, the depth of focus of the process will increase if the ILS is improved such that the intensity response to focus is minimized. The focus is accounted for by the pupil K(α,β). The pupil, K(α,β), is shown in Equation 41, where focus is denoted z. Equation 41 can be divided into two terms, terms dependant on z (the defocus term) and terms independent of z (the non-defocus term), as shown in Equation 42.

$$K(\alpha,\beta)=\underbrace{\left[\frac{1-(\alpha^2+\beta^2)/M^2}{1-(\alpha^2+\beta^2)}\right]^{1/4}}_{\text{obliquity factor}}\underbrace{exp\left[-i\frac{2\pi}{\lambda}z\sqrt{1-\alpha^2-\beta^2}\right]}_{\text{defocus}}\underbrace{exp\left[-i\frac{2\pi}{\lambda}W(\alpha,\beta)\right]}_{\text{aberrations}} \qquad \text{Eqn. 41}$$

$$K(\alpha,\beta)=\underbrace{K_{nd}(\alpha,\beta)}_{\text{non-defocused}}\underbrace{\exp\left[-i\frac{2\pi}{\lambda}z\sqrt{1-\alpha^2-\beta^2}\right]}_{\text{defocus}}=K_{nd}(\alpha,\beta)K_d(\alpha,\beta) \qquad \text{Eqn. 42}$$

The variation in intensity due to focus, z, can be minimized by setting the derivative of intensity with respect to z to zero. By substituting Equation 42 into Equations 1 through 3, a cost function f(α,β,z) can be defined as shown in Equation 43 which is the cost function of the intensity imaging terms which depend on z.

$$f(\alpha,\beta,z)=K_d\left(\alpha+\frac{m\lambda}{P_xNA},\beta+\frac{n\lambda}{P_yNA}\right)K_d^*\left(\alpha-\frac{p\lambda}{P_xNA},\beta-\frac{q\lambda}{P_yNA}\right) \qquad \text{Eqn. 43}$$

The cost function, f(α,β,z), is in turn minimized when g(α,β,m,n,p,q) equals zero (see Equation 44, below). In Equation 44 the phase terms have been removed as the derivative with respect to z equals zero only when the magnitude terms equal zero.

When g(α,β,m,n,p,q) is zero, the areas (α,β) of the pupil for a given order (m,n,p,q) are minimally sensitive to focus. These are the most desired areas of the pupil for constructing the illumination configuration. A weighting function, $w_{focus}(\alpha,\beta,m,n,p,q)$, is defined in Equation 45. This weighting function is equal to 1 for areas least sensitive to focus and is equal 0 for areas most sensitive to focus. A new weighting function which maximizes ILS through focus can then be defined by Equation 46 and used to modify the illumination configuration.

$$g(\alpha,\beta,n,n,p,q)=\frac{\partial}{\partial z}f(\alpha,\beta,z)$$
$$=\left[-i\frac{2\pi}{\lambda}\sqrt{1-\left(\alpha+\frac{m\lambda}{P_xNA}\right)^2-\left(\beta+\frac{n\lambda}{P_yNA}\right)^2}+i\frac{2\pi}{\lambda}\sqrt{1-\left(\alpha-\frac{p\lambda}{P_xNA}\right)^2-\left(\beta-\frac{q\lambda}{P_yNA}\right)^2}\right]$$

Eqn. 44

$$w_{focus}(\alpha,\beta,m,n,p,q)=1-|g(\alpha,\beta,m,n,p,q)| \qquad \text{Eqn. 45}$$

$$w(\alpha,\beta,m,n,p,q)=w_{ILS}(m,n,p,q)w_{focus}(\alpha,\beta,m,n,p,q) \qquad \text{Eqn. 46}$$

The above methodology allows the sensitivity of the intensity to be minimized to the influence of focus, an aberration. Since the impact of focus on intensity can be minimized, the impact of intensity can be minimized to a specific aberration. This is desirable for certain patterns which demonstrate a high sensitivity to a particular aberration. The projection pupil in Equation 19 can be written as an unaberrated term, $K_0(\alpha,\beta)$, multiplied by an aberrated term, $K_a(\alpha,\beta)$ as shown in Equation 47.

$$K(\alpha,\beta)=K_0(\alpha,\beta)K_a(\alpha,\beta) \qquad \text{Eqn. 47}$$

The sensitivity of the intensity to a particular aberration Z_i can be minimized by setting the derivative of the intensity with respect to Z_i to zero. By substituting

Equation 47 into Equations 1 through 3 and taking the derivative of the intensity, the aberration sensitivity is minimized when h(α,β,m,n,p,q) in Equation 48 is equal to zero.

$$\frac{\partial}{\partial Z_i} I(x,y) = 0 \Rightarrow$$

$$h(\alpha,\beta,m,n,p,q) = K_a\left(\alpha + \frac{m\lambda}{P_x NA}, \beta + \frac{n\lambda}{P_y NA}\right)\frac{\partial}{\partial Z_i}K_a^*\left(\alpha - \frac{p\lambda}{P_x NA}, \beta - \frac{q\lambda}{P_y NA}\right)$$
$$+ \frac{\partial}{\partial Z_i}K_a\left(\alpha + \frac{m\lambda}{P_x NA}, \beta + \frac{n\lambda}{P_y NA}\right)K_a^*\left(\alpha - \frac{p\lambda}{P_x NA}, \beta - \frac{q\lambda}{P_y NA}\right) = 0$$

Eqn. 48

$$h(\alpha,\beta,m,n,p,q) = \left[R_i\left(\alpha - \frac{p\lambda}{P_x NA}, \beta - \frac{q\lambda}{P_y NA}\right) - R_i\left(\alpha + \frac{m\lambda}{P_x NA}, \beta + \frac{n\lambda}{P_y NA}\right)\right] = 0$$

Eqn. 49

Equation 48 may be simplified and written as Equation 49. A weighting function $w_{ab}(\alpha,\beta,m,n,p,q)$ is defined in Equation 50, which equates to 1 for areas (α,β) of the pupil that are least sensitive to Z_i and to 0 for areas most sensitive to Z_i.

$$w_{ab}(\alpha,\beta,m,n,p,q) = 1 - \frac{1}{2}\left|h(\alpha,\beta,m,n,p,q)\right| \qquad \text{Eqn. 50}$$

The weighting function to minimize ILS sensitivity to a particular aberration, Z_i, can then be defined in Equation 51. Furthermore, a weighting function to minimize ILS sensitivity to a particular aberration, Z_i, and to maximize ILS through focus can also be defined in Equation 52. Either of these equations can be substituted into Equation 34 to calculate the illuminator with the optimal response to a given metric.

$$w(\alpha,\beta,m,n,p,q) = w_{NILS}(m,n,p,q)\,w_{ab}(\alpha,\beta,m,n,p,q) \qquad \text{Eqn. 51}$$

$$w(\alpha,\beta,m,n,p,q) = w_{NILS}(m,n,p,q)w_{focus}(\alpha,\beta,m,n,p,q)w_{ab}(\alpha,\beta,m,n,p,q)$$

Eqn. 52

Figure 15 is a schematic representation of an example of a lithography apparatus for use according to the present invention. The apparatus includes a radiation system. The radiation system is made up of a lamp LA (which may be an excimer laser, for example) and an illumination system which may comprise beam shaping optics EX, an integrator IN, and a condenser lens CO, for example. The radiation system supplies a projection beam PB of radiation. For example, the radiation system may provide ultraviolet, deep ultraviolet or extreme ultraviolet radiation. In general, the radiation system may also provide soft x-ray or other forms of radiation.

A first object table, or mask table MT holds a mask MA. The mask MA includes a pattern area C which contains the mask pattern to be imaged. The mask table MT is movable relative to the projection beam PB so that different portions of the mask may be irradiated. Alignment marks $M_1$and M_2 are used for determining whether the mask is properly aligned with the substrate, or wafer, W.

A projection system PL projects the projection beam PB onto the wafer W. The wafer W includes two alignment marks P_1 and P_2 which are aligned with the marks M_1 and M_2 prior to beginning imaging. The wafer W is supported by a substrate table WT which is moveable relative to the projection beam for exposing different parts of the wafer W; in this way, the mask pattern C may be imaged onto different target portions c of the wafer W. An interferometric position monitor IF is used to insure that the wafer table WT is in the correct position relative to the position of the mask table MT.

While the invention has been described in connection with particular embodiments, it is to be understood that the invention is not limited to the disclosed embodiments, but on the contrary it is intended to cover various modifications and equivalent arrangement included within the scope of the claims which follow.

4 Brief Description of Drawings

Figure 1 is a diagram of the transmission cross coefficient function for a generalized image forming system;

Figure 2 is an example of a brick wall isolation pattern microlithographic mask feature;

Figure 3 is a representation of the diffraction orders of the mask feature of Figure 2;

Figure 4 is a map of the calculated optimized four dimensional illumination configuration for the mask feature of Figure 2;

Figure 5 is a calculated starting gray scale illumination configuration (J_{m1}) for the mask feature of Figure 2;

Figure 6 is a binary representation of the illumination configuration of Figure 5;

Figure 7 shows analysis of a print of the mask feature of Figure 2 printed with an annular illumination configuration;

Figure 8 shows analysis of a print of the mask feature of Figure 2 printed with an optimized elliptical illumination configuration;

Figure 9 is a map of the calculated optimized four dimensional illumination configuration for the mask feature of Figure 2 scaled to 110nm design rules;

Figure 10 is a calculated starting gray scale illumination configuration for the mask feature of Figure 2 scaled to 110nm design rules;

Figures 11a and 11b are binary representations of the illumination configuration of Figure 10 with differing values of σ;

Figure 12 is an example of a mask pattern with critical gates and cells indicated;

Figure 13 is the mask pattern of Figure 12 with assist features added to reduce the number of pitches in the pattern;

Figure 14 compares probability density functions of space widths of the mask patterns of Figures 12 and 13; and

Figure 15 is a schematic representation of an apparatus for microphotolithography.

In the various Figures, like parts are identified by like references.

Fig.1.

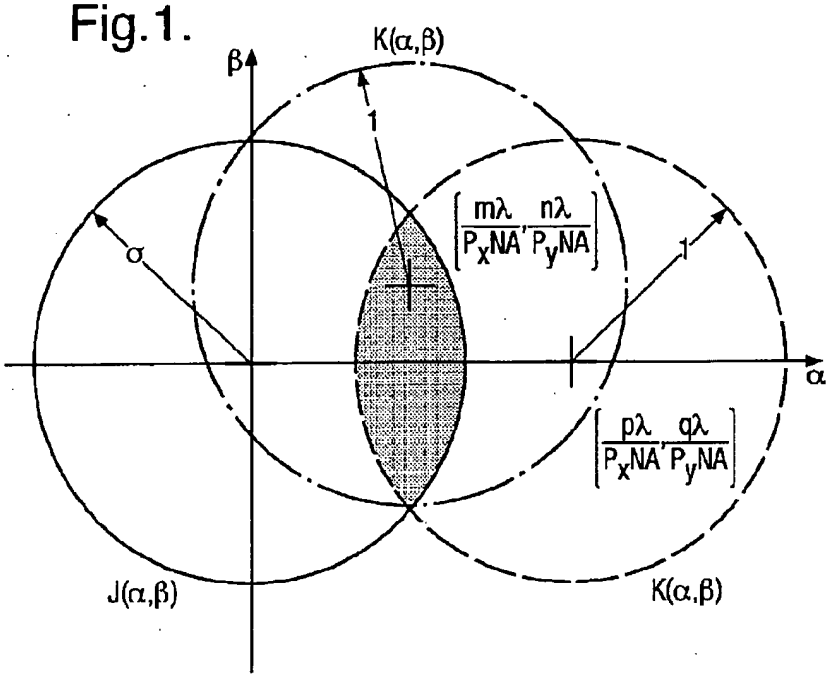
K(α,β)
β
1
σ
$\left[\frac{m\lambda}{P_xNA}, \frac{n\lambda}{P_yNA}\right]$
1
α
$\left[\frac{p\lambda}{P_xNA}, \frac{q\lambda}{P_yNA}\right]$
J(α,β)
K(α,β)

Fig.2.

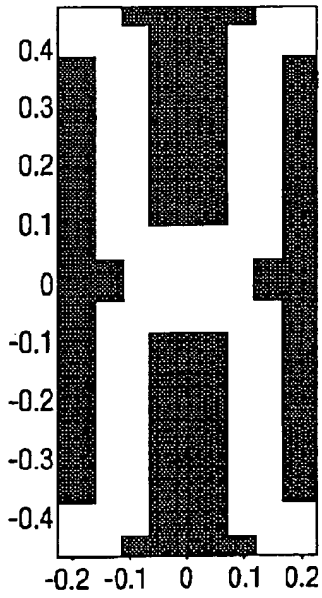
0.4
0.3
0.2
0.1
0
-0.1
-0.2
-0.3
-0.4
-0.2 -0.1 0 0.1 0.2

Fig.3.

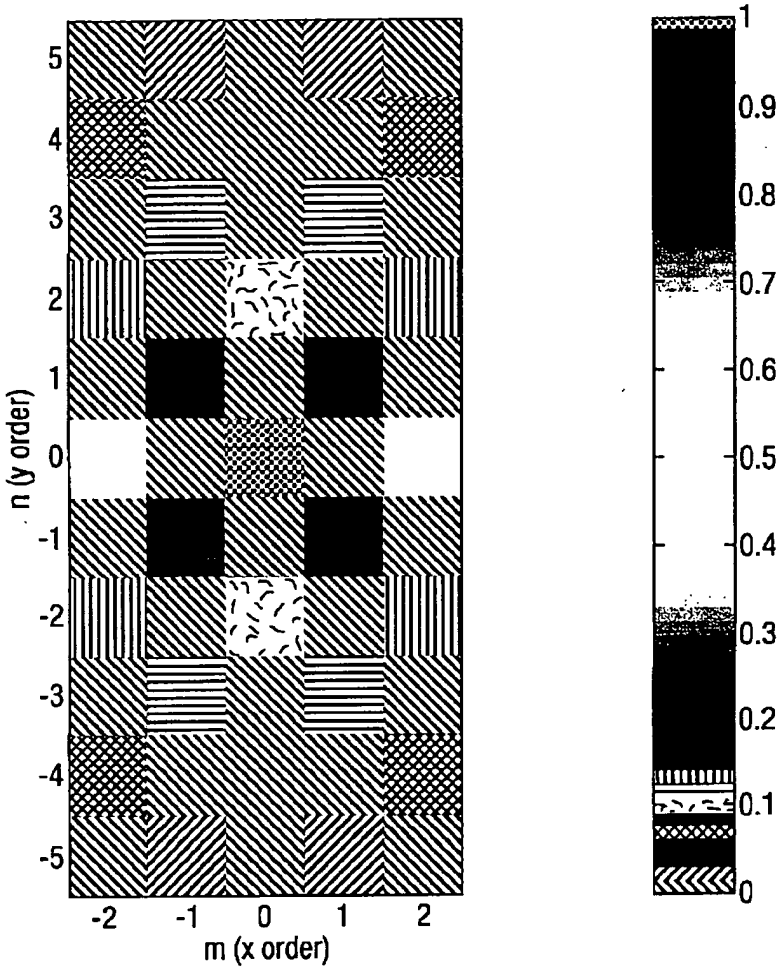
5
4
3
2
1
0
-1
-2
-3
-4
-5
n (y order)
-2
-1
0
1
2
m (x order)
1
0.9
0.8
0.7
0.6
0.5
0.4
0.3
0.2
0.1
0

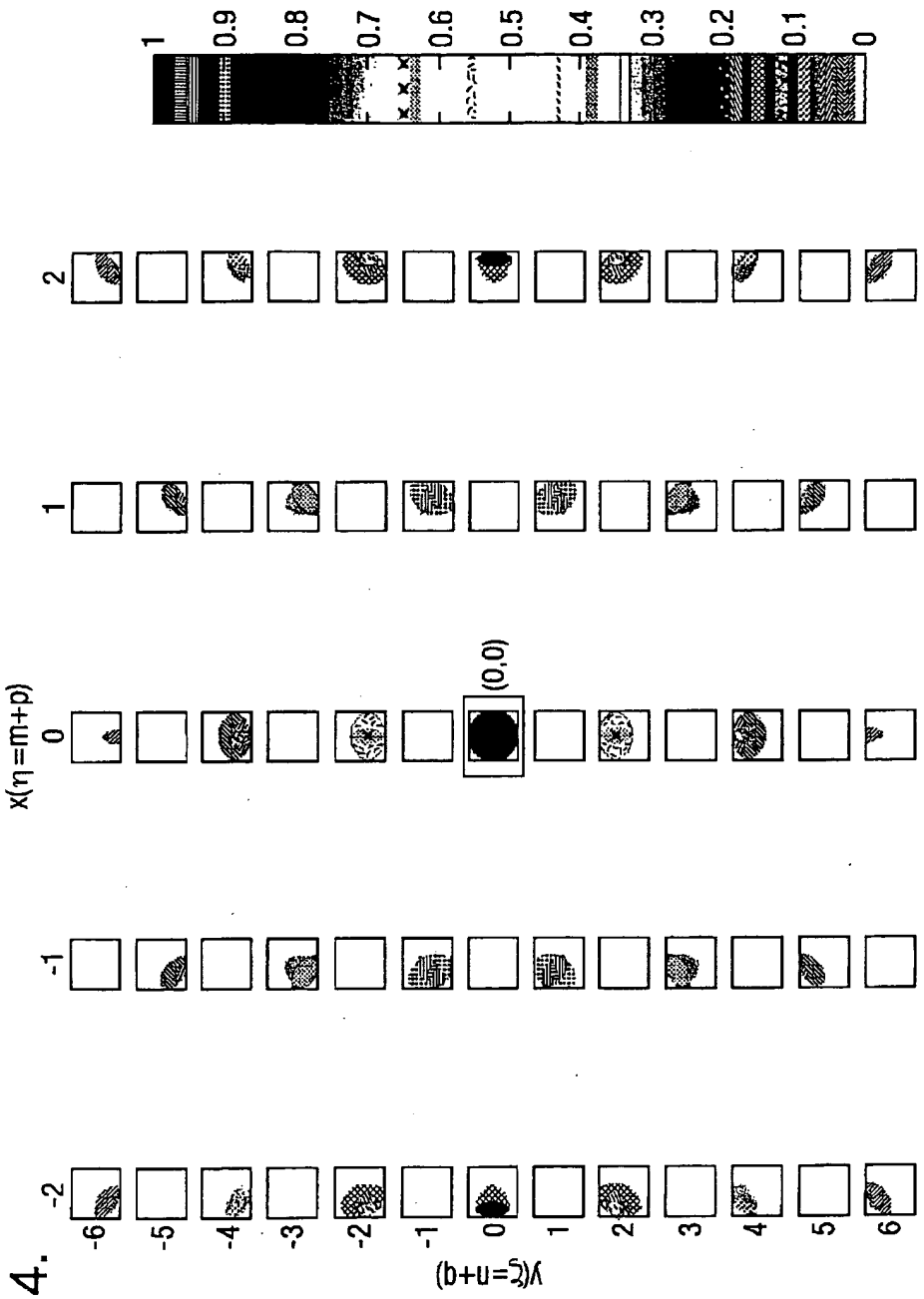

Fig.4.

Fig.5.

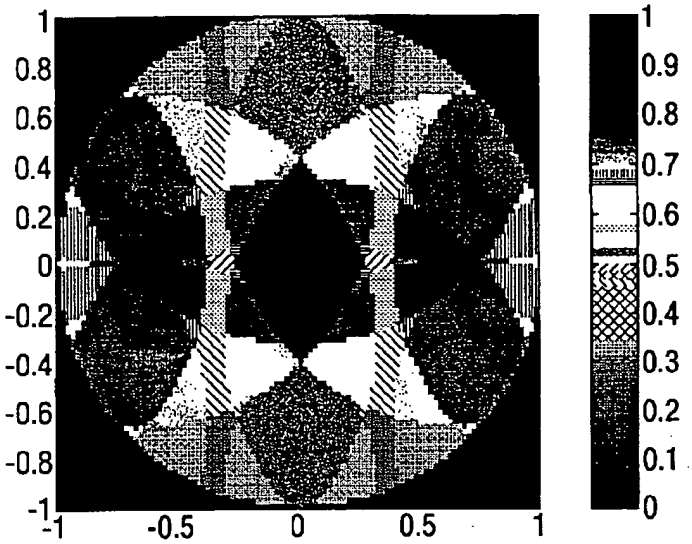

Fig.6.

Fig.7.

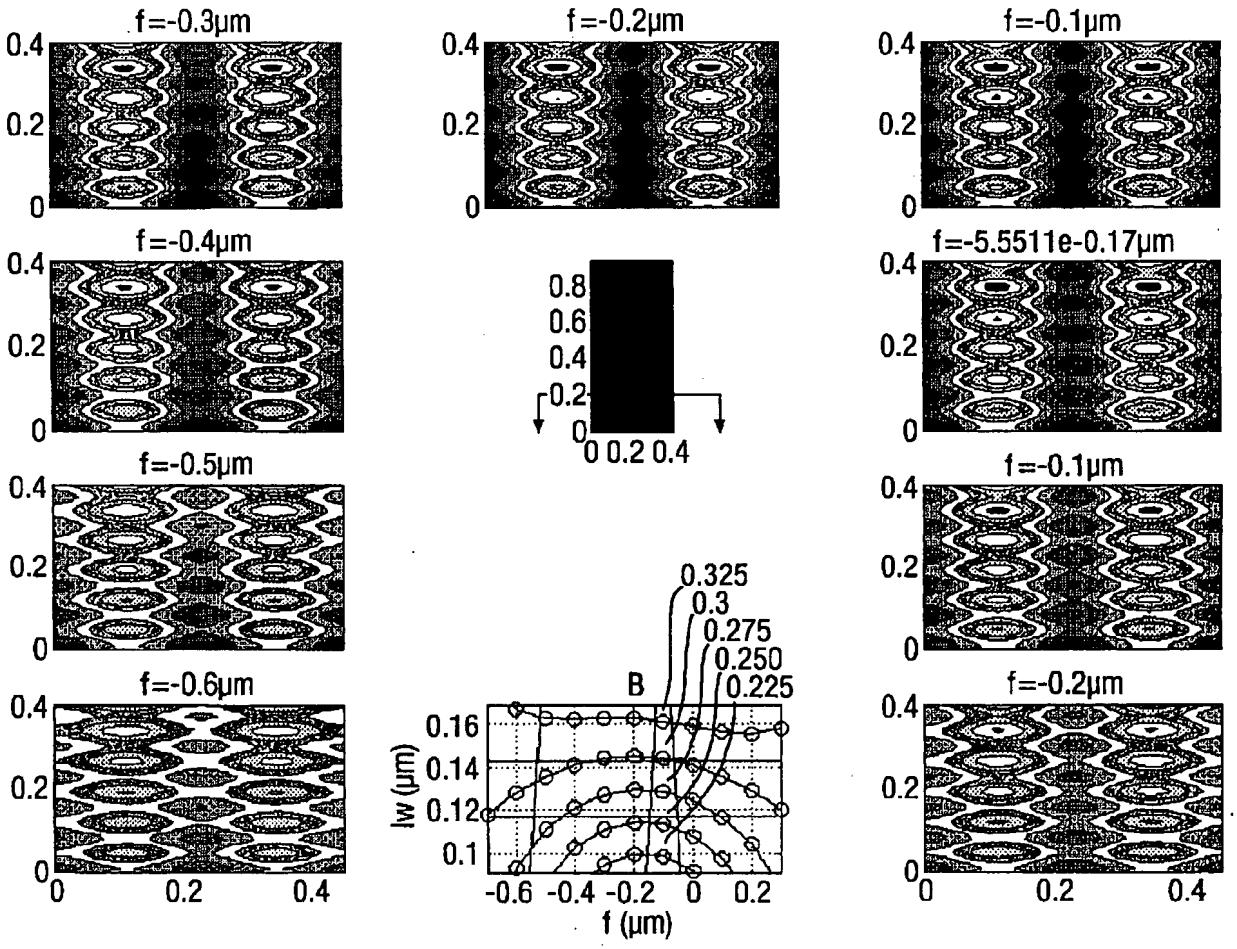

(番3)102-334836(P2002-<136

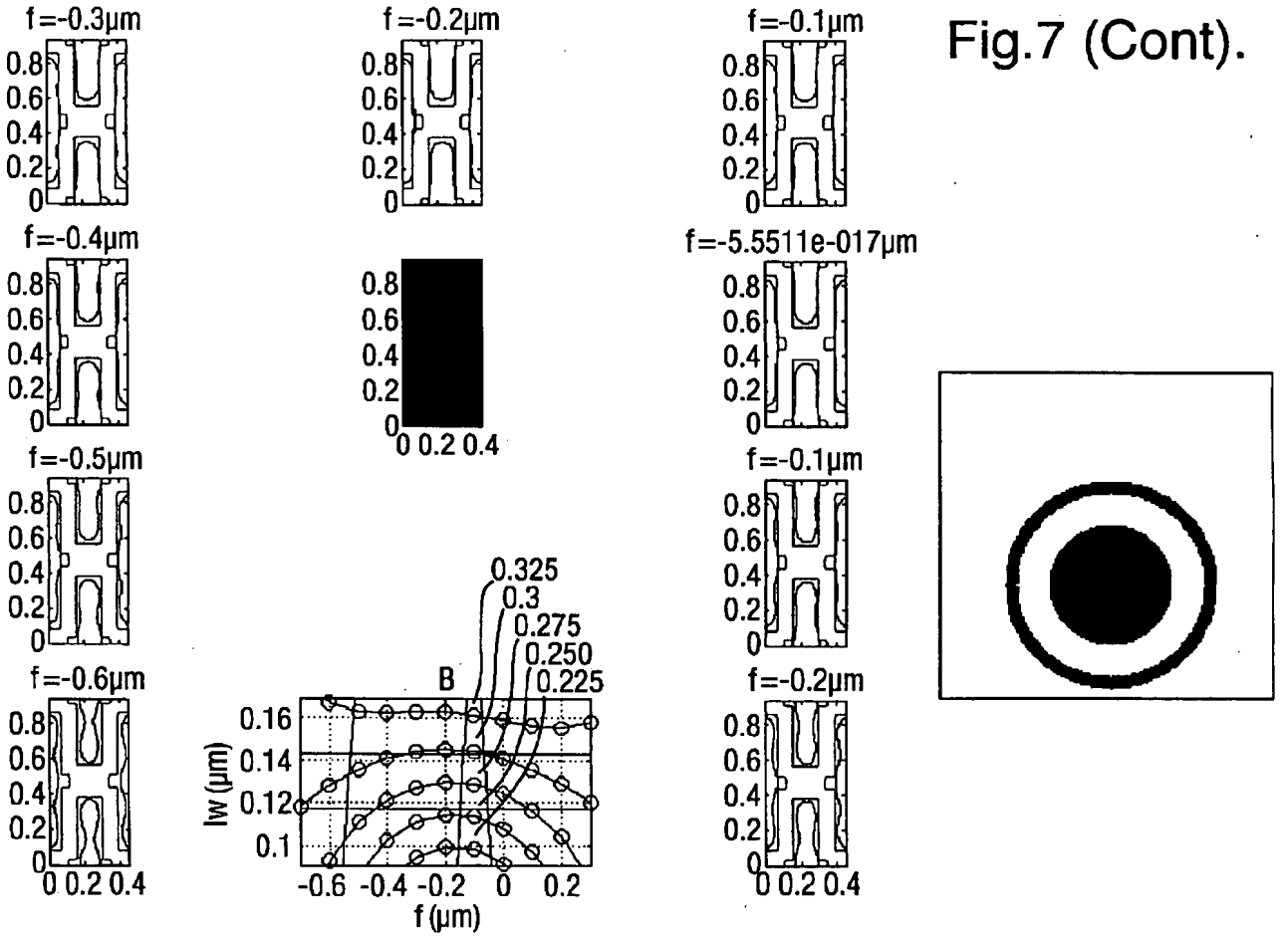

Fig.7 (Cont).

(第4)102-334836(P2002-*拔械

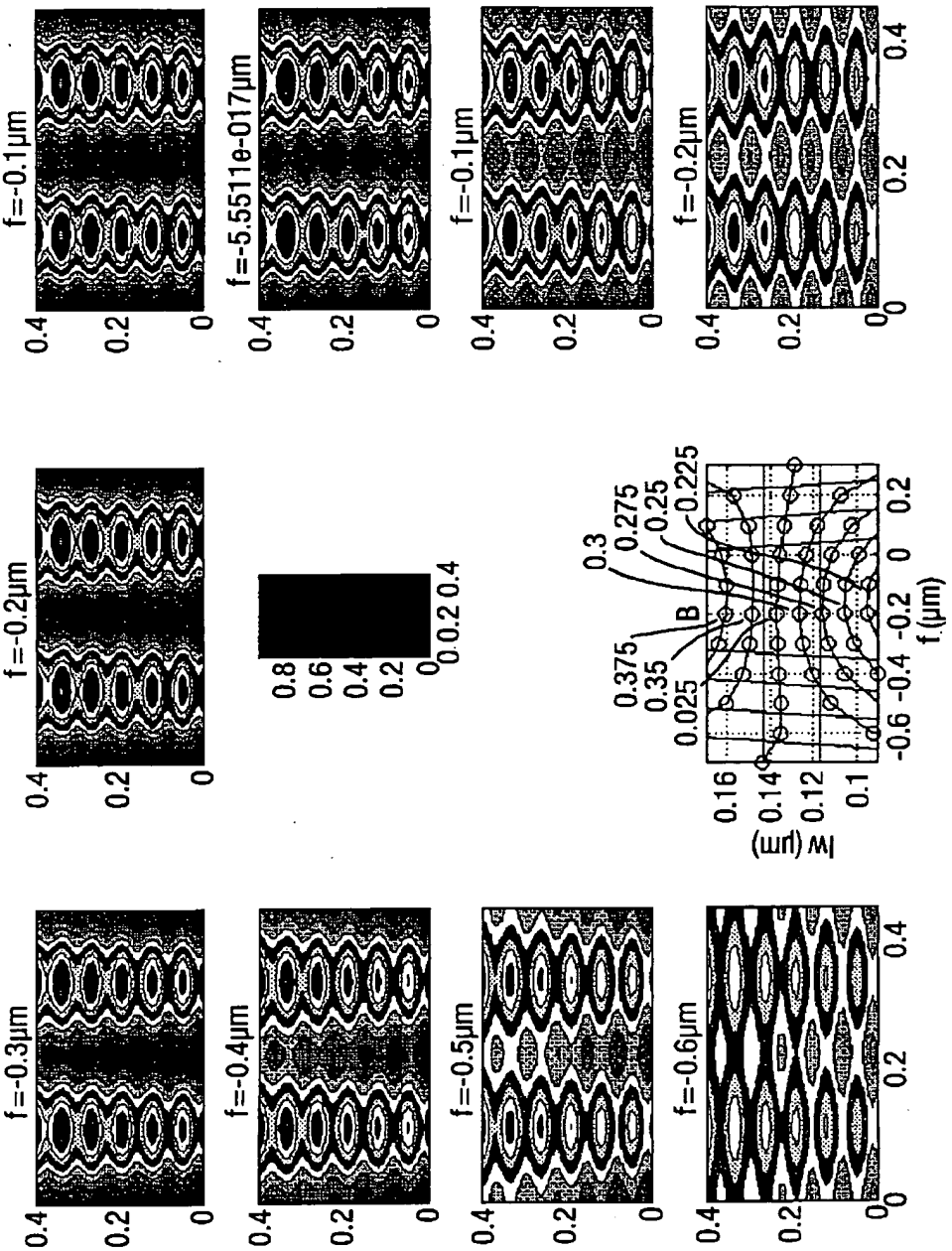
f=-0.1μm
f=-5.5511e-017μm
f=-0.1μm
f=-0.2μm
f=-0.2μm
f=-0.3μm
f=-0.4μm
f=-0.5μm
f=-0.6μm
0.4
0.2
0
0.8
0.6
0.4
0.2
0
0.2 0.4
0.3
0.275
0.25
0.225
0.375
0.35
0.025
B
0.2
0
-0.2
-0.4
-0.6
f (μm)
0.16
0.14
0.12
0.1
lw (μm)

Fig.8.

Fig.8 (Cont).

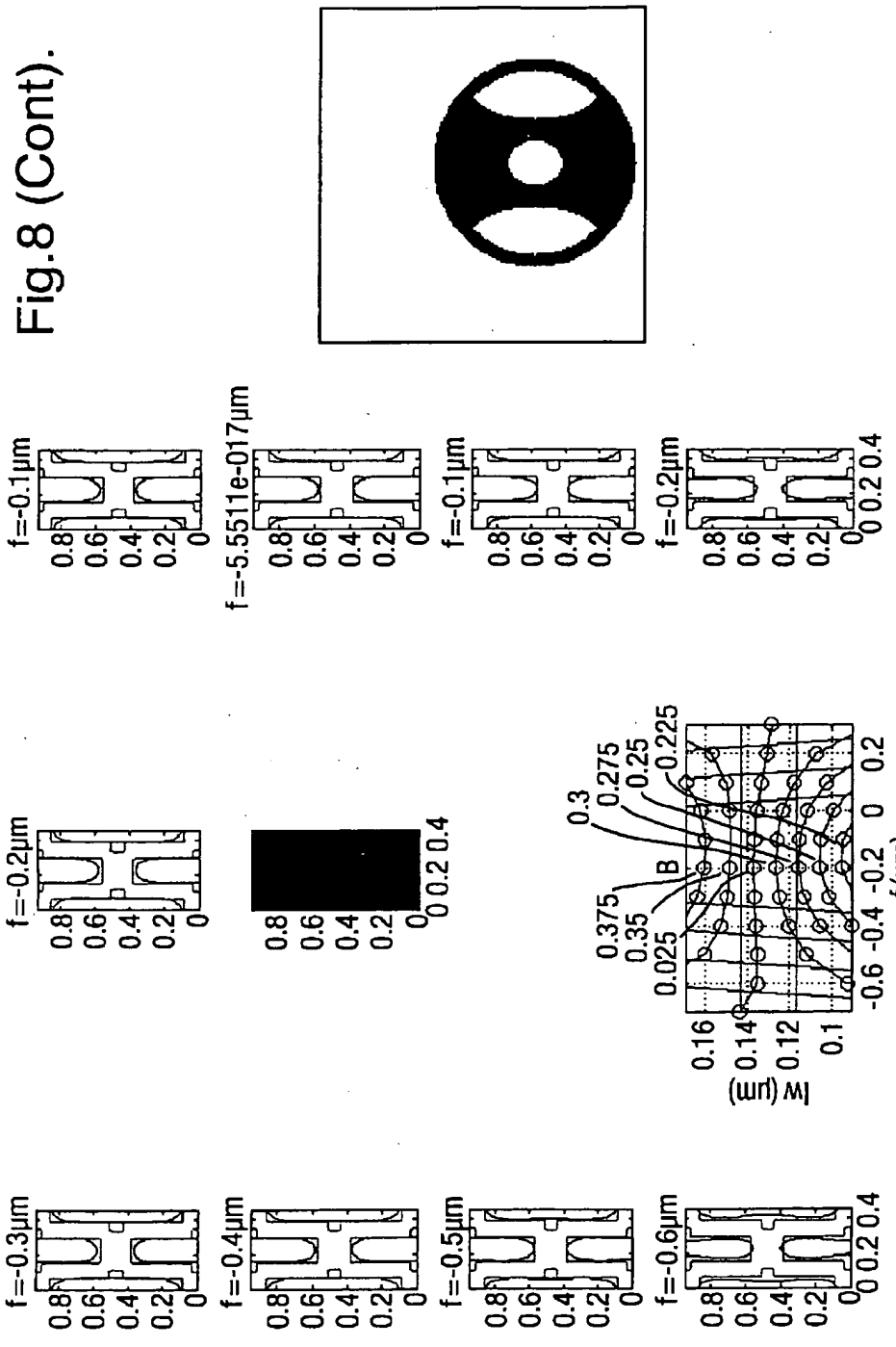
f=-0.1μm
f=-5.5511e-017μm
f=-0.1μm
f=-0.2μm
f=-0.2μm
0.8
0.6
0.4
0.2
0
0 0.2 0.4
0.3
0.275
0.25
0.225
0.375
0.35
B
0.025
0.16
0.14
0.12
0.1
lw (μm)
-0.6 -0.4 -0.2 0 0.2
f(μm)
f=-0.3μm
f=-0.4μm
f=-0.5μm
f=-0.6μm

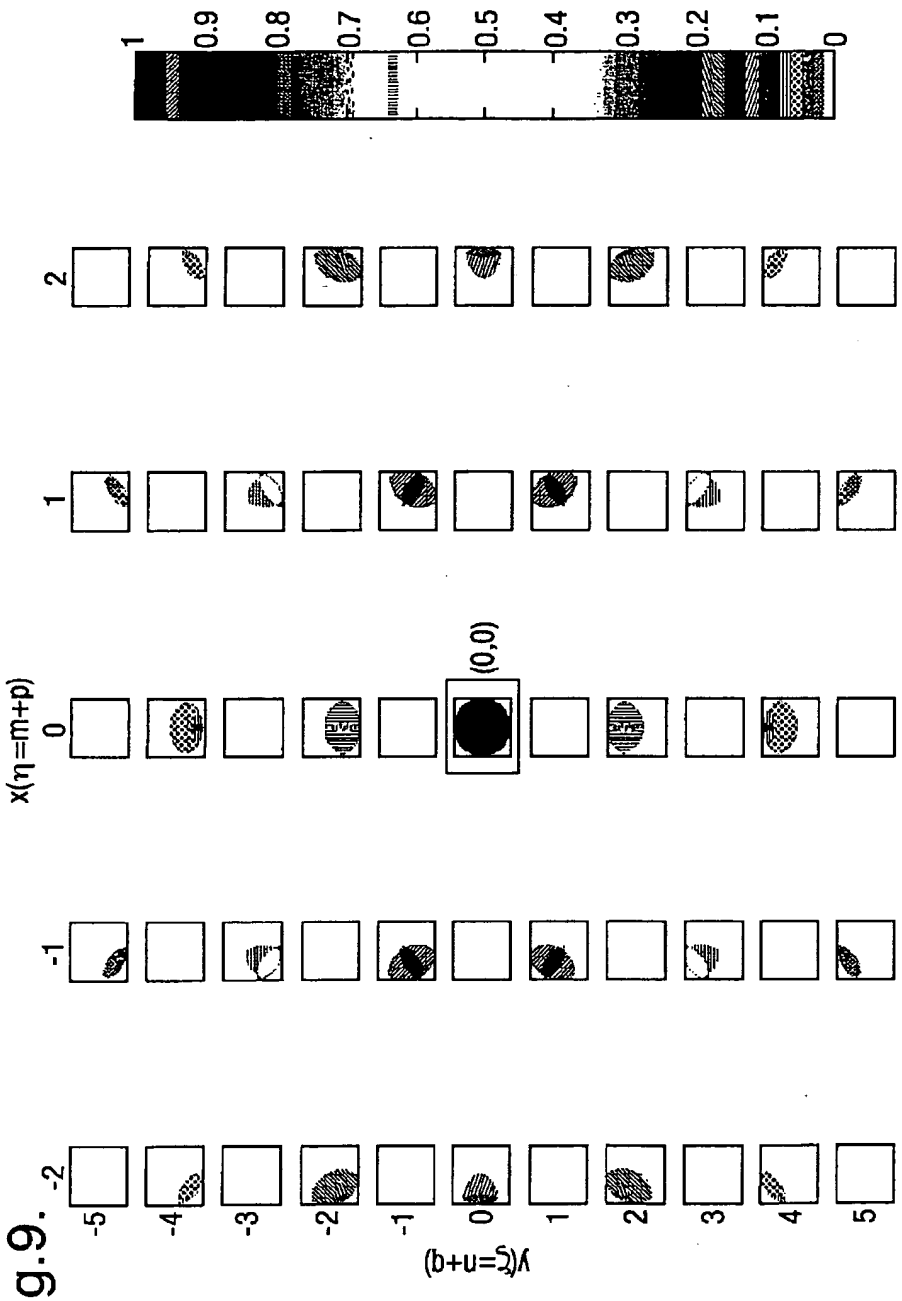

Fig.9.

Fig.10.

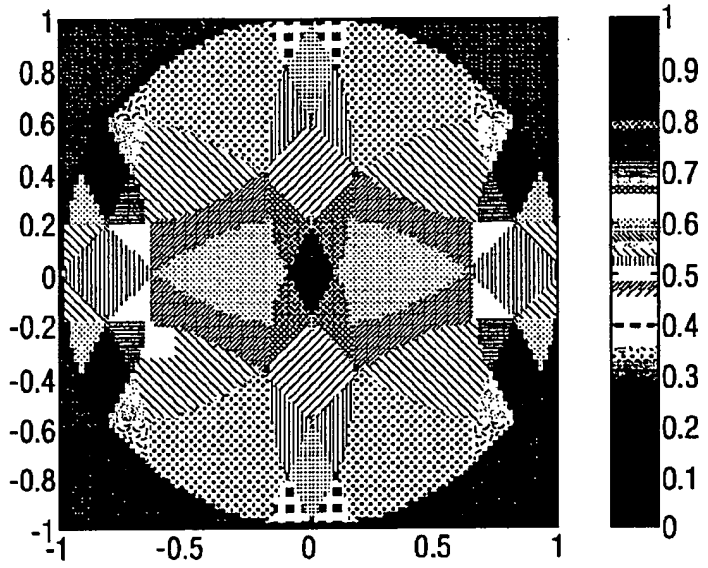

Fig.11a.

Fig.11b.

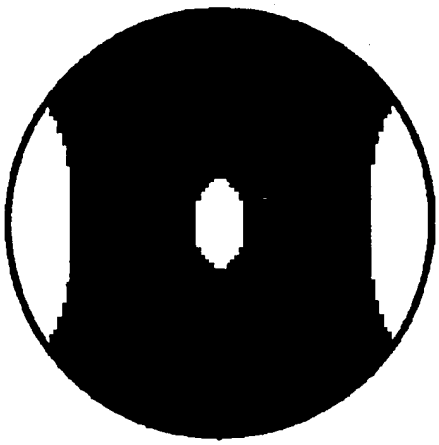

Fig.12.

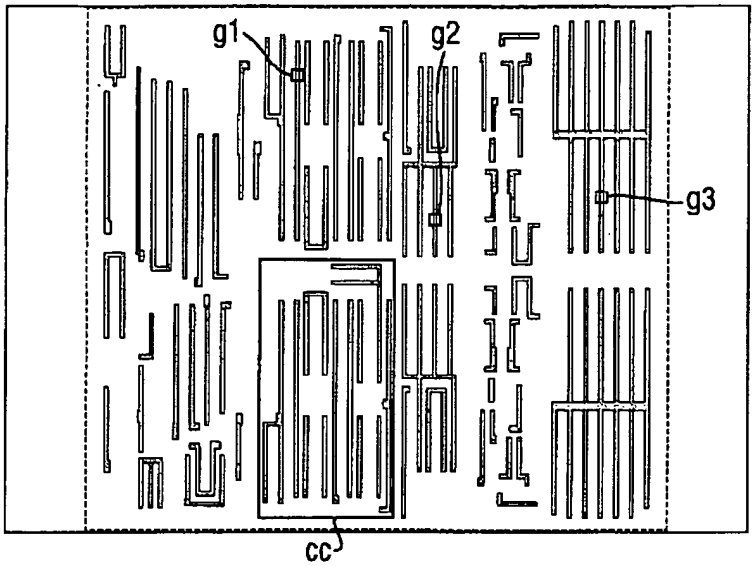

Fig.13.

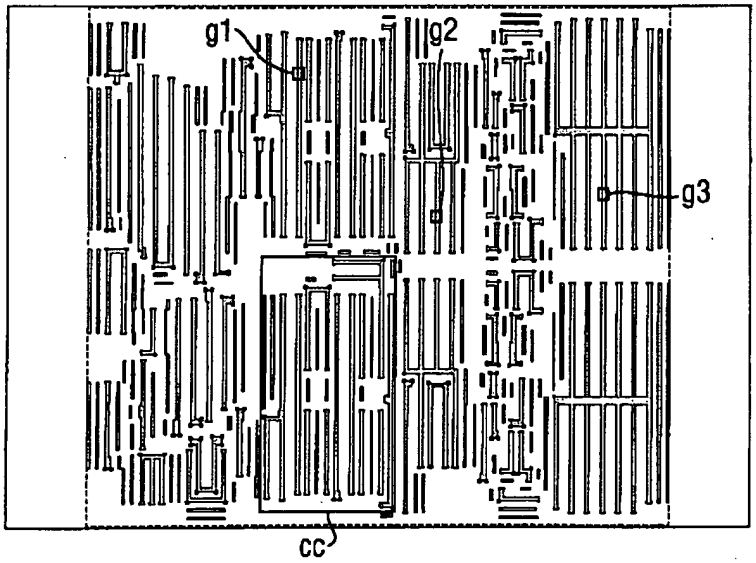

Fig.14.

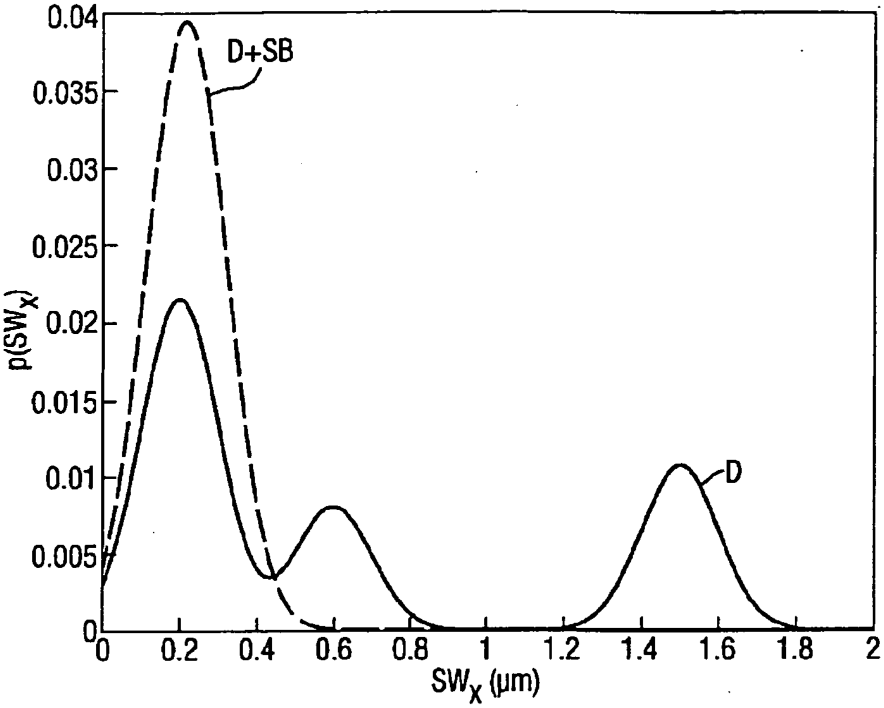
0.04
0.035
0.03
0.025
0.02
0.015
0.01
0.005
0
p(SWx)
D+SB
D
0
0.2
0.4
0.6
0.8
1
1.2
1.4
1.6
1.8
2
SWx (μm)

Fig.15.

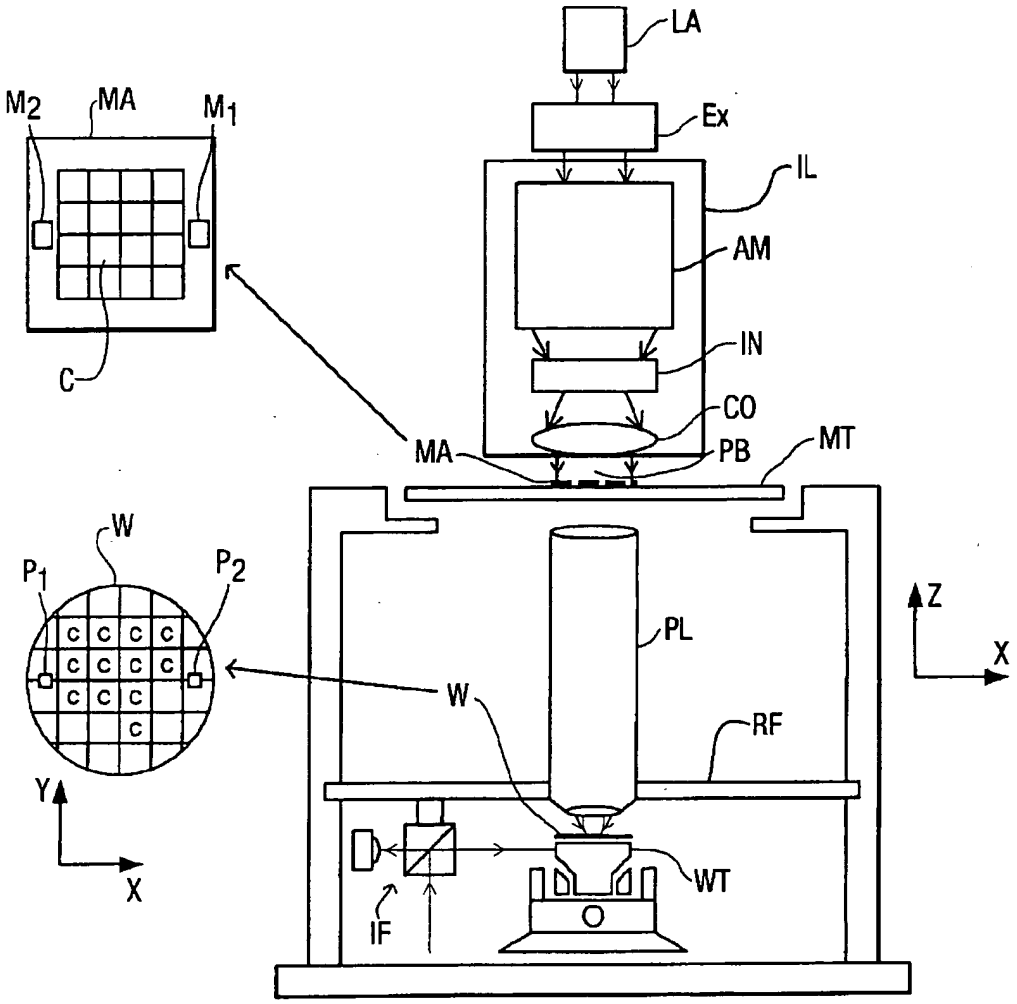

1 Abstract

A method and apparatus for microlithography. The method and apparatus include optimizing illumination modes based on characteristics of a specific mask pattern. The illumination is optimized by determining an appropriate illumination mode based on diffraction orders of the reticle, and the autocorrelation of the projection optic. By elimination of parts of the illumination pattern which have no influence on modulation, excess DC light can be reduced, thereby improving depth of focus. Optimization of mask patterns includes addition of sub-resolution features to reduce pitches and discretize the probability density function of the space width.

2 Representative Drawing

Fig. 1